The effects of climate change and fire on tundra vegetation change in the western Canadian Arctic

by

Angel Chen
B.Sc., University of Saskatchewan, 2017

A Thesis Submitted in Partial Fulfillment
of the Requirements for the Degree of

MASTER OF SCIENCE

in the School of Environmental Studies

Supervisory Committee

The effects of climate change and fire on tundra vegetation change in the western Canadian Arctic

by

Angel Chen
B.Sc., University of Saskatchewan, 2017

Supervisory Committee

Dr. Trevor C. Lantz, School of Environmental Studies
Supervisor

Dr. Joe Antos, Department of Biology
Outside Committee Member

Abstract

Supervisory Committee

Dr. Trevor C. Lantz, School of Environmental Studies
Supervisor

Dr. Joe Antos, Department of Biology
Outside Committee Member

Rapid climate change is driving increases in tundra vegetation productivity and altering the frequency and severity of natural disturbances across the Arctic. While tundra vegetation change has been widespread, there is still uncertainty about the influence of fine-scale factors on change and the role of interactions between warming, disturbance, and vegetation change. In my MSc research I investigated how Arctic tundra vegetation is responding to ongoing climate change and more severe tundra fire in the western Canadian Arctic. In the first part of my thesis I measured post-fire soil and vegetation recovery along a burn severity gradient at six fires, which burned in 2012 in the Northwest Territories. My observations suggest that deciduous shrub communities (dominated by *Betula glandulosa*) are resilient to high severity fire and that severe fire promotes edaphic conditions that favor the persistence of this vegetation type. In the second part of my thesis, I investigated the spatial patterns of trends in tundra vegetation productivity over the past three decades using Random Forests machine learning to analyze Enhanced Vegetation Index (EVI) data derived from Landsat imagery. My Random Forests models of the relationship between Landsat EVI trends and biophysical variables showed that two-thirds of the western Canadian Arctic productivity has increased during the past three decades and that this change is occurring most rapidly in dwarf and upright shrub-dominated regions. Taken together, my research demonstrates that shrub tundra communities are well adapted to

severe fire and show increasing productivity in response to warming Arctic temperature. My research also indicates that these relationships can be highly complex at finer scales, where they are mediated by local variations in microclimate, topography, and moisture.

Table of Contents

List of Tables

List of Figures

Acknowledgments

Thank you to the many funding and research institutions that enabled me to conduct this research and to learn on the territories of the Gwich'in and Inuvialuit. This research possible through logistical and financial support from the University of Victoria, the Natural Resources and Engineering Resource Council of Canada, Compute Canada – Westgrid, the Aurora Research Institute – Western Arctic Research Centre, Gwich'in Helicopters, the Northern Scientific Training Program, the Polar Continental Shelf Program, and the Arctic Institute of North America.

Thank you to my supervisor, Trevor Lantz, for believing in me and supporting me through this entire process, as well as my supervisory committee member, Joe Antos, for all his inputs along the way.

I am grateful to live on Lekwungen territories and for the community I have found here the past few years. I am so appreciative of all the incredible Team Rhubarb and Group ENVI folks for years of big laughs, kindness, and support through all the breakdowns and breakthroughs. Special thanks to all my wonderful past and present lab mates in the Arctic Landscape Ecology Lab (Kiyo Campbell, Tracey Proverbs, Jordan Seider, Nicola Shipman, Zander Chila, Hana Travers-Smith, and Tait Overeem) for always sharing your wisdom, your encouragement, and of course, your snacks.

Thank you to all my friends and to my parents, May and Daniel, for your love, patience, and encouragement through it all. I could never have done it without all of you.

1 Introduction

1.1 Study Rationale

Global air temperatures have increased by 1° C since pre-industrial levels and it has been proven beyond a reasonable doubt to be linked to anthropogenic global greenhouse gas emissions (IPCC, 2019). The Arctic is the fastest warming region in the northern hemisphere and in recent decades warming has surpassed twice the average global rate (ACIA, 2004) and lengthened the growing season by over one week during the past three decades (Park et al., 2016). Increases in the size of individuals, cover density, and range limits of shrub species in tundra vegetation have been observed in response to warming size (Myers-Smith, et al., 2011). This overall increase in tundra productivity, commonly referred to as "greening", has been observed across the Yukon (Myers-Smith, et al., 2011), Northwest Territories (Lantz et al., 2010), Nunavik (Tremblay et al., 2012), Nunatsiavut (Davis et al., 2020), and Nunavut (Hill & Henry, 2011). As the Arctic greens, it has inevitably altered surface energy exchange (Blok et al., 2011), permafrost (Wang et al., 2019), hydrology (Drake et al., 2019), and global carbon cycling (Christiansen et al., 2018). Longer growing seasons, warming temperatures, and increasing biomass will only continue to increase the frequency and severity of fire events in the greening Arctic (Chipman et al., 2015; Higuera et al., 2008). These compounding changes have regional and global-scale implications, as increased high latitude fire threatens to release massive carbon pools from permafrost into the atmosphere (Mack et al., 2011).

Arctic vegetation change is widespread, but there is still uncertainty about the interactions between climate and biophysical factors and the mechanism and impacts of change (Myers-Smith et al., 2020). With polar amplification pushing the rate of Arctic warming towards

three times the global rate of increase (Wang et al., 2017) it is becoming increasingly important to understand ecological responses to warming at high latitudes. The overall objective of my MSc research is to understand how Arctic tundra vegetation is responding to ongoing climate change and more severe tundra fire. To accomplish this, I undertook two unique but complimentary research projects. These studies are presented as stand-alone manuscripts in Chapters 2 and 3 of this thesis.

In Chapter 2, I use remote sensing to map burn severity (Allen and Sorbel, 2008) at six recent fires in the Northwest Territories and evaluate how tundra vegetation responds to increasing burn severity. In Chapter 3, I examine the factors that best explain changes in satellite estimates of vegetation productivity across the Western Canadian Arctic. Specifically, I use Random Forests classification and regression tree modelling to evaluate the relationship between vegetation productivity and microclimatic, topographic, and edaphic properties. Both data chapters are important for investigating recent changes in tundra vegetation and they contribute to our overall understanding of the interactions between warming, disturbance, and vegetation. In Chapter 4, I synthesize my findings from Chapters 2 and 3 and discuss the overall importance of my research, the implications of my findings, and provide recommendations for future opportunities.

1.2 Critical Context

1.2.1 High Latitude Fire

Research on high latitude fires has predominantly centered on northern boreal ecosystems, but interest in tundra fire research has expanded in recent decades as large, severe tundra fires become more prevalent (Mack et al., 2014). Historically, tundra fires have been low or moderate intensity, largely constrained by low biomass, and carried predominantly on

the surface through peat smouldering (Rocha et al., 2012; Wein, 1976). Most tundra fire activity is observed in July and August, but fires can also occur as early as May - as soon as snow melts and vegetation dries (Wein, 1976). Unlike canopied boreal forest vegetation that has greater moisture retention, tundra vegetation is fast-drying and can become highly susceptible to fire without extensive drought periods (York et al., 2017). It was previously thought that tundra fire has been a relatively rare disturbance in the past 11 000 years compared to boreal forest fire, but charcoal records from tundra regions of Noatak, Alaska reveal that ancient shrub tundra burned at a frequency similar to northern boreal forests (~144 ±90 years) under the correct climatic conditions and suggests that ongoing climate warming and increasing shrub cover will facilitate increasing tundra fire activity (Higuera et al., 2008). Recent changes in temperatures and aridity have promoted fire in Alaskan shrub tundra in the past half century and is projected to continue (Higuera et al., 2008). Widespread increases in the productivity and northward expansion of shrub-dominated vegetation (Jia et al., 2003; Stow et al., 2004; Tape et al., 2012) is increasing the rate of biomass accumulation and can enable a shorter fire return interval than southern ecosystems below the treeline (Parks et al., 2018). An increase in fire season length in Canada by over two weeks has also increased the fire susceptibility of northern ecosystems (Hanes et al., 2019). The Anaktuvuk River Fire, a large tundra fire of unprecedented size that burned in the Alaskan North Slope released approximately 2.1 teragrams of carbon into the atmosphere, demonstrating that increased fire activity can have major implications on the global carbon budget (Mack et al., 2011).

Modelling of future climate scenarios from historical climate-fire relationships across the circumpolar region have revealed that tundra fires may double in frequency and the

probability of large tundra fires (>1000 km^2) will be 2-3 times higher by 2100 than they have been in the past half century (Hu et al., 2015). With increases in tundra fire, more research is needed to examine the successional trajectories and ecological feedbacks that follow these disturbances.

1.2.2 **Remote Sensing**

In remote locations of the Canadian Arctic where limited resources and accessibility can make fieldwork impossible, remote sensing has become a popular tool for conducting research and environmental monitoring (Stow et al., 2004). Remote sensing technology can acquire near-real time environmental data over large spatial areas and short time return intervals, which are characteristics that can be critical for vegetation analysis, vegetation mapping, and change detection. Global coverage of remote sensing data has become increasingly accessible over the last few decades and created opportunities for researchers and practitioners to conduct long-term research on earth system dynamics. Earth Observation Systems (EOS), which are readily available for high latitude remote sensing include: the Moderate Resolution Imaging Spectraradiometer (MODIS), the Advanced Spaceborne Thermal Emission and Reflection Radiometer (ASTER), the Advanced Very High Resolution Radiometer (AVHRR), the PlanetScope constellation, the Landsat satellites, and Sentinel-2. (Table 1).

The Landsat program, a collaborative project of the United States Geological Survey (USGS) and the National Aeronautics and Space Administration (NASA), has been collecting earth observations since 1971 (Wulder et al., 2012). Landsat occupies a unique spatiotemporal niche, providing a spatial resolution fine enough for identifying land use

Table 1.1 Summary of high latitude earth observation systems.

Sensor	Spatial Resolution (m)	Temporal Resolution (days)	Data Timeline
MODIS	250-1000	8-16	2000 - Present
ASTER	15-90	16	2000 – Present
Landsat	15 – 30	16	1984 - Present
Sentinel 2	10 – 60	10	2015 – Present
AVHRR	1100	15	1978 – Present
PROBA-V	100-1000	2	2013 – Present
Spot	6	1	1986 – Present
Planetscope	3	1	2016-Present

and land cover change and broad enough for application across large land areas, while also having temporal dimensionality that captures long-term trends (Wulder et al., 2012; White et al., 2014). The 30-meter pixel resolution and 16-day revisit intervals provides moderately high spatial and temporal resolution imagery suitable for environmental monitoring (Wulder et al., 2012). This has allowed Landsat to gain recognition for its application in generating vegetation indices capable of evaluating landscape level interannual vegetation dynamics. Landsat was not widely utilized until 2008, when USGS changed its data policy to allow free and open access of all USGS-held Landsat data to all users (Wulder et al., 2012). This unrestricted access provides more than 1200 scenes across Canada for government, private sector, and public usage, which can be used for global scale change detection and environmental monitoring (Wulder et al. 2012). The opening of the Landsat archive, granting free and unlimited access of archived and new data for all users has revolutionized environmental monitoring research (Txomin Hermosilla et al., 2015; Wulder et al., 2012).

Data at high latitudes is often limited by availability of cloud-free scenes, limiting the capabilities of scene-based analyses. Best Available Pixel (BAP) composites are derived from pixel-based image composition and enable a robust method for deriving gap-free data

sets over large spatial scales (White et al., 2014). By selecting the most suitable data available or interpolated from imagery archives, pixel-based composition provides complete datasets that incorporate the most relevant information to the user and overcome the data limitations of scene-based analysis. BAP has been developed to create composites that allocate proxy values for cloud, shadow, and haze cover (Hermosilla et al., 2015). By using a scoring system that ranks pixel suitability based on individual scoring for sensor type, date, proximity to cloud cover, and opacity, BAP selection can be customized to suit individual user needs (White et al., 2014). With the limited availability of cloud-free images at northern latitudes, BAP composites create a promising opportunity to evaluate long-term Arctic trends in remotely sensed vegetation indices. Annual BAP imagery used in this project was generated by the Canadian Forest Service using the pixel scoring method where the values at each pixel location were assigned a score based on suitability of: (1) sensor, (2) date of data acquisition, (3) image noise, and (4) atmospheric opacity (White et al., 2014; Hermosilla et al., 2015). Final data value for the BAP composite is assigned based on the highest cumulative score. Synthetic proxy values can be generated for missing or low-score data by assigning value based on data available for years before and after the missing data.

1.2.3 **Vegetation Indices**

Development of increasingly sophisticated remote sensing products has allowed researchers to maximize on this rich dataset to suit specific research objectives. Vegetation indices have emerged as a popular application of remote sensing to quantify vegetation change across multiple spatiotemporal scales (Osunmadewa et al., 2018). Continuous time series data of vegetation index products can be used to detect trends in vegetation

productivity, and evaluate the relationships between changes in vegetation productivity and environmental changes (Stow et al., 2003). Vegetation indices employing specific wavelength ranges captured by satellites are commonly used as proxies for vegetation properties such as: productivity or biomass (Bannari et al., 1995). Chlorophyll in plant cells absorbs light ranging from 400 to 700 nanometers (nm) for photosynthesis and reflects near-infrared (NIR) light ranging from 700 to 1300 nanometers (Tarpley et al., 1984). Satellites with sensors that detect these wavelengths can be used to measure the intensity of reflectance from visible and NIR spectrums to estimate the photosynthetic capacity of vegetation. Productive vegetation absorbs the most visible light and reflects the most NIR light. This knowledge has led to the development of the Normalized Difference Vegetation Index (NDVI) which measures the proportion of light absorbed and reflected from the photosynthetically active radiation (PAR) spectral range (Huemmrich & Goward, 1997).

The Enhanced Vegetation Index (EVI) is a modified version of NDVI which employs blue wavelengths in addition to red and NIR to correct for atmospheric perturbations and allow greater sensitivity to subtle species compositional change, canopy structure, and leaf area index (Huete et al., 2002).

$$EVI = 2.5 \times \frac{NIR - Red}{NIR + 6 \times Red - 7.5 \times Blue + 1}$$

The Normalized Burn Ratio (NBR) is a modified version of NDVI that uses NIR and shortwave infrared (SWIR) wavelengths to capture the greatest contrast in the reflectance response of healthy and burned vegetation (Key & Benson, 2006). Properties that affect radiative characteristics including fuel consumption, ash presence, transpiration and increased surface temperature can result in reduced surface reflectance in the Near Infrared

(NIR) wavelength range and increased reflectance in the Shortwave Infrared (SWIR) range (Chen & Huang, 2008). Living vegetation has higher NIR reflectance and lower SWIR reflectance compared to burned vegetation (Keeley et al., 2008). Differenced NBR (dNBR) using pre and post-fire NBR imagery approximately one year before and after fire can be used to calculate the magnitude of per-pixel change initiated by fire (Key & Benson, 2006).

1.2.4 **Random Forests**

To understand the relationships between vegetation, climate, and disturbance, machine learning methods have become increasingly popular in ecological research (Cutler et al., 2007; Olden et al., 2008). Machine learning algorithms 'learn' and model relationships between user-inputted predictor and response data by acquiring knowledge from training data (Mellor et al., 2012). Classification and regression trees (CARTs) are a method of inferential machine learning that partitions data from predictor variables into classes or nodes of increasing homogeneity (Cutler et al., 2007). Tree-based learning can simulate relationships among variables across multiple spatiotemporal scales, allowing the complex, often non-linear, interactions between vegetation, climate, and disturbance to be effectively modelled. Random Forests (RF) modelling is an ensemble method of machine learning that combines many individual "weak learner" CARTs and operates as a "strong learner" by utilizing the average response of all individual CARTs to achieve a higher overall modeling accuracy (Rodriguez-Galiano et al., 2012). While improved accuracy of ensemble methods can come at the cost of more difficult interpretation and more intensive computing (Gómez et al., 2016), RF is a relatively simple method compared to other ensemble methods, such as artificial neural networks and support vector machines, as it requires only two user-defined parameters: (1) number of trees and (2) number of predictor variables to sample

per branch (Rodriguez-Galiano et al., 2012). By selecting a random subset of variables per branch, RF addresses the limitations of CARTs and reduces the strength of individual trees as well as the correlation between them (Rodriguez-Galiano et al., 2012).

Beyond simplicity, RF can also handle large sets of input predictor variables without deletion (Cutler et al., 2007) and is not limited by Gaussian distributional assumptions (Faivre et al., 2016). Traditional statistical methods such as linear regression assume constant variance of the response variable across the observations, and normal (Gaussian) distribution of errors – conditions which may not be valid for many ecological studies (Cutler et al., 2007). RF can also better handle the inclusion of correlated variables, an issue which can hinder the process of variable selection in regression-based modelling methods (Faivre et al., 2016).

Bibliography

ACIA. (2004). Impacts of a Warming Arctic: Arctic Climate Impact Assessment. Cambridge University Press, 144.

Bannari, A., Morin, D., Bonn, F., & Huete, A. R. (1995). A review of vegetation indices. *Remote Sensing Reviews*, *13*(1–2), 95–120. https://doi.org/10.1080/02757259509532298

Blok, D., Schaepman-Strub, G., Bartholomeus, H., Heijmans, M. P. D., Maximov, T. C., & Berendse, F. (2011). The response of Arctic vegetation to the summer climate: Relation between shrub cover, NDVI, surface albedo and temperature. *Environmental Research Letters*, *6*(3). https://doi.org/10.1088/1748-9326/6/3/035502

Chen, X., & Huang, C. (2008). *Use of multiple spectral indices to estimate burn severity in the Black Hills of South Dakota*. https://www.researchgate.net/publication/229043901

Chipman, M. L., Hudspith, V., Higuera, P. E., Duffy, P. A., Kelly, R., Oswald, W. W., & Hu, F. S. (2015). Spatiotemporal patterns of tundra fires: Late-Quaternary charcoal records from Alaska. *Biogeosciences*. https://doi.org/10.5194/bg-12-4017-2015

Christiansen, C. T., Lafreniére, M. J., Henry, G. H. R., & Grogan, P. (2018). Long-term deepened snow promotes tundra evergreen shrub growth and summertime ecosystem net CO2 gain but reduces soil carbon and nutrient pools. *Global Change Biology*, *24*(8), 3508–3525. https://doi.org/10.1111/gcb.14084

Cutler, D. R., Edwards, T. C., Beard, K. H., Cutler, A., Hess, K. T., Gibson, J., & Lawler, J. J. (2007). RANDOM FORESTS FOR CLASSIFICATION IN ECOLOGY. *Ecology*, *88*(11), 2783–2792.

Davis, E., Trant, A., Hermanutz, L., Way, R. G., Lewkowicz, A. G., Siegwart Collier, L., Cuerrier, A., & Whitaker, D. (2020). Plant–Environment Interactions in the Low Arctic Torngat Mountains of Labrador. *Ecosystems*, 1–21. https://doi.org/10.1007/s10021-020-00577-6

Drake, T. W., Holmes, R. M., Zhulidov, A. V., Gurtovaya, T., Raymond, P. A., McClelland, J. W., & Spencer, R. G. M. (2019). Multidecadal climate-induced changes in Arctic tundra lake geochemistry and geomorphology. *Limnology and Oceanography*, *64*(S1), S179–S191. https://doi.org/10.1002/lno.11015

Faivre, N. R., Jin, Y., Goulden, M. L., & Randerson, J. T. (2016). Spatial patterns and controls on burned area for two contrasting fire regimes in Southern California. *Ecosphere*, *7*(5), e01210. https://doi.org/10.1002/ecs2.1210

Gómez, C., White, J. C., & Wulder, M. A. (2016). *Optical remotely sensed time series data for land cover classification: A review*.

https://doi.org/10.1016/j.isprsjprs.2016.03.008

Hanes, C. C., Wang, X., Jain, P., Parisien, M.-A., Little, J. M., & Flannigan, M. D. (2019). Fire-regime changes in Canada over the last half century. *Canadian Journal of Forest Research*, *49*(3), 256–269. https://doi.org/10.1139/cjfr-2018-0293

Hermosilla, T., Wulder, M. A., White, J. C., Coops, N. C., & Hobart, G. W. (2015). Regional detection, characterization, and attribution of annual forest change from 1984 to 2012 using Landsat-derived time-series metrics. *Remote Sensing of Environment*, *170*, 121–132. https://doi.org/10.1016/j.rse.2015.09.004

Higuera, P. E., Brubaker, L. B., Anderson, P. M., Brown, T. A., Kennedy, A. T., & Hu, F. S. (2008). Frequent fires in ancient shrub tundra: implications of paleorecords for arctic environmental change. *PloS One*, *3*(3), e0001744. https://doi.org/10.1371/journal.pone.0001744

Hill, G. B., & Henry, G. H. R. (2011). Responses of High Arctic wet sedge tundra to climate warming since 1980. *Global Change Biology*, *17*(1), 276–287. https://doi.org/10.1111/j.1365-2486.2010.02244.x

Hu, F. S., Higuera, P. E., Duffy, P., Chipman, M. L., Rocha, A. V, Young, A. M., Kelly, R., & Dietze, M. C. (2015). Arctic tundra fires: natural variability and responses to climate change. *Frontiers in Ecology and the Environment*, *13*(7), 369–377. https://doi.org/10.1890/150063

Huemmrich, K. F., & Goward, S. N. (1997). Vegetation canopy PAR absorptance and NDVI: An assessment for ten tree species with the SAIL model. *Remote Sensing of Environment*, *61*(2), 254–269. https://doi.org/10.1016/S0034-4257(97)00042-4

Huete, A., Didan, K., Miura, T., Rodriguez, E. P., Gao, X., & Ferreira, L. G. (2002). Overview of the radiometric and biophysical performance of the MODIS vegetation indices. *Remote Sensing of Environment*, *83*(1–2), 195–213. https://doi.org/10.1016/S0034-4257(02)00096-2

Jia, G. J., Epstein, H. E., & Walker, D. A. (2003). Greening of arctic Alaska, 1981-2001. *Geophysical Research Letters*, *30*(20). https://doi.org/10.1029/2003GL018268

Keeley, J. E., Brennan, T., & Pfaff, A. H. (2008). FIRE SEVERITY AND ECOSYTEM RESPONSES FOLLOWING CROWN FIRES IN CALIFORNIA SHRUBLANDS. *Ecological Applications*, *18*(6), 1530–1546. https://doi.org/10.1890/07-0836.1

Key, C. H., & Benson, N. C. (n.d.). *LA-1 Landscape Assessment (LA) Sampling and Analysis Methods*. Retrieved February 16, 2018, from https://www.fs.fed.us/rm/pubs/rmrs_gtr164/rmrs_gtr164_13_land_assess.pdf

Lantz, T. C., Gergel, S. E., & Henry, G. H. R. (2010). Response of green alder (Alnus viridis subsp. fruticosa) patch dynamics and plant community composition to fire and regional temperature in north-western Canada. *Journal of Biogeography*, *37*(8),

no-no. https://doi.org/10.1111/j.1365-2699.2010.02317.x

Mack, M. C., Bret-Harte, S. M., Hollingsworth, T. N., Jandt, R. R., Schuur, E. A. G., Shaver, G. R., & Verbyla, D. L. (2011). Carbon loss from an unprecedented Arctic tundra wildfire. *Nature*, *475*. https://doi.org/10.1038/nature10283

Mellor, A., Haywood, A., Jones, S., Wilkes, P., Mellor, A., Haywood, A., Jones, S., & Wilkes, P. (2012). Forest Classification using Random forests with multisource remote sensing and ancillary GIS data. . *16th Australasian Remote Sensing and Photogrammetry Conference Proceedings*, 40–44. https://www.researchgate.net/publication/265382341

Myers-Smith, I. H., Forbes, B. C., Wilmking, M., Hallinger, M., Lantz, T., Blok, D., Tape, K. D., Macias-Fauria, M., Sass-Klaassen, U., Lévesque, E., Boudreau, S., Ropars, P., Hermanutz, L., Trant, A., Collier, L. S., Weijers, S., Rozema, J., Rayback, S. A., Schmidt, N. M., … Hik, D. S. (2011). Shrub expansion in tundra ecosystems: dynamics, impacts and research priorities. *Environmental Research Letters*, *6*(4), 045509. https://doi.org/10.1088/1748-9326/6/4/045509

Myers-Smith, I. H., Hik, D. S., Kennedy, C., Cooley, D., Johnstone, J. F., Kenney, A. J., & Krebs, C. J. (2011). Expansion of canopy-forming willows over the twentieth century on Herschel Island, Yukon Territory, Canada. *Ambio*, *40*(6), 610–623. https://doi.org/10.1007/s13280-011-0168-y

Myers-Smith, I. H., Kerby, J. T., Phoenix, G. K., Bjerke, J. W., Epstein, H. E., Assmann, J. J., John, C., Andreu-Hayles, L., Angers-Blondin, S., Beck, P. S. A., Berner, L. T., Bhatt, U. S., Bjorkman, A. D., Blok, D., Bryn, A., Christiansen, C. T., Hans, J., Cornelissen, C., Cunliffe, A. M., … Wipf, S. (2020). Complexity revealed in the greening of the Arctic. *Nature Climate Change*, *10*, 106–117. https://doi.org/10.1038/s41558-019-0688-1

Olden, J. D., Lawler, J. J., & Poff, N. L. (2008). MACHINE LEARNING METHODS WITHOUT TEARS: A PRIMER FOR ECOLOGISTS. *The Quarterly Review of Biology*, *83*(2). https://www.journals.uchicago.edu/doi/pdfplus/10.1086/587826

Osunmadewa, B. A., Gebrehiwot, W. Z., Csaplovics, E., & Adeofun, O. C. (2018). Spatio-temporal monitoring of vegetation phenology in the dry sub-humid region of Nigeria using time series of AVHRR NDVI and TAMSAT datasets. *Open Geosciences*, *10*(1), 1–11. https://doi.org/10.1515/geo-2018-0001

Park, T., Ganguly, S., TØmmervik, H., Euskirchen, E. S., HØgda, K. A., Karlsen, S. R., Brovkin, V., Nemani, R. R., & Myneni, R. B. (2016). Changes in growing season duration and productivity of northern vegetation inferred from long-term remote sensing data. *Environmental Research Letters*, *11*(8), 084001. https://doi.org/10.1088/1748-9326/11/8/084001

Parks, S. A., Parisien, M.-A., Miller, C., Holsinger, L. M., & Baggett, L. S. (2018). Fine-scale spatial climate variation and drought mediate the likelihood of reburning.

Ecological Applications, *28*(2), 573–586. https://doi.org/10.1002/eap.1671

Rocha, A. V., Loranty, M. M., Higuera, P. E., MacK, M. C., Hu, F. S., Jones, B. M., Breen, A. L., Rastetter, E. B., Goetz, S. J., & Shaver, G. R. (2012). The footprint of Alaskan tundra fires during the past half-century: Implications for surface properties and radiative forcing. *Environmental Research Letters*, *7*(4), 044039. https://doi.org/10.1088/1748-9326/7/4/044039

Rodriguez-Galiano, V. F., Ghimire, B., Rogan, J., Chica-Olmo, M., & Rigol-Sanchez, J. P. (2012). An assessment of the effectiveness of a random forest classifier for land-cover classification. *ISPRS Journal of Photogrammetry and Remote Sensing*, *67*(1), 93–104. https://doi.org/10.1016/j.isprsjprs.2011.11.002

Stow, D. A., Hope, A., McGuire, D., Verbyla, D., Gamon, J., Huemmrich, F., Houston, S., Racine, C., Sturm, M., Tape, K., Hinzman, L., Yoshikawa, K., Tweedie, C., Noyle, B., Silapaswan, C., Douglas, D., Griffith, B., Jia, G., Epstein, H., … Myneni, R. (2004). Remote sensing of vegetation and land-cover change in Arctic Tundra Ecosystems. *Remote Sensing of Environment*, *89*(3), 281–308. https://doi.org/10.1016/j.rse.2003.10.018

Stow, D., Daeschner, S., Hope, A., Douglas, D., Petersen, A., Myneni, R., Zhou, L., & Oechel, W. (2003). Variability of the Seasonally Integrated Normalized Difference Vegetation Index Across the North Slope of Alaska in the 1990s. □□□. *24*, □□, *5*, 1111–1117. https://doi.org/10.1080/0143116021000020144

Tape, K. D., Hallinger, M., Welker, J. M., & Ruess, R. W. (2012). Landscape Heterogeneity of Shrub Expansion in Arctic Alaska. *Ecosystems*, *15*(5), 711–724. https://doi.org/10.1007/s10021-012-9540-4

Tarpley, J. D., Schneider, S. R., & Money, R. L. (1984). Global Vegetation Indices from the NOAA-7 Meteorological Satellite. *Journal of Climate and Applied Meteorology*, *23*(3), 491–494. https://doi.org/10.1175/1520-0450(1984)023%3C0491:GVIFTN%3E2.0.CO;2%0A

Tremblay, B., Lévesque, E., & Boudreau, S. (2012). Recent expansion of erect shrubs in the Low Arctic: evidence from Eastern Nunavik. *Environmental Research Letters*, *7*(3), 035501. https://doi.org/10.1088/1748-9326/7/3/035501

Wang, K., Zhang, T., Zhang, X., Clow, G. D., Jafarov, E. E., Overeem, I., Romanovsky, V., Peng, X., & Cao, B. (2017). Continuously amplified warming in the Alaskan Arctic: Implications for estimating global warming hiatus. *Geophysical Research Letters*, *44*(17), 9029–9038. https://doi.org/10.1002/2017GL074232

Wang, Z., Kim, Y., Seo, H., Um, M. J., & Mao, J. (2019). Permafrost response to vegetation greenness variation in the Arctic tundra through positive feedback in surface air temperature and snow cover. *Environmental Research Letters*, *14*(4), 044024. https://doi.org/10.1088/1748-9326/ab0839

Wein, R. W. (1976). Frequency and Characteristics of Arctic Tundra Fires. *ARCTIC*, *29*(4), 213–222. https://doi.org/10.14430/arctic2806

White, J. C., Wulder, M. A., Hobart, G. W., Luther, J. E., Hermosilla, T., Griffiths, P., Coops, N. C., Hall, R. J., Hostert, P., Dyk, A., Guindon, L., & White, ©j C. (2014). Pixel-Based Image Compositing for Large-Area Dense Time Series Applications and Science. *Canadian Journal of Remote Sensing*, *40*, 192–212. https://doi.org/10.1080/07038992.2014.945827

Wulder, M. A., Masek, J. G., Cohen, W. B., Loveland, T. R., & Woodcock, C. E. (2012). Opening the archive: How free data has enabled the science and monitoring promise of Landsat. *Remote Sensing of Environment*, *122*, 2–10. https://doi.org/10.1016/j.rse.2012.01.010

2 Ecological response of Arctic tundra to burn severity in the Northwest Territories

Angel Chen[1], Trevor Lantz[1], Joe Antos[2]

1. School of Environmental Studies, University of Victoria

2. Department of Biology, University of Victoria

2.1 Introduction

Over the past half century, the length of the fire season in Canada has increased substantially and the national trend in annual area burned has increased three-fold (Hanes et al., 2019). Fire activity has increased most rapidly in boreal regions of northern Canada (Brown & Johnstone, 2011; Walker et al., 2019), where air temperatures are warming at three times the global rate (Bush & Lemmen, 2019; Vincent et al., 2015). High-latitude tundra fires have historically been constrained by low biomass, making them less common and severe than boreal forest fires (Viereck & Schandelmeier, 1980; Wein, 1976). However, warming Arctic temperatures (Vincent et al., 2015) and the proliferation of deciduous shrubs (creating surface fuels) (Lantz et al., 2013b; Moffat et al., 2016) are projected to dramatically increase fire probability in the tundra biome by the end of the 21st century (Moritz et al., 2012) and increase the fire return interval from over 800 years to less than 200 years (Higuera et al., 2008; Rocha et al., 2012). To date, Low Arctic tundra regions of Alaska (Sae-Lim et al., 2019), Canada (Versaverbeke et al., 2017), and Siberia (Moskovchenko et al., 2020) have seen increases in the number of ignitions in the past half century (Bret-Harte et al., 2013), demonstrating that fire regimes are already changing in the circumpolar tundra.

Studies on the effects of fire in subarctic forest ecosystems show that rapid climate warming is increasing fire frequency and intensity and initiating successional sequences that have not previously been observed previously (Johnstone & Chapin, 2006; Kelly et al., 2013). Less is known about the impacts that altered fire regimes will have on tundra landscapes. Resilience in ecological systems is a measurement of persistence and the capacity of a system to absorb change or disturbance and return to its original state (Holling, 1973). Subarctic boreal forest ecosystems, like black spruce forests, have

historically been resilient to wildfire, maintaining consistent recovery pathways where post-fire succession leads to pre-fire community structure (Johnstone & Chapin, 2006). However, this cycle of resiliency can be broken by unusual disturbance events, such as high severity fires or shorter fire return intervals (Johnstone, et al., 2010a). Studies in the boreal have shown that the combustion of the soil organic layer during severe fire can interrupt the successional return of pre-fire type communities and favor alternative trajectories of successional change and alternative species assemblages (Hollingsworth et al., 2013; Johnstone, et al., 2010b), and accelerate permafrost degradation and thermokarst development (Jafarov et al., 2013; Jones et al., 2015).

Research in tundra ecosystems indicates that vegetation can recover quickly following fire. In Alaska, tussock tundra ecosystems can reach pre-fire structure and composition within 5-10 years (Jandt et al., 2012; Jones et al., 2009; Racine et al., 2004), while shrub tundra ecosystems typically recover on a decadal scale (Frost et al., 2020; Heim et al., 2019; Lantz et al. 2010). There is some evidence that severe tundra fire can alter successional trajectories and not return to pre-fire conditions by promoting changes in community composition. In tussock-shrub tundra communities fire typically initiates a rapid recovery and dominance of tussock-forming sedges (*Eriophorum vaginatum*), but can shift towards shrub-domination at the decadal scale (Racine et al. 2004). Studies from the Tuktoyaktuk Coastlands have also shown that severe fire can facilitate the landscape-scale dominance of upright shrubs (Lantz et al., 2013a; Travers-Smith &ff Lantz, 2020). In tussock-tundra the recovery of vascular species is predominantly driven by resprouting of individuals, and seedling establishment and success is typically limited (Bret-Harte et al., 2013; Gartner et al., 1986). Though the leaves of *E. vaginatum* are destroyed by severe fire, the rhizomes

and meristems can survive and resprout rapidly within the moist tussock core, where it is enclosed and protected (Bret-Harte et al., 2013). While belowground stems of deciduous and evergreen shrub species also survive, the recovery of aboveground biomass following fire is slower, and does not usually reach or surpass pre-fire conditions until at least a decade after fire (Narita et al., 2015; Racine et al., 2004).

Changes to tundra vegetation structure can increase snow cover (Jia et al., 2009; Ropars and Boudreau, 2012) and evapotranspiration (Swann et al., 2010; Zhang and Walsh, 2006), and alter wildlife habitat (Fauchald et al., 2017; Gustine et al., 2014; Jandt et al., 2008; Joly et al., 2009). Permafrost thaw and thermokarst subsidence (Jones et al., 2015; Myers-Smith et al., 2008) triggered by severe tundra fires can remain evident decades after fire (Racine et al., 2004). At a global scale more widespread fire is predicted to cause a fourfold increase in fire-driven global carbon flux by 2100 (Abbott et al., 2016; Mack et al., 2011; Walker et al., 2019), with model projections suggesting the relative increase in carbon emissions from tundra fire will be up to two times higher than from boreal fires (Abbott et al., 2016). Identifying how variation in burn severity can affect successional trajectories is critical to understanding how increasing tundra fire frequency and severity will impact regional and global ecological processes.

To date, most research on multi-year and decadal (Frost et al., 2020; Racine et al., 2004) recovery following tundra fire has focused on individual fire disturbances and few studies have evaluated recovery patterns across gradients of burn severity (Rocha and Shaver, 2011; Tsuyuzaki et al., 2017). Remotely sensed vegetation indices can be used to delineate severity in tundra fires (Fraser et al., 2017; Kolden and Rogan, 2013), which can streamline field monitoring efforts and allow more efficient sampling design. The objective of this

study was to evaluate the resilience of tundra ecosystems across a gradient of burn severity. To accomplish this, we used remote sensing to map burn severity (Allen and Sorbel, 2008) and measured community composition, soil properties and permafrost conditions at six tundra fires that burned in the Northwest Territories in 2012.

2.2 Methods

2.2.1 Study Area

We conducted this study within the Tuktoyaktuk Coastal Plain and Anderson River Plain Ecoregions, in the Northwest Territories (Fig. 2.1). This area is located within the continuous permafrost zone, where soils are typically ice-rich, and the rolling landscape is characterized by hummocky uplands and lowlands typically occupied by polygonal peatlands (Ecosystem Classification Group, 2012). These ecoregions span the forest-tundra ecotone with landscapes in the southern part of the study area dominated by tall shrubs (*Salix* spp., *Alnus viridis*, and *Betula glandulosa)* and scattered spruce woodlands (Timoney et al., 1992; Travers-Smith and Lantz, 2020), and in the northern part by dwarf shrubs (*Vaccinium* spp., *Ledum decumbens*, *Empetrum nigrum*, *Rubus chamaemorus*), sedges (*Eriophorum* spp., *Carex* spp.), and grasses (Poaceae spp.) (Hernandez, 1973; Kokelj et al., 2017). Our study sites were predominantly within upland terrain where vegetation was dominated by shrub tundra communities comprised of tall (*Alnus*, *Betula*, *Salix*) and dwarf (*Ledum, Empetrum, Vaccinium*) shrubs and graminoids (*Carex*, *Eriophorum*, Poaceae). At lower micro-positions where moisture was higher, some sites were dominated by tussock tundra comprised mainly of *Eriphorum* and graminoids.

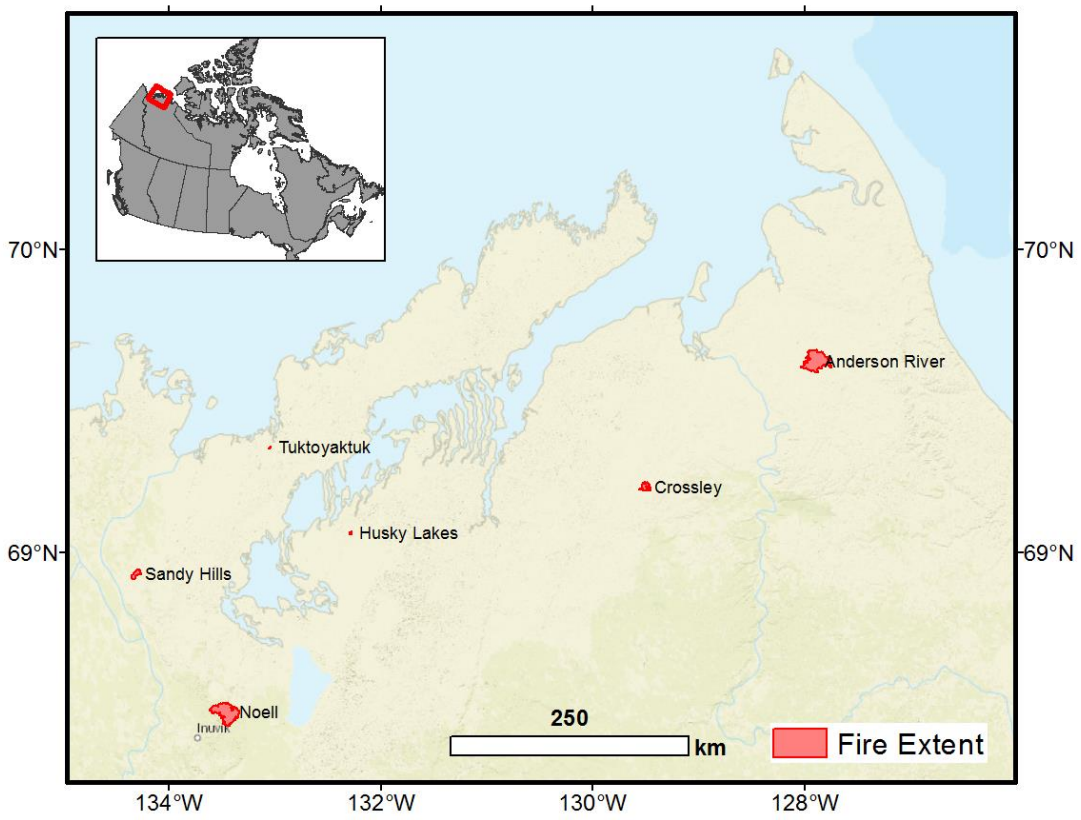

Figure 2.1 Map of study area and perimeter of six tundra fires examined. Inset map in upper area shows the location of the study area in northwestern Canada.

The regional climate of this area is characterized by long cold winters and short summers (Rampton, 1988). Mean annual temperatures (MAT) in Inuvik and Tuktoyaktuk are -8.2° C, and -10.1°C, respectively. Annual precipitation is approximately 240 mm in Inuvik and 160 mm in Tuktoyaktuk (Environment Canada, 2018). Continuous permafrost in this region is ice rich and thermokarst landforms (thaw slumps, thermokarst lakes, polygonal terrain) are common (Ecosystem Classification Group, 2012). Increasing MAT has been observed across all weather stations in the western Canadian Arctic over the past half century (Burn and Kokelj, 2009; Vincent et al., 2015) and warming has driven an increase

in ground temperatures and thaw depths in the past half century (Burn and Kokelj, 2009; Kokelj et al., 2017).

2.2.2 Site Selection

To examine the effects of burn severity on tundra landscapes we used Landsat false colour imagery to locate and identify six tundra fires that burned in 2012. To map spatial variation in the severity of each fire we determined the approximate dates of ignition and downloaded pre- and post-fire Landsat scenes, which were used to calculate the Normalized Burn Ratio (García and Caselles, 1991; Key and Benson, 1999) (Appendix A). The NBR is a modified version of the NDVI index, which uses the shortwave infrared (SWIR) and near infrared (NIR) bands to identify burned areas:

$$NBR = \frac{NIR - SWIR}{NIR + SWIR}$$

Unburned vegetation has high NIR reflectance and low SWIR reflectance and burned vegetation has low NIR and high SWIR reflectance (Keeley et al., 2008). Differenced NBR (dNBR) is calculated by subtracting post-fire NBR from pre-fire NBR to estimate burn severity and the magnitude of post-fire surface change (Chen and Huang, 2008). All of our fires burned in June, 2012 and Landsat scenes for dNBR calculation were selected based on proximity to the anniversary of the burn date pre- (June 2011) and post-fire (June, 2013) using the method described by Key and Benson (2006). Top of Atmosphere (ToA) Landsat Thematic Mapper (TM), Enhanced Thematic Mapper Plus (ETM+), and Operational Land Imager (OLI) images were downloaded from the United States Geological Survey (USGS) Earth Resources Observation and Sciences (EROS) Center Science processing Architecture (ESPA) for fire mapping. Burn severity calculations and classifications were

performed in R (R Core Team, 2018). To derive gapless dNBR calculations where Landsat images were affected by SLC-off, OLI reflectance values were transformed and calibrated to correspond with ETM+ values using the 'raster' package in R (Hijmans, 2019).

Fire severity classes were delineated using dNBR thresholds from the US Forest Service's *Fire Effects Monitoring and Inventory System* (FIREMON). This classification system was designed for forest monitoring in the contiguous United States, but has also been used in northern boreal regions (Epting et al., 2005). We adapted the classification scheme from Epting et al. (2005) by defining our severity classes as: (1) unburned (dNBR <100), (2) moderate severity (dNBR ≥ 100 and <400), and (3) high severity (dNBR ≥ 400) (Appendix B). We did not apply atmospheric correction to calculations of the NBR, as previous studies have found that the effects of atmospheric scattering are limited in the NIR and SWIR wavelengths used in this calculation (Miller et al., 2009). Atmospheric correction can also introduce errors when using imagery from multiple dates that likely differ in atmospheric effects (Fang and Yang, 2014; Miller et al., 2009).

2.2.3 Field Sampling

In July 2018, six years after the fires, we measured a suite of biotic and abiotic variables at six tundra fires identified using Landsat (Table 2.1, Fig. 2.1). and six unburned reference sites adjacent to each fire. To compare ecological recovery among fires and severity classes, we used field sampling to describe vegetation structure and composition and soil and permafrost conditions within moderately and severely burned regions of each fire, and adjacent unburned regions as control sites. We used randomized stratified sampling was to select sampling areas from satellite-derived burn severity classes. At each fire we selected randomly selected two sampling sites each in moderately burned regions, severely burned

regions, and unburned regions outside of the burn perimeter (n=6). All unburned sites were located at least 10 m beyond the perimeter of the fire. At each site, five sampling plots were randomly selected for a total of 180 plots across the study area. To measure vegetation structure and composition at each plot, we used a nested quadrat approach. 4 m^2 quadrats were used to visually estimate the percent cover of upright shrubs and trees and to measure tree or shrub canopy height. Percent cover of dwarf shrub, graminoid, herbaceous dicot and non-vascular species was estimated in 0.25 m^2 quadrats, located inside the 4m^2 quadrats. Percent cover estimates were made for all species, except graminoids, lichens, and mosses, which were estimated at the family (graminoids) or functional group (mosses and lichens) level.

Table 2.1 Size and estimated timing of the six fires sampled in this study and the Landsat scenes used to calculate the severity of each fire.

Fire Name	**Size (km^2)**	**Start Date**	**End Date**	**Pre-fire Scene**	**Post-fire Scene**
Crossley (CY)	56.6	24-Jun-12	10-July-12	LT05_L1TP_059012_20110623_20161008_01_T1	LE07_L1TP_060011_20130627_20161124_01_T1
Anderson River (AR)	392.7	24-June-12	19-July-12	LE07_L1TP_060011_20110622_20161208_01_T1	LE07_L1TP_060011_20130627_20161124_01_T1
Tuktoyaktuk (TK)	0.63	04-Jun-12	20-Jun-12	LT05_L1TP_064011_20110626_20161008_01_T1	LE07_L1TP_064011_20130607_20161124_01_T1
Husky Lakes (HL)	3.5	22-Jun-12	24-Jul-12	LE07_L1TP_062011_20110620_20161208_01_T1	LE07_L1TP_061012_20130618_20161123_01_T1
Sandy Hills (SH)	36.0	27-Jun-12	13-Jul-12	LT05_L1TP_063012_20110619_20161008_01_T1	LE07_L1TP_065011_20130614_20161123_01_T1
Noell Lake (NL)	362.6	13-Jun-12	09-Aug-12	LT05_L1TP_063012_20110619_20161008_01_T1	LE07_L1TP_061012_20130618_20161123_01_T1

Soil properties were measured at the centre and corners of each 4 m^2 quadrat (n=5). Volumetric soil water content was estimated in the field at the top of the mineral soil horizon using a Delta ThetaProbe Soil Moisture Sensor and HH2 moisture meter. Thaw depth was measured by depressing an active layer probe to the depth of refusal. To standardize thaw depth measurements made throughout the thaw season we estimated maximum thaw depth by adding 0.2 cm day^{-1} (Ovenden and Brassard, 1989) for measurements made before August 1st. Soil samples from the top 10 cm of soil matrix below the litter and organic horizon, were placed in plastic bags, labeled, and frozen until they were prepared for lab analysis.

We installed 12 thermistors to measure air and ground temperature at one severely burned and one unburned control site within each fire (n=6). To measure near surface and top-of-permafrost temperature we drilled shallow boreholes (100 cm) and attached thermistors to a PVC pipe, which was positioned in the borehole at depths of 5 cm and 100 cm. To measure air temperature thermistors were positioned at 1.5 m above the ground inside RS1 solar radiation shields (Onset Computing Corporation, Pocasset, MA, USA). We used Hobo Pro U23-003 data loggers with our thermistors, which have accuracy and precision of ±0.21 °C and 0.02 °C. Loggers were set to continuously record measurements every two hours.

2.2.4 Lab Analysis

In late August 2018, thawed soil samples were homogenized and used to estimate soil moisture and to prepare pore water extracts used to measure the concentration of major ions, conductivity, and pH. Samples were weighed before and after being oven dried to calculate gravimetric water content as:

$$\frac{Mass\ of\ water\ (\mathrm{g})}{Mass\ of\ oven\ dry\ soil\ (\mathrm{g})}$$

Samples for pore water extracts were air-dried, passed through a 2 mm sieve and used to create a 1:5 solution of soil to deionized water (He et al., 2012; Klaustermeier et al., 2016). Soil solutions were agitated continuously for ten seconds bihourly for a total of twelve hours then left to settle for twelve hours, agitated again for ten seconds, and centrifuged at 8000 rotations per minute for 30 minutes. The temperature-corrected electrical conductivity (EC) and pH of the supernatant were measured using an ExStik PH100 pH meter (Extech Instruments, Waltham, MA, USA) and a TDSTestr 3 conductivity meter (Oakton Instruments, Vernon Hills, IL, USA). After pH and EC were measured, we filtered the supernatant using 45 µm syringe filters, placed the samples into vials and shipped them to Taiga Labs in Yellowknife, NT for major ion analysis using Inductively Coupled Plasma – Mass Spectrometer

2.2.5 Statistical Analysis

To assess differences in community composition among severity classes we conducted a non-metric multidimensional scaling ordination using the 'vegan' package (Oksanen et al., 2019) in R (R Core Team, 2018). A matrix of species and functional group cover data was log (x+1) transformed prior to calculating a Bray Curtis distance matrix. We visualized differences in community composition among severity classes with ordination plots and used the envfit and bioenv functions in vegan to test for significant relationships among environmental variables and NMDS scores. Analysis of Similarity (ANOSIM) was performed in PRIMER v6 (Clarke and Gorley, 2006) to test for significant differences in community composition among severity classes (severe burn, moderate burn, and unburned). The null hypothesis of our ANOSIM was that there is no difference in average

rank dissimilarity between severity classes. We used SIMPER analysis to identify the species that made the largest contribution to dissimilarity between severity classes.

We used the GLIMMIX procedure in SAS (SAS Institute, 2015) and 'lme4' package (Bates et al., 2015) in R to fit generalized linear mixed effects models of the relationships between burn severity and abiotic site properties. In models of edaphic properties (thaw depth, organic layer depth, and soil moisture) burn severity was treated as a fixed factor and burns and sites were treated as random factors. Degrees of freedom were estimated using the Kenward-Roger approximation (Kenward and Roger, 1997).

2.3 Results

2.3.1 Plant Community Response

The effect of tundra fire on plant community composition and vegetation structure six years after fire depended on fire severity. Areas impacted by high severity fire were characterized by increased abundance of ruderals (*Chamerion angustifolium*, and *Senecio congestus*) and graminoids (*Carex* spp., Poaceae spp.) and decreased cover of shrubs (*B. glandulosa, V. vitis-idaea*) and lichen (Figs. 2.2B and 2.3). One-way analysis of similarity (ANOSIM) showed that plant community composition at severely burned was moderately distinct from unburned control sites (R_{ANOSIM} = 0.221), whereas plant community composition at moderate and severely burn sites (R_{ANOSIM} = 0.083) and moderate and unburned control sites (R_{ANOSIM} = 0.063) could not be clearly distinguished. Differences in plant community composition between severely burned sites and controls were driven by lower abundance of deciduous and evergreen shrubs and lichen in severely burned plots and an increase in the cover of bryophytes, grasses (Poaceae), mosses and litter (Table 2.2; Figs. 2.2 and 2.3). Indicators of disturbance such as bare ground and remnants of burned vegetation persisted

in moderately burned and severely burned sites six years after fire (Fig. 3A). Bare ground was observed in 47 out of 80 burned sites but only 3 out of 40 unburned sites.

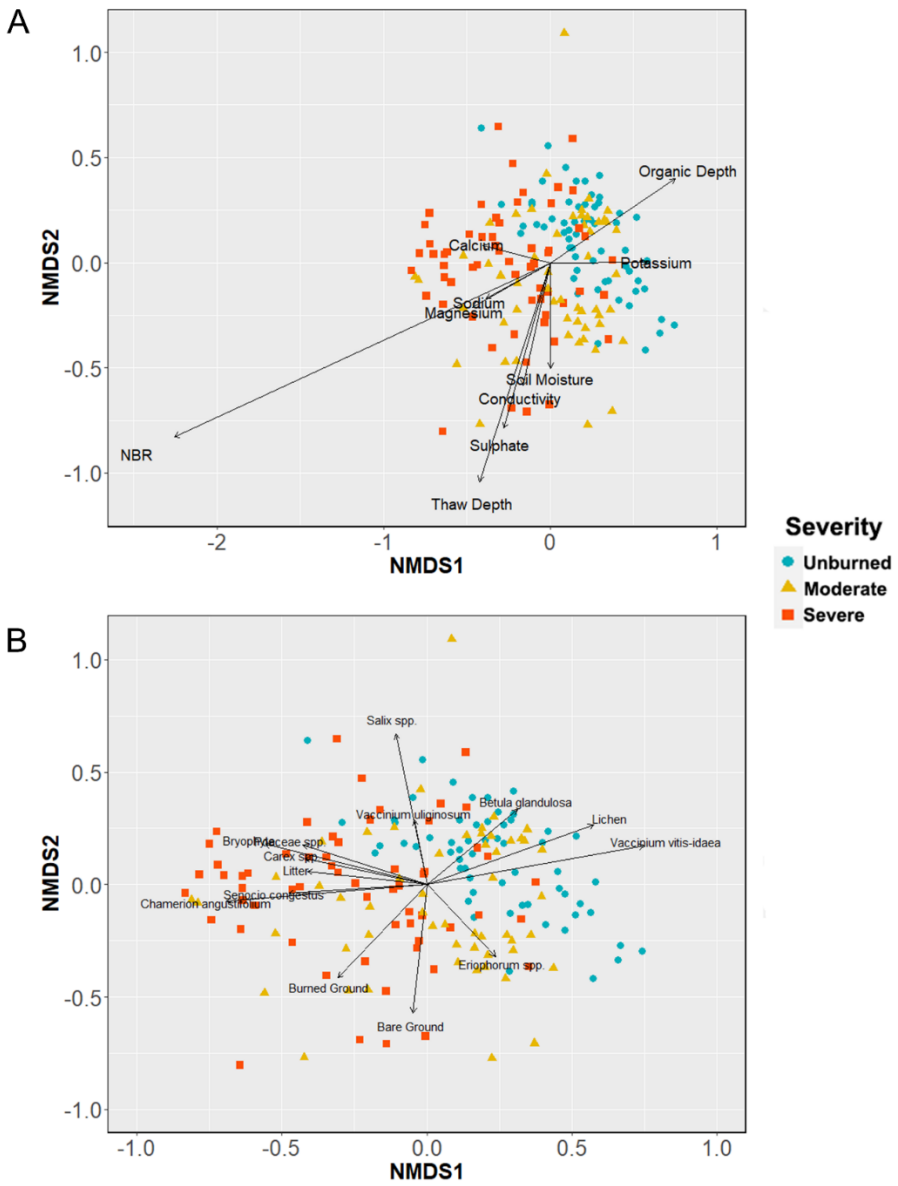

Figure 2.2 Non-metric multidimensional scaling (NMDS) ordination plot showing community similarity/dissimilarity among burned (two severity classes) and unburned sites. Points are sample plots (n=60) and are coloured by burn severity. Vectors in (A) show correlations between edaphic variables and NMDS scores. Vectors in (B) show correlations between percent cover of individual species or species groups and NMDS scores. The NMDS ordination had a final stress of 0.22 after

50 iterations. Clarke and Warwick (2001) state a stress around 0.2 to be within the range for useful for 2D interpretations.

Table 2.2 SIMPER analysis showing the top ten species or species group making the greatest contribution to Bray-Curtis dissimilarity among burn severity classes.

Site Types	**Site type 1 Abundance (%)**	**Site type 2 Abundance (%)**	**Cumulative Dissimilarity (%)**
Control and Severely Burned			
Bryophytes	19.12	36.36	15.76
Litter	22.82	30.12	28.24
Betula glandulosa	16.27	11.00	35.94
Vaccinium vitis-idaea	16.48	6.53	43.53
Lichen	13.22	2.74	50.46
Eriophorum spp.	7.12	4.38	56.06
Ledum decumbens	11.27	6.03	61.55
Empetrum nigrum	9.53	2.31	66.96
Poaceae spp.	1.33	7.64	71.73
Salix spp.	5.63	4.59	75.37
Moderately Burned and Severely Burned			
Bryophytes	22.05	36.36	16.82
Litter	25.16	30.12	29.57
Eriophorum spp.	11.95	4.38	37.65
Vaccinium vitis-idaea	11.98	6.53	44.44
Betula glandulosa	12.62	11.00	51.13
Ledum decumbens	11.55	6.03	57.26
Poaceae spp.	3.64	7.54	63.28
Vaccinium uliginosum	2.38	4.66	67.59
Empetrum nigrum	4.25	2.31	71.22
Salix spp.	3.33	4.59	74.70
Control and Moderately Burned			
Bryophytes	19.12	22.05	12.41
Litter	22.82	25.16	24.28
Eriophorum spp.	7.12	11.95	33.46
Vaccinium vitis-idaea	16.48	11.98	41.95
Betula glandulosa	16.27	12.62	50.11
Lichen	13.22	3.91	57.67
Ledum decumbens	11.27	11.55	64.33
Empetrum nigrum	9.53	4.25	70.46
Rubus chamaemorous	3.40	4.44	74.25
Salix spp.	5.63	3.33	77.78

Community composition at unburned sites was mainly characterized by presence of deciduous (*Betula glandulosa, Vaccinium uliginosum, Salix* spp.) and evergreen (*Empetrum nigrum, Vaccinium vitis-idaea, Ledum decumbens*) shrubs, and sedges (*Carex* spp., *Eriophorum* spp.) and grasses (Poaceae) (Table 2.2; Figs. 2.3 and 2.4). Cover of both deciduous and evergreen shrubs was negatively and linearly related to burn severity as indicated by post-fire NBR – a continuous variable indicating burn severity (Fig. 2.4). Herbaceous dicot cover was relatively uncommon across all site types regardless of burn severity (Fig. 2.3).

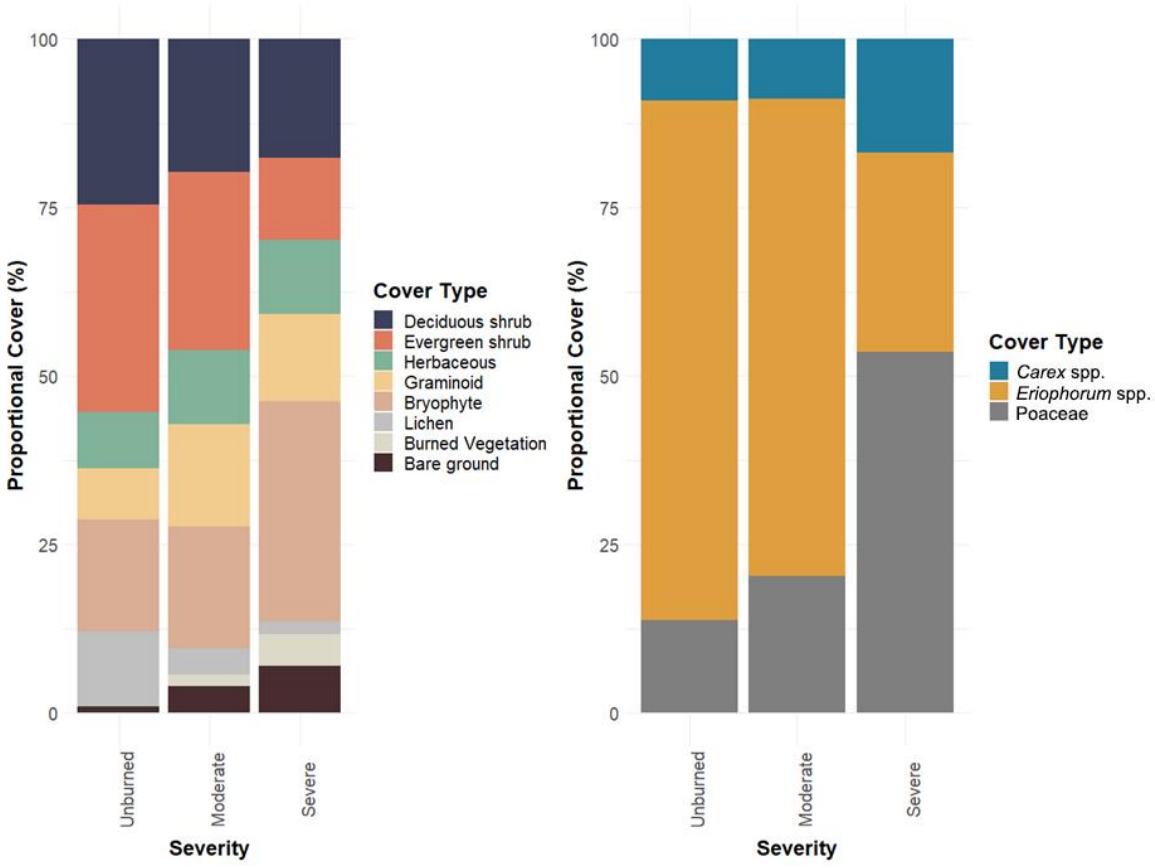

Figure 2.3 Average proportional percent cover of (A) plant functional types and (B) sub-groups of graminoids in unburned, moderately burned, and severely burned tundra types.

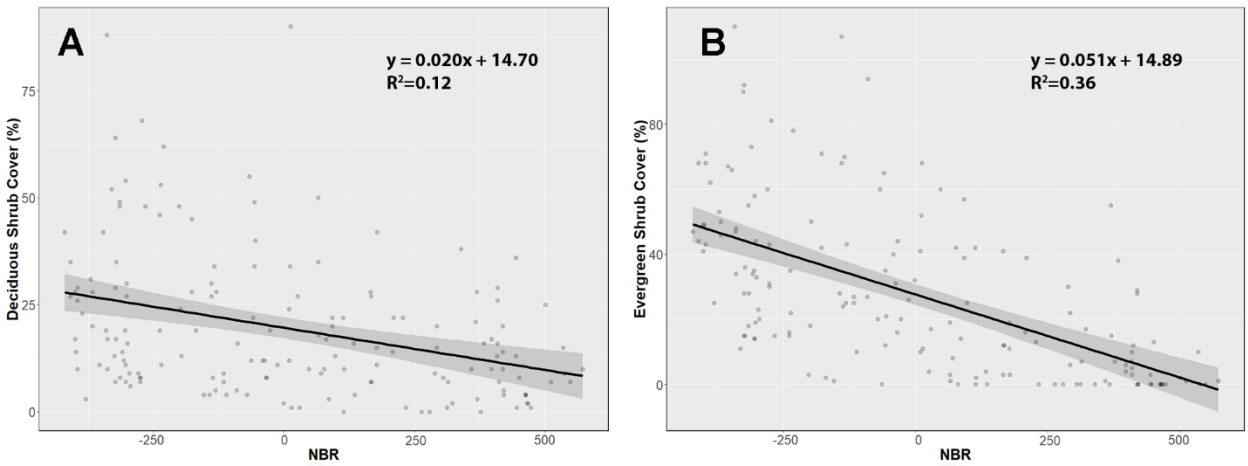

Figure 2.4 Linear fit of relationships between NBR and (A) deciduous shrubs, and (B) evergreen shrubs. The solid lines show the linear fit and the gray shaded area represents the standard error.

2.3.2 Edaphic Response

The MDS ordination (Fig. 2.2) indicates major shifts in community composition with burn severity, and these were associated with various abiotic factors (Appendix C), including decreased organic thickness and increased thaw depth, bare ground, electrical conductivity and micronutrient concentrations (Ca^{2+}, $SO4^{-}$, Na^{-}, Mg^{2+}).

Thaw depth was highly variable (Range: 13.6-103.0 cm) but exhibited a significant positive relationship with burn severity (Fig. 2.5A), and least square mean thaw depth at severely burned sites was 12 cm higher than at unburned sites (Fig. 2.5A). Organic layer thickness was also highly variable (Range: 0-40 cm) but was deepest at unburned controls and shallowest at severely burned sites, where, average organic thickness was 4 cm shallower than unburned controls (Fig. 2.5B). Thaw depth was inversely related to organic layer thickness and increased by approximately 1 cm for every 1 cm decrease in organic layer depth (Fig. 2.5C). Soil moisture was variable across all sites but was generally higher when thaw depth was shallower (Fig. 2.5D).

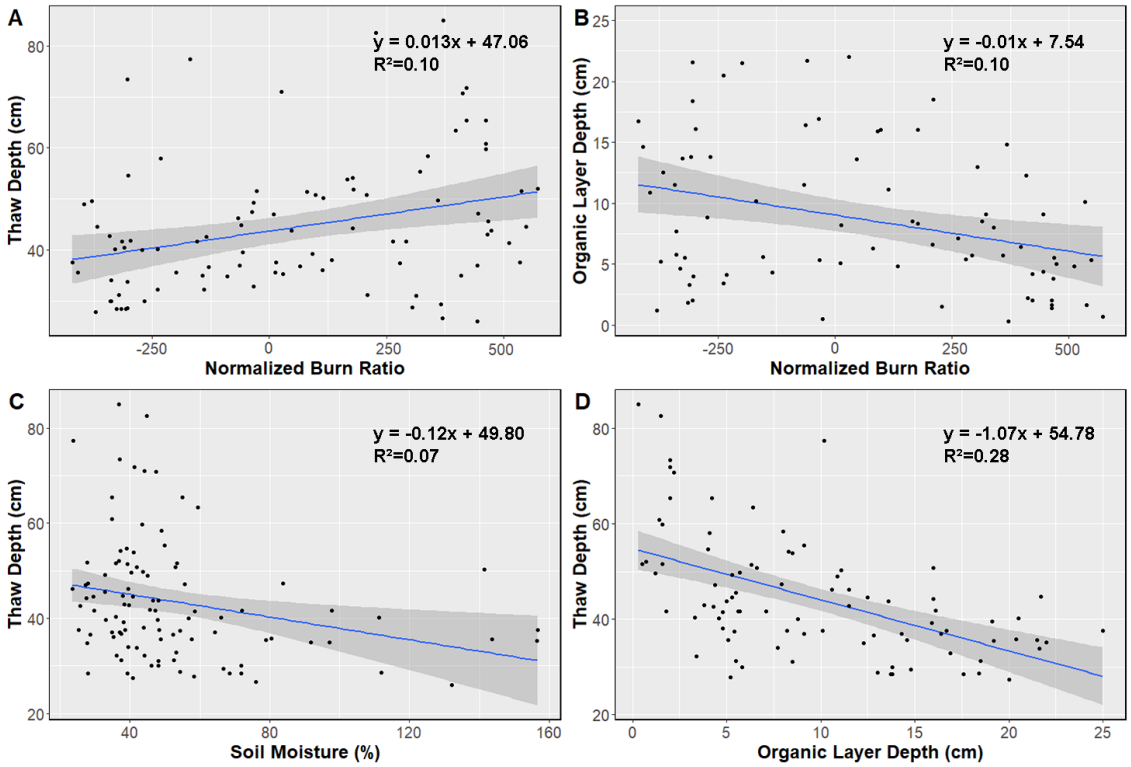

Figure 2.5 Linear fit of relationships between: (A) thaw depth and post-fire Normalized Burn Ratio, (B) organic layer depth and post-fire Normalized Burn Ratio, (C) thaw depth and organic layer depth, and (D) thaw depth and soil moisture. The solid lines show the linear fit and the gray shaded area represents the standard error.

Average ground surface soil temperature was consistently higher at severely burned sites compared to unburned control sites (Fig. 2.6A). This difference was largest in late June, when average temperature across burned sites was up to approximately 12°C higher than adjacent unburned control sites (Fig. 2.6A). Differences in soil temperatures between burned and unburned sites were also apparent at 1 meter below the surface (Fig. 2.6), where the average date of freeze-back was close to a month (Dec. 1st) later in severely burned sites compared to unburned controls (Nov. 4th). Severely burned sites also exhibited an early increase in spring temperature at the ground surface and the top of permafrost compared to controls (Fig. 2.6).

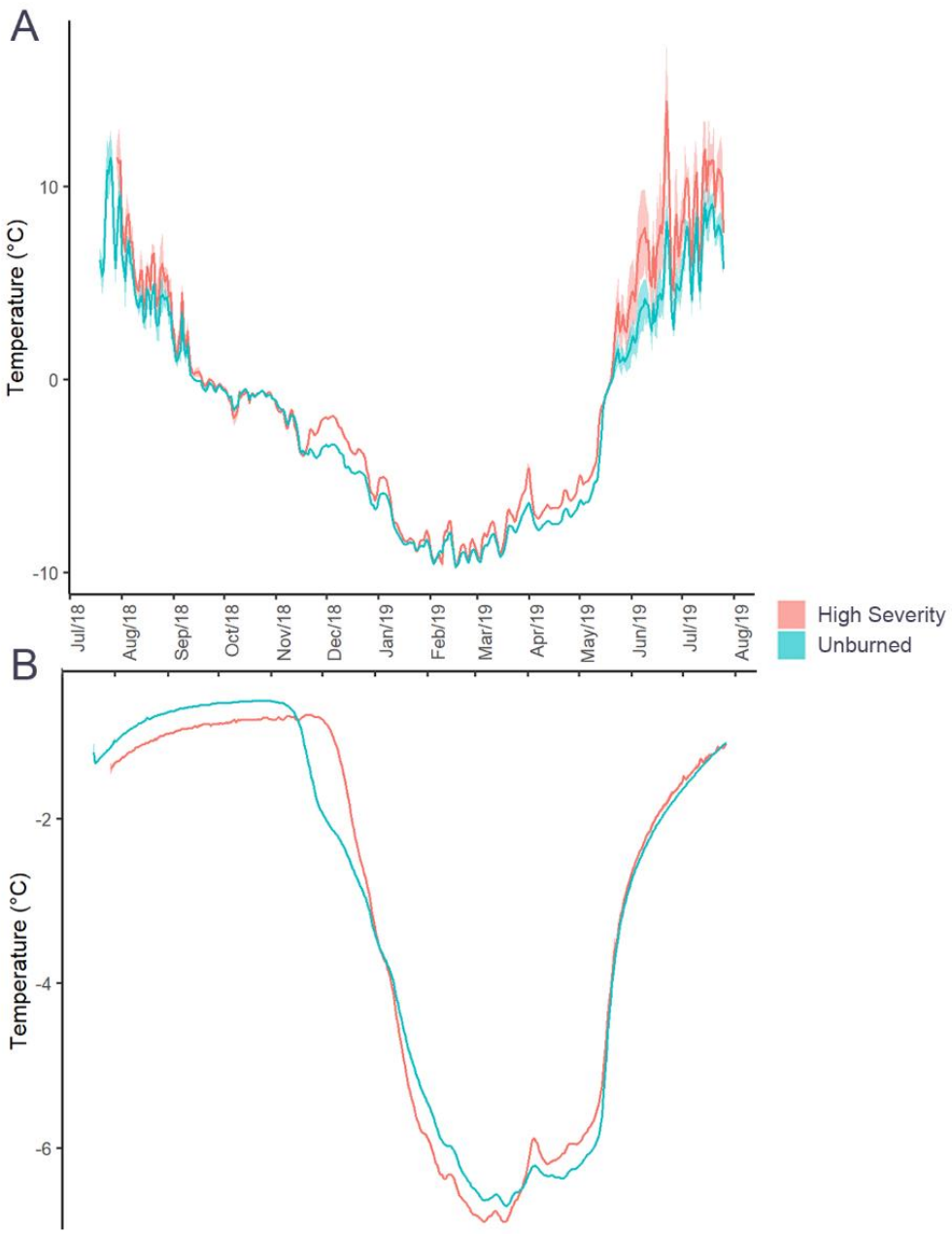

Figure 2.6 Mean daily temperatures at severely burned sites (red line) and unburned sites (blue lines) where thermistors were installed: (A) at the ground surface (5 cm below surface) and (B) at the top of permafrost (100 cm below surface)

2.4 Discussion

Our analysis shows that the impact of tundra fire depends on burn severity, which must be high enough to kill aboveground meristems and reduce the surface organic layer to affect

vegetation and soil conditions. The similarity of plant community composition at moderately burned and unburned sites shows that tundra vegetation structure is resilient to lower severity fire. However, where fire was severe, community composition and abiotic conditions were distinct from unburned and moderately burned areas. The persistence of thermal changes six years following fire also indicates that severe tundra fire can initiate positive feedbacks impacting abiotic conditions. Higher ground temperatures at severely burned sites can be attributed to increased ground heat flux in the summer (Nossov et al., 2013) following the partial combustion of the soil organic layer. Higher burn severity was associated with the loss of surface cover and organics, which increased thaw depths, and extended the thaw season by reducing surface insulation and albedo (Figs. 2.5 and 2.6). These increases in thaw depths are noteworthy because they may exacerbate long-term carbon loss by accelerating decomposition rates (O'Donnell et al., 2011; Racine et al., 2004). Thermal recovery can take decades following tundra fire (Jiang et al., 2015), and when the disturbance is severe, it can also facilitate thermal erosion (Chipman and Hu, 2017), and thermokarst development (Jones et al., 2015; Mackay, 1995).

Our observations of community composition and soils in areas where tundra burning was severe show that shrub tundra has been recovering rapidly and suggests that ongoing succession may promote shrub dominance, as many studies indicate (Higuera et al., 2008; Jones et al., 2009; Racine et al., 2004). After six years, the cover of shrubs was still lower in areas of severe burning (Figs. 3 and 4), but our observations, combined with previous studies, suggest that full recovery of shrub cover is likely to occur within several decades. Ultimately, ongoing monitoring is required to track successional change and test this prediction. Fire destroyed most to all aboveground vegetation at severely burned sites, but

recovery was rapid at these sites. Our field observations indicate that the rapid recovery of vegetation at our study sites was driven by the sprouting of near-surface buds, which is a common reproductive strategy for tundra species following disturbance (Au Yeung and Li, 2018; Bret-Harte et al., 2013; Wein and Bliss, 1973). Previous tundra fire recovery studies have shown that re-sprouting can return aboveground cover to pre-fire levels within a few years (Au Yeung and Li, 2018; Racine et al., 2004).

The rapid recovery of deciduous shrubs particularly in areas where fire consumed most aboveground biomass suggests that succession may result in the dominance of these species relative to other vegetation. Aboveground biomass of deciduous shrubs such as *Betula glandulosa* and *Vaccinium uliginosum* is typically destroyed by fire, but can recover quickly via re-sprouting and exceed pre-fire abundance (De Groot and Wein, 2004; Dyrness and Norum, 1983; Wein and Bliss, 1973). Sprouting can occur from dormant buds on root crowns and rhizomes (De Groot, 1998; Zasada, 1986), which facilitates rapid regeneration after fire, even when burning is severe (De Groot and Wein, 2004).

Previous studies have shown that tundra disturbances that reduce or remove organic soils can also promote the dominance of deciduous shrubs (Gibson et al., 2016; Johnstone, Chapin, et al., 2010; Landhausser and Wein, 1993; Lantz et al., 2009, 2010; Racine et al., 2004). Increased thaw depth at severely burned sites was also associated with higher concentrations of soluble nutrients (Ca^{2+}, $SO4^{-}$, Na^{-}, Mg^{2+}), which has been linked to rapid increases in aboveground biomass of deciduous shrubs (Hu et al., 2015; Lantz et al., 2009; Wein and Bliss, 1973). Tundra shrubs, particularly *Betula glandulosa* show increased stem biomass, density, and dominance over graminoid species in response to increased thaw depth, pH and nutrient availability (Ca^{2+}, $SO4^{-}$) (Abbott and Jones, 2015; Lantz et al., 2009;

Schuur et al., 2007) and in greenhouse treatments where below and aboveground temperatures have increased (Bret-Harte et al., 2001; Bret-Harte et al., 2004; Shaver et al., 2001).

At our sites severe burning suppressed lichen and evergreen shrub cover, but promoted the rapid establishment of graminoids and "weedy" herbs such as *Chamerion angustifolium* and *Senecio congestus*, which may also facilitate abiotic conditions that favor deciduous shrub dominance in the long-term. In the subarctic, the dominance of herb and graminoid understories in early succession following fire accelerates nutrient cycling, which limits organic layer development and promotes the development of deciduous shrub communities that are better adapted to shallow organic layers (Chapin et al., 1996; Gibson et al., 2016; Johnstone, Chapin, et al., 2010).

The greater decline in evergreen shrub cover relative to deciduous shrub cover that we observed with increasing burn severity was likely driven by high plant and seed mortality, which prevented re-sprouting in this functional group. *Vaccinium vitis-idaea* typically regrows after disturbance via resprouting from aerial stems (Viereck and Schandelmeier, 1980). While this can allow quick recovery under light to moderate severity fire (Racine et al., 2004), when high severity fire destroys aboveground stems the recovery of *Vaccinium vitis-idaea* is limited (Racine, 1981). The post-fire recovery of evergreen shrubs such as *Vaccinium vitis-idaea*, *Ledum decumbens*, and *Empetrum nigrum* can take decades because of dispersal limitation and the requirement of an organic seedbed (Bell and Tallis, 1973; Landhausser and Wein, 1993; Viereck and Schandelmeier, 1980).

Our observation that changes in community composition and soil conditions were greatest in areas of severe burning indicates that the nature of tundra recovery is a function of disturbance severity. Although short-term recovery at severely burned sites differed from areas of moderate fire, our observations suggest that the fires we sampled were not severe enough to facilitate the development of novel successional trajectories as has been observed in the subarctic, but additional study on higher severity fires over longer timeframes is needed for this to be conclusive (Hollingsworth et al., 2013; Johnstone, Chapin, et al., 2010; Landhausser and Wein, 1993; Lantz et al., 2010).

Modelling suggests that climate warming will decrease the tundra fire return interval to less than 200 years, a level unprecedented in the Holocene (Young et al., 2017). As warming increases the severity of fire, it is possible that fires will become severe enough to drive the total combustion of soil organic layer and promote altered successional trajectories where resprouting recovery is overtaken by the establishment of new seedlings (Hollingsworth et al., 2013), but additional study is needed. Modelling of vegetation succession indicates that increasing burn severity can lead to the long-term replacement of shrub tundra by graminoid tundra (Barrett et al., 2012). Conversely, palynological studies indicate that during the mid-Holocene shrub tundra landscapes dominated by *Betula glandulosa* burned as frequently (~144 years) as modern northern boreal black spruce landscapes (Higuera et al., 2008, 2011). Given the potential impacts of widespread changes in tundra vegetation structure on regional and global ecological processes, such as hydrology (Drake et al., 2019), global carbon storage (Christiansen et al., 2018; Schuur et al., 2015), and permafrost dynamics (Blok et al., 2011; Wilcox et al., 2019), additional research on the long-term effects of tundra fire is critical. The limited availability of reliable

data on tundra wildfire has made it difficult to document the effects of severe fire on tundra. Remote sensing and plot-based monitoring should be used to assess how landscapes will change in the decades following disturbance. The fine-scale variation in tundra terrain requires that future research utilize very high spatial resolution data. The emergence of hyperspectral remote sensing and very-high resolution platforms, such as microsatellites and unmanned aerial systems (Fraser et al., 2017), which can quantify high resolution burn severity provides an exciting opportunity to examine landscape-scale successional responses following tundra fire and other disturbances.

Bibliography

Abbott, B.W., Jones, J. B., Schuur, E. A. G., Chapin Iii, F. S., Bowden, W. B., Bret-Harte, M. S., Epstein, H. E., Flannigan, M. D., Harms, T. K., Hollingsworth, T. N., Mack, M. C., McGuire, A. D., Natali, S. M., Rocha, A. V., Tank, S. E., Turetsky, M. R., Vonk, J. E., Wickland, K. P., Aiken, G. R., … Zimov, S. (2016). Biomass offsets little or none of permafrost carbon release from soils, streams, and wildfire: An expert assessment. *Environmental Research Letters*, *11*(3). https://doi.org/10.1088/1748-9326/11/3/034014

Abbott, Benjamin W., and Jones, J. B. (2015). Permafrost collapse alters soil carbon stocks, respiration, CH4 , and N 2O in upland tundra. *Global Change Biology*, *21*(12), 4570–4587. https://doi.org/10.1111/gcb.13069

Allen, J. L., and Sorbel, B. (2008). Assessing the differenced Normalized Burn Ratio's ability to map burn severity in the boreal forest and tundra ecosystems of Alaska's national parks. *International Journal of Wildland Fire*, *17*, 463–475. https://doi.org/10.1071/WF08034

Au Yeung, C., and Li, R. (2018). Comparison of vegetation regeneration after wildfire between Mediterranean and tundra ecosystems by using Landsat images. *Annals of GIS*, *24*(2), 99–112. https://doi.org/10.1080/19475683.2018.1424740

Bates, D., Mächler, M., Bolker, B., and Walker, S. (2015). Fitting Linear Mixed-Effects Models Using {lme4}. *Journal of Statistical Software*, *67*(1), 1–48. https://doi.org/10.18637/jss.v067.i01

Bell, J. N. B., and Tallis, J. H. (1973). Empetrum Nigrum L. *The Journal of Ecology*, *61*(1), 289. https://doi.org/10.2307/2258934

Blok, D., Schaepman-Strub, G., Bartholomeus, H., Heijmans, M. P. D., Maximov, T. C., and Berendse, F. (2011). The response of Arctic vegetation to the summer climate: Relation between shrub cover, NDVI, surface albedo and temperature. *Environmental Research Letters*, *6*(3). https://doi.org/10.1088/1748-9326/6/3/035502

Bret-Harte, M. S., Mack, M. C., Shaver, G. R., Huebner, D. C., Johnston, M., Mojica, C. A., Pizano, C., and Reiskind, J. A. (2013). The response of Arctic vegetation and soils following an unusually severe tundra fire. *Philosophical Transactions of the Royal Society B: Biological Sciences*, *368*(1624). https://doi.org/10.1098/rstb.2012.0490

Bret-Harte, S. M., Garcia, E. A., Sacre, V. M., Whorley, J. R., Wagner, J. L., Lippert, S. C., and Chapin, S. F. (2004). Plant and soil responses to neighbour removal and fertilization in Alaskan tussock tundra. *Journal of Ecology*, *92*(4), 635–647. https://doi.org/10.1111/j.0022-0477.2004.00902.x

Bret-Harte, S. M., Shaver, G. R., Zoerner, J. P., Johnstone, J. F., Wagner, J. L., Chavez,

A. S., Gunkelman IV, R. F., Lippert, S. C., and Laundre, J. A. (2001). Developmental plasticity allows betula nana to dominate tundra subjected to an altered environment. *Ecology*, *82*(1), 18–32. https://doi.org/10.1890/0012-9658(2001)082[0018:dpabnt]2.0.co;2

Brown, C. D., and Johnstone, J. F. (2011). *How does increased fire frequency affect carbon loss from fire? A case study in the northern boreal forest*. https://doi.org/10.1071/WF10113

Burn, C. R., and Kokelj, S. V. (2009). The environment and permafrost of the Mackenzie Delta area. *Permafrost and Periglacial Processes*, *20*(2), 83–105. https://doi.org/10.1002/ppp.655

Bush, E., and Lemmen, D. S. (2019). *Canada's Changing Climate Report*. http://www.changingclimate.ca/CCCR2019

Chapin, F. S., Bret-Harte, M. S., Hobbie, S. E., and Zhong, H. (1996). Plant functional types as predictors of transient responses of arctic vegetation to global change. *Journal of Vegetation Science*, *7*(3), 347–358. https://doi.org/10.2307/3236278

Chen, X., and Huang, C. (2008). *Use of multiple spectral indices to estimate burn severity in the Black Hills of South Dakota*. https://www.researchgate.net/publication/229043901

Chipman, M. L., and Hu, F. S. (2017). Linkages Among Climate, Fire, and Thermoerosion in Alaskan Tundra Over the Past Three Millennia. *Journal of Geophysical Research: Biogeosciences*. https://doi.org/10.1002/2017JG004027

Christiansen, C. T., Lafreniére, M. J., Henry, G. H. R., and Grogan, P. (2018). Long-term deepened snow promotes tundra evergreen shrub growth and summertime ecosystem net CO_2 gain but reduces soil carbon and nutrient pools. *Global Change Biology*, *24*(8), 3508–3525. https://doi.org/10.1111/gcb.14084

Clarke, K., and Gorley, R. N. (2006). Primer v6: User Manual/Tutorial. In *PRIMER-E*.

De Groot, W. J. (1998). *Fire ecology of betula glandulosa Michx.* [Univeristy of Alberta]. https://doi.org/10.7939/R3CN6Z51D

De Groot, W. J., and Wein, R. W. (2004). Effects of fire severity and season of burn on Betula glandulosa growth dynamics. *International Journal of Wildland Fire*, *13*(3), 287–295. https://doi.org/10.1071/WF03048

Drake, T. W., Holmes, R. M., Zhulidov, A. V., Gurtovaya, T., Raymond, P. A., McClelland, J. W., and Spencer, R. G. M. (2019). Multidecadal climate-induced changes in Arctic tundra lake geochemistry and geomorphology. *Limnology and Oceanography*, *64*(S1), S179–S191. https://doi.org/10.1002/lno.11015

Dyrness, C. T., and Norum, R. A. (1983). The effects of experimental fires on black

spruce forest floors in interior Alaska. *Canadian Journal of Forest Research*, *13*(5), 879–893. https://doi.org/10.1139/x83-118

Epting, J., Verbyla, D., and Sorbel, B. (2005). Evaluation of remotely sensed indices for assessing burn severity in interior Alaska using Landsat TM and ETM+. *Remote Sensing of Environment*, *96*(3–4), 328–339. https://doi.org/10.1016/J.RSE.2005.03.002

Fang, L., and Yang, J. (2014). Atmospheric effects on the performance and threshold extrapolation of multi-temporal Landsat derived dNBR for burn severity assessment. *International Journal of Applied Earth Observation and Geoinformation*, *33*(1), 10–20. https://doi.org/10.1016/j.jag.2014.04.017

Fauchald, P., Park, T., Tømmervik, H., Myneni, R., and Hausner, V. H. (2017). Arctic greening from warming promotes declines in caribou populations. *Science Advances*, *3*(4), e1601365. https://doi.org/10.1126/sciadv.1601365

Fraser, R., van der Sluijs, J., and Hall, R. (2017). Calibrating Satellite-Based Indices of Burn Severity from UAV-Derived Metrics of a Burned Boreal Forest in NWT, Canada. *Remote Sensing*, *9*(3), 279. https://doi.org/10.3390/rs9030279

Frost, G. V., Loehman, R. A., Saperstein, L. B., Macander, M. J., Nelson, P. R., Paradis, D. P., and Natali, S. M. (2020). Multi-decadal patterns of vegetation succession after tundra fire on the Yukon-Kuskokwim Delta, Alaska. In *Environmental Research Letters* (Vol. 15, Issue 2, p. 025003). Institute of Physics Publishing. https://doi.org/10.1088/1748-9326/ab5f49

García, M. J. L., and Caselles, V. (1991). Mapping burns and natural reforestation using thematic Mapper data. *Geocarto International*, *6*(1), 31–37. https://doi.org/10.1080/10106049109354290

Gartner, B. L., Chapin Iii, F. S., and Shavert, G. R. (1986). Reproduction of Eriophorum Vaginatu by Seed in Alaskan Tussock Tundra. *Journal of Ecology*, *74*(1), 1–18. https://doi.org/https://doi.org/10.2307/2260345

Gibson, C. M., Turetsky, M. R., Cottenie, K., Kane, E. S., Houle, G., and Kasischke, E. S. (2016). Variation in plant community composition and vegetation carbon pools a decade following a severe fire season in interior Alaska. *Journal of Vegetation Science*, *27*(6), 1187–1197. https://doi.org/10.1111/jvs.12443

Gustine, D. D., Brinkman, T. J., Lindgren, M. A., Schmidt, J. I., Rupp, T. S., and Adams, L. G. (2014). Climate-Driven Effects of Fire on Winter Habitat for Caribou in the Alaskan-Yukon Arctic. *PLoS ONE*, *9*(7), e100588. https://doi.org/10.1371/journal.pone.0100588

Hanes, C. C., Wang, X., Jain, P., Parisien, M.-A., Little, J. M., and Flannigan, M. D. (2019). Fire-regime changes in Canada over the last half century. *Canadian Journal of Forest Research*, *49*(3), 256–269. https://doi.org/10.1139/cjfr-2018-0293

He, Y., DeSutter, T., Prunty, L., Hopkins, D., Jia, X., and Wysocki, D. A. (2012). Evaluation of 1:5 soil to water extract electrical conductivity methods. *Geoderma, 185–186*, 12–17. https://doi.org/10.1016/j.geoderma.2012.03.022

Hernandez, H. (1973). Natural plant recolonization of surficial disturbances, Tuktoyaktuk Peninsula Region, Northwest Territories. *Canadian Journal of Botany*, *51*(11), 2177–2196. https://doi.org/10.1139/b73-280

Higuera, P. E., Brubaker, L. B., Anderson, P. M., Brown, T. A., Kennedy, A. T., and Hu, F. S. (2008). Frequent fires in ancient shrub tundra: implications of paleorecords for arctic environmental change. *PloS One*, *3*(3), e0001744. https://doi.org/10.1371/journal.pone.0001744

Higuera, P. E., Chipman, M. L., Barnes, J. L., Urban, M. A., and Hu, F. S. (2011). Variability of tundra fire regimes in Arctic Alaska: millennial-scale patterns and ecological implications. *Ecological Applications*, *21*(8), 3211–3226. https://doi.org/10.1890/11-0387.1

Hijmans, R. J. (2019). *raster: Geographic Data Analysis and Modeling*. https://cran.r-project.org/package=raster

Holling, C. S. (1973). Resilience and Stability of Ecological Systems. *Annual Review of Ecology and Systematics*, *4*(1), 1–23. https://doi.org/10.1146/annurev.es.04.110173.000245

Hollingsworth, T. N., Johnstone, J. F., Bernhardt, E. L., and Chapin, F. S. (2013). Fire Severity Filters Regeneration Traits to Shape Community Assembly in Alaska's Boreal Forest. *PLoS ONE*, *8*(2), e56033. https://doi.org/10.1371/journal.pone.0056033

Hu, F. S., Higuera, P. E., Duffy, P., Chipman, M. L., Rocha, A. V, Young, A. M., Kelly, R., and Dietze, M. C. (2015). Arctic tundra fires: natural variability and responses to climate change. *Frontiers in Ecology and the Environment*, *13*(7), 369–377. https://doi.org/10.1890/150063

Jafarov, E. E., Romanovsky, V. E., Genet, H., McGuire, A. D., and Marchenko, S. S. (2013). The effects of fire on the thermal stability of permafrost in lowland and upland black spruce forests of interior Alaska in a changing climate. *Environmental Research Letters*, *8*(3), 035030. https://doi.org/10.1088/1748-9326/8/3/035030

Jandt, R., Joly, K., Meyers, C. R., and Racine, C. (2008). Slow Recovery of Lichen on Burned Caribou Winter Range in Alaska Tundra: Potential Influences of Climate Warming and Other Disturbance Factors. *Source: Arctic, Antarctic, and Alpine Research*, *40*(1), 89–95. http://www.jstor.org/stable/20181768

Jandt, R. R., Miller, E. A., Yokel, D. A., Bret-Harte, M. S., Kolden, C. A., and Mack, M. C. (2012). *Findings of Anaktuvuk River Fire Recovery Study*.

Jia, G. J., Epstein, H. E., and Walker, D. A. (2009). Vegetation greening in the canadian arctic related to decadal warming. *Journal of Environmental Monitoring*, *11*(12), 2231–2238. https://doi.org/10.1039/b911677j

Jiang, Y., Rocha, A. V., O'Donnell, J. A., Drysdale, J. A., Rastetter, E. B., Shaver, G. R., and Zhuang, Q. (2015). Contrasting soil thermal responses to fire in Alaskan tundra and boreal forest. *Journal of Geophysical Research: Earth Surface*, *120*(2), 363–378. https://doi.org/10.1002/2014JF003180

Johnstone, J. F., and Chapin, F. S. (2006). Effects of Soil Burn Severity on Post-Fire Tree Recruitment in Boreal Forest. *Ecosystems*, *9*(1), 14–31. https://doi.org/10.1007/s10021-004-0042-x

Johnstone, J. F., Chapin, S. F., Hollingsworth, T. N., Mack, M. C., Romanovsky, V., and Turetsky, M. (2010). Fire, climate change, and forest resilience in interior alaska1. *Canadian Journal of Forest Research*, *40*(7), 1302–1312. https://doi.org/10.1139/X10-061

Johnstone, J. F., Hollingsworth, T. N., Chapin, F. S., and Mack, M. C. (2010). Changes in fire regime break the legacy lock on successional trajectories in Alaskan boreal forest. *Global Change Biology*, *16*(4), 1281–1295. https://doi.org/10.1111/j.1365-2486.2009.02051.x

Joly, K., Jandt, R. R., and Klein, D. R. (2009). Decrease of lichens in Arctic ecosystems: the role of wildfire, caribou, reindeer, competition and climate in north-western Alaska. *Polar Research*, *28*(3), 433–442. https://doi.org/10.1111/j.1751-8369.2009.00113.x

Jones, B. M., Grosse, G., Arp, C. D., Miller, E., Liu, L., Hayes, D. J., and Larsen, C. F. (2015). Recent Arctic tundra fire initiates widespread thermokarst development. *Scientific Reports*, *5*, 15865. https://doi.org/10.1038/srep15865

Jones, B. M., Kolden, C. A., Jandt, R., Abatzoglou, J. T., Urban, F., and Arp, C. D. (2009). Fire Behavior, Weather, and Burn Severity of the 2007 Anaktuvuk River Tundra Fire, North Slope, Alaska. *Arctic, Antarctic, and Alpine Research*, *41*(3), 309–316. https://doi.org/10.1657/1938-4246-41.3.309

Keeley, J. E., Brennan, T., and Pfaff, A. H. (2008). FIRE SEVERITY AND ECOSYTEM RESPONSES FOLLOWING CROWN FIRES IN CALIFORNIA SHRUBLANDS. *Ecological Applications*, *18*(6), 1530–1546. https://doi.org/10.1890/07-0836.1

Kelly, R., Chipman, M. L., Higuera, P. E., Stefanova, I., Brubaker, L. B., and Hu, F. S. (2013). Recent burning of boreal forests exceeds fire regime limits of the past 10,000 years. *Proceedings of the National Academy of Sciences of the United States of America*, *110*(32), 13055–13060. https://doi.org/10.1073/pnas.1305069110

Kenward, M. G., and Roger, J. H. (1997). Small Sample Inference for Fixed Effects from Restricted Maximum Likelihood. *Biometrics*, *53*(3), 983.

https://doi.org/10.2307/2533558

Key, C. H., and Benson, N. C. (1999). Measuring and Remote Sensing of Burn Severity. *Proceedings Joint Fire Science Conference and Workshop*. https://www.researchgate.net/publication/241687936_Measuring_and_remote_sensing_of_burn_severity_the_CBI_and_NBR

Key, C. H., and Benson, N. C. (2006). *LA-1 Landscape Assessment (LA) Sampling and Analysis Methods*. https://www.fs.fed.us/rm/pubs/rmrs_gtr164/rmrs_gtr164_13_land_assess.pdf

Klaustermeier, A., Tomlinson, H., Daigh, A. L. M., Limb, R., DeSutter, T., and Sedivec, K. (2016). Comparison of soil-to-water suspension ratios for determining electrical conductivity of oil-productionwater-contaminated soils. *Canadian Journal of Soil Science*, *96*(2), 233–243. https://doi.org/10.1139/cjss-2015-0097

Kokelj, S. V, Palmer, M. J., Lantz, T. C., and Burn, C. R. (2017). *Ground Temperatures and Permafrost Warming from Forest to Tundra, Tuktoyaktuk Coastlands and Anderson Plain, NWT, Canada*. https://doi.org/10.1002/ppp.1934

Kolden, C. A., and Rogan, J. (2013). Mapping Wildfire Burn Severity in the Arctic Tundra from Downsampled MODIS Data. *Source: Arctic, Antarctic, and Alpine Research Published By: Institute of Arctic and Alpine Research Arctic, Antarctic, and Alpine Research*, *45*(1), 64–76. https://doi.org/10.1657/1938-4246-45.1.64

Landhausser, S. M., and Wein, R. W. (1993). Postfire Vegetation Recovery and Tree Establishment at the Arctic Treeline: Climate-Change-Vegetation-Response Hypotheses. *The Journal of Ecology*, *81*(4), 665. https://doi.org/10.2307/2261664

Lantz, T. C., Gergel, S. E., and Henry, G. H. R. (2010). Response of green alder (Alnus viridis subsp. fruticosa) patch dynamics and plant community composition to fire and regional temperature in north-western Canada. *Journal of Biogeography*, *37*(8), no-no. https://doi.org/10.1111/j.1365-2699.2010.02317.x

Lantz, T. C., Kokelj, S. V., Gergel, S. E., and Henry, G. H. R. (2009). Relative impacts of disturbance and temperature: persistent changes in microenvironment and vegetation in retrogressive thaw slumps. *Global Change Biology*, *15*(7), 1664–1675. https://doi.org/10.1111/j.1365-2486.2009.01917.x

Lantz, T. C., Marsh, P., and Kokelj, S. V. (2013a). Recent Shrub Proliferation in the Mackenzie Delta Uplands and Microclimatic Implications. *Ecosystems*, *16*(1), 47–59. https://doi.org/10.1007/s10021-012-9595-2

Lantz, T. C., Marsh, P., and Kokelj, S. V. (2013b). Recent Shrub Proliferation in the Mackenzie Delta Uplands and Microclimatic Implications. *Ecosystems*, *16*(1), 47–59. https://doi.org/10.1007/s10021-012-9595-2

Mack, M. C., Bret-Harte, S. M., Hollingsworth, T. N., Jandt, R. R., Schuur, E. A. G.,

Shaver, G. R., and Verbyla, D. L. (2011). Carbon loss from an unprecedented Arctic tundra wildfire. *Nature*, *475*. https://doi.org/10.1038/nature10283

Mackay, J. (1995). Active Layer Changes (1968 to 1993) Following the Forest-Tundra Fire near Inuvik, N.W.T., Canada. *Arctic and Alpine Research*, *27*(4), 323–336. http://www.jstor.org/stable/1552025

Miller, J. D., Knapp, E. E., Key, C. H., Skinner, C. N., Isbell, C. J., Creasy, R. M., and Sherlock, J. W. (2009). Calibration and validation of the relative differenced Normalized Burn Ratio (RdNBR) to three measures of fire severity in the Sierra Nevada and Klamath Mountains, California, USA. *Remote Sensing of Environment*, *113*(3), 645–656. https://doi.org/10.1016/j.rse.2008.11.009

Moffat, N. D., Lantz, T. C., Fraser, R. H., and Olthof, I. (2016). Recent Vegetation Change (1980–2013) in the Tundra Ecosystems of the Tuktoyaktuk Coastlands, NWT, Canada. *Arctic, Antarctic, and Alpine Research*. https://doi.org/10.1657/AAAR0015-063

Moritz, M. A., Parisien, M.-A., Batllori, E., Krawchuk, M. A., Van Dorn, J., Ganz, D. J., and Hayhoe, K. (2012). Climate change and disruptions to global fire activity. *Ecosphere*, *3*(6), art49. https://doi.org/10.1890/es11-00345.1

Moskovchenko, D. V., Aref'ev, S. P., Moskovchenko, M. D., and Yurtaev, A. A. (2020). Spatiotemporal Analysis of Wildfires in the Forest Tundra of Western Siberia. *Contemporary Problems of Ecology*, *13*(2), 193–203. https://doi.org/10.1134/S1995425520020092

Narita, K., Harada, K., Saito, K., Sawada, Y., Fukuda, M., and Tsuyuzaki, S. (2015). Vegetation and Permafrost Thaw Depth 10 Years after a Tundra Fire in 2002, Seward Peninsula, Alaska. *Arctic, Antarctic, and Alpine Research*, *47*(3), 547–559. https://doi.org/10.1657/AAAR0013-031

Nossov, D. R., Torre Jorgenson, M., Kielland, K., and Kanevskiy, M. Z. (2013). Edaphic and microclimatic controls over permafrost response to fire in interior Alaska. *Environmental Research Letters*, *8*(3), 035013. https://doi.org/10.1088/1748-9326/8/3/035013

O'Donnell, J. A., Harden, J. W., McGuire, A. D., and Romanovsky, V. E. (2011). Exploring the sensitivity of soil carbon dynamics to climate change, fire disturbance and permafrost thaw in a black spruce ecosystem. *Biogeosciences*, *8*, 1367–1382. https://www.biogeosciences.net/8/1367/2011/bg-8-1367-2011.pdf

Oksanen, J., Blanchet, F. G., Friendly, M., Kindt, R., Legendre, P., McGlinn, D., Minchin, P. R., O'Hara, R. B., Simpson, G. L., Solymos, P., Stevens, M. H. H., Szoecs, E., and Wagner, H. (2019). *vegan: Community Ecology Package*. https://cran.r-project.org/package=vegan

Ovenden, L., and Brassard, G. R. (1989). Wetland vegetation near Old Crow, northern

Yukon. *Canadian Journal of Botany*, *67*(4), 954–960. https://doi.org/10.1139/b89-127

R Core Team. (2018). *R: A Language and Environment for Statistical Computing*. https://www.r-project.org/

Racine, C. H. (1981). Tundra Fire Effects on Soils and Three Plant Communities Along a Hill-Slope Gradient in the Seward Peninsula, Alaska. *ARCTIC*, *34*(1), 71–84. https://doi.org/10.14430/arctic2508

Racine, C., Jandt, R., Meyers, C., and Dennis, J. (2004). Tundra Fire and Vegetation Change along a Hillslope on the Seward Peninsula, Alaska, U.S.A. *Source: Arctic, Antarctic, and Alpine Research Arctic, Antarctic, and Alpine Research*, *36*(1), 1–10. http://www.jstor.org/stable/1552423

Rocha, A. V., Loranty, M. M., Higuera, P. E., MacK, M. C., Hu, F. S., Jones, B. M., Breen, A. L., Rastetter, E. B., Goetz, S. J., and Shaver, G. R. (2012). The footprint of Alaskan tundra fires during the past half-century: Implications for surface properties and radiative forcing. *Environmental Research Letters*, *7*(4), 044039. https://doi.org/10.1088/1748-9326/7/4/044039

Rocha, A. V., and Shaver, G. R. (2011). Burn severity influences postfire CO2 exchange in arctic tundra. *Ecological Applications*, *21*(2), 477–489. https://doi.org/10.1890/10-0255.1

Ropars, P., and Boudreau, S. (2012). Shrub expansion at the foresttundra ecotone: Spatial heterogeneity linked to local topography. *Environmental Research Letters*, *7*(1). https://doi.org/10.1088/1748-9326/7/1/015501

Sae-Lim, J., Russell, J. M., Vachula, R. S., Holmes, R. M., Mann, P. J., Schade, J. D., and Natali, S. M. (2019). Temperature-controlled tundra fire severity and frequency during the last millennium in the Yukon-Kuskokwim Delta, Alaska. *The Holocene*, *29*(7), 1223–1233. https://doi.org/10.1177/0959683619838036

SAS Institute. (2015). *Base SAS 9.4 procedures guide.* SAS Institute.

Schuur, E. A.G., McGuire, A. D., Schädel, C., Grosse, G., Harden, J. W., Hayes, D. J., Hugelius, G., Koven, C. D., Kuhry, P., Lawrence, D. M., Natali, S. M., Olefeldt, D., Romanovsky, V. E., Schaefer, K., Turetsky, M. R., Treat, C. C., and Vonk, J. E. (2015). Climate change and the permafrost carbon feedback. In *Nature* (Vol. 520, Issue 7546, pp. 171–179). Nature Publishing Group. https://doi.org/10.1038/nature14338

Schuur, Edward A.G., Crummer, K. G., Vogel, J. G., and MacK, M. C. (2007). Plant species composition and productivity following permafrost thaw and thermokarst in Alaskan tundra. *Ecosystems*, *10*(2), 280–292. https://doi.org/10.1007/s10021-007-9024-0

Shaver, G. R., Syndonia Bret-Harte, M., Jones, M. H., Johnstone, J., Gough, L., Laundre, J., and Stuart Chapin, F. (2001). Species composition interacts with fertilizer to control long-term change in tundra productivity. *Ecology*, *82*(11), 3163–3181. https://doi.org/10.1890/0012-9658(2001)082[3163:SCIWFT]2.0.CO;2

Swann, A. L., Fung, I. Y., Levis, S., Bonan, G. B., and Doney, S. C. (2010). Changes in arctic vegetation amplify high-latitude warming through the greenhouse effect. *Proceedings of the National Academy of Sciences of the United States of America*, *107*(4), 1295–1300. https://doi.org/10.1073/pnas.0913846107

Timoney, K. P., La Roi, G. H., Zoltai, S. C., and Robinson, A. L. (1992). The high subarctic forest-tundra of northwestern Canada: position, width, and vegetation gradients in relation to climate. *Arctic*, *45*(1), 1–9. https://doi.org/10.14430/arctic1367

Travers-Smith, H., and Lantz, T. C. (2020). Leading edge disequilibrium in sub-Arctic alder and spruce populations. *Ecosphere*.

Tsuyuzaki, S., Iwahana, G., and Saito, K. (2017). Tundra fire alters vegetation patterns more than the resultant thermokarst. *Polar Biology*, 1–9. https://doi.org/10.1007/s00300-017-2236-7

Veraverbeke, S., Rogers, B. M., Goulden, M. L., Jandt, R. R., Miller, C. E., Wiggins, E. B., and Randerson, J. T. (2017). Lightning as a major driver of recent large fire years in North American boreal forests. *Nature Climate Change*, *7*(7), 529–534. https://doi.org/10.1038/nclimate3329

Viereck, L. A., and Schandelmeier, L. A. (1980). Effects of Fire in Alaska and Adjacent Canada - A Literature Review. In *Technical Report 6*.

Vincent, L. A., Zhang, X., Brown, R. D., Feng, Y., Mekis, E., Milewska, E. J., Wan, H., and Wang, X. L. (2015). Observed trends in Canada's climate and influence of low-frequency variability modes. *Journal of Climate*, *28*(11), 4545–4560. https://doi.org/10.1175/JCLI-D-14-00697.1

Walker, X. J., Baltzer, J. L., Cumming, S. G., Day, N. J., Ebert, C., Goetz, S., Johnstone, J. F., Potter, S., Rogers, B. M., Schuur, E. A. G., Turetsky, M. R., and Mack, M. C. (2019). Increasing wildfires threaten historic carbon sink of boreal forest soils. *Nature*, *572*(7770), 520–523. https://doi.org/10.1038/s41586-019-1474-y

Wein, R. W. (1976). Frequency and Characteristics of Arctic Tundra Fires. *ARCTIC*, *29*(4), 213–222. https://doi.org/10.14430/arctic2806

Wein, R. W., and Bliss, L. C. (1973). Changes in Arctic Eriophorum Tussock Communities Following Fire. *Ecology*, *54*(4), 845–852. https://doi.org/10.2307/1935679

Wilcox, E. J., Keim, D., de Jong, T., Walker, B., Sonnentag, O., Sniderhan, A. E., Mann,

P., and Marsh, P. (2019). Tundra shrub expansion may amplify permafrost thaw by advancing snowmelt timing. *Arctic Science*, *5*(4), 202–217. https://doi.org/10.1139/as-2018-0028

Young, A. M., Higuera, P. E., Duffy, P. A., and Hu, F. S. (2017). Climatic thresholds shape northern high-latitude fire regimes and imply vulnerability to future climate change. *Ecography*, *40*(5), 606–617. https://doi.org/10.1111/ecog.02205

Zasada, J. (1986). *Natural Regeneration of Trees and Tall Shrubs on Forest Sites in Interior Alaska* (pp. 44–73). Springer, New York, NY. https://doi.org/10.1007/978-1-4612-4902-3_4

Zhang, J., and Walsh, J. E. (2006). Thermodynamic and hydrological impacts of increasing greenness in northern high latitudes. *Journal of Hydrometeorology*, *7*(5), 1147–1163. https://doi.org/10.1175/JHM535.1

Appendix A: Flowchart for differenced Normalized Burn Ratio calculation using Landsat 7 ETM+ imagery

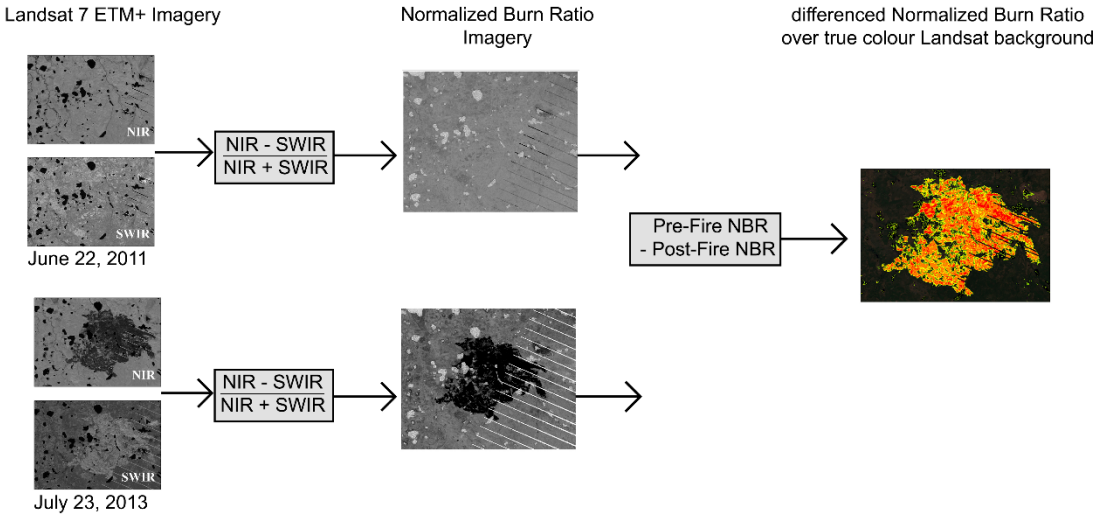

Appendix B: Flowchart for burn severity classification using differenced Normalized Burn Ratio (dNBR)

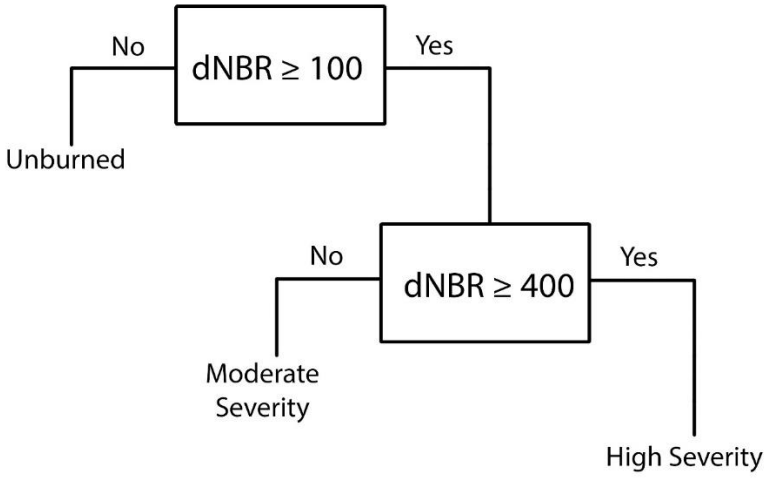

Appendix C: Significant Kendall correlations between NMDS Axes 1 and 2 and species and site properties

Site Properties	**NMDS1**	**NMDS2**
Bare Ground	-0.08	-0.99
Burned ground	0.59	-0.80
Thaw depth	-0.38	-0.93
Organic layer depth	0.88	0.47
NBR	-0.94	-0.34
Sulphate	-0.33	-0.94
Electrical conductivity	-0.27	-0.96
Soil Moisture	0.01	-0.99
Species	**NMDS1**	**NMDS2**
Betula glandulosa	0.68	0.73
Carex spp.	-0.96	0.27
Chamerion angustifolium	-0.99	-0.11
Eriophorum spp.	0.59	-0.80
Poaceae	-0.93	0.38
Salix spp.	-0.16	0.99
Vaccinium uliginosum	-0.99	-0.08
Vaccinium vitis-idaea	-0.15	0.99
Bryophytes	0.97	0.22
Lichen	-0.95	0.31
Litter	-0.99	0.14

3 Biophysical controls of increased tundra productivity in the western Canadian Arctic

Angel Chen[1], Trevor C. Lantz[1], Txomin Hermosilla[2], Michael A. Wulder[2]

[1]School of Environmental Studies, University of Victoria
[2]Pacific Forestry Centre, Canadian Forest Service

3.1 Introduction

Increases in temperature are predicted to profoundly alter the structure and function of global vegetation (Serreze et al., 2000; Stocker et al., 2013). In Arctic ecosystems, where temperatures are warming at more than twice the average global rate (Cowtan and Way, 2014; Pithan and Mauritsen, 2014), shifts in vegetation are already widespread (Bhatt et al., 2013; Jia et al., 2009). Analysis of satellite imagery from the last three decades across the Canadian Arctic has revealed rapid increases in vegetation productivity in the Yukon, Northwest Territories, Nunavut, and northern Quebec and Labrador (Ju and Masek, 2016). Several lines of evidence indicate that changes in vegetation productivity have been driven primarily by increases in air temperature, a factor which significantly limits vegetation growth and reproduction at northern latitudes (Bunn et al., 2006; Myers-Smith et al., 2015; Ohse et al., 2012; Tape et al., 2012). Tundra warming experiments and fine-scale monitoring show that increasing temperatures can drive rapid expansion of deciduous shrubs (Elmendorf et al., 2012; Moffat et al., 2016; Travers-Smith and Lantz, 2020) and dwarf evergreen shrubs (Fraser et al., 2014; Rozema et al., 2009), but the magnitude of these changes is also regionally variable (Elmendorf et al., 2015; Tape et al., 2012). Pronounced heterogeneity in vegetation productivity trends have been observed at broad scales, with some tundra regions exhibiting rapid greening, while others show little to no change in productivity over the past few decades (Jorgenson et al., 2018; Tape et al., 2012). Some regions also show trends towards decreasing vegetation productivity, or browning (Berner et al., 2020; Phoenix and Bjerke, 2016)

Heterogeneity of tundra productivity trends suggests that the effects of temperature are mediated by broad-scale variation in local topography (Campbell et al., 2020; Ropars and Boudreau, 2012), surficial geology and geological history (Raynolds et al., 2006; Rickbeil

et al., 2018), soil moisture (Cameron and Lantz, 2016; Campbell et al., 2020; Myers-Smith et al., 2015), and land cover (Bunn et al., 2006; Ju and Masek, 2016; Silapaswan et al., 2001). Research to determine the causes of this variability is critical because vegetation change affects ecological processes that strongly influence the climate system (Bhatt et al., 2017; Bunn et al., 2006; de Jong et al., 2013; Mcguire et al., 2009). Specifically, changes in the structure and function of tundra vegetation are expected to alter soil and permafrost conditions (Blok et al., 2010), hydrological processes (Drake et al., 2019), global carbon storage (Christiansen et al., 2018), and surface energy exchange (Blok et al., 2011).

In this study we used a time-series of Landsat imagery (Wulder et al., 2019) to analyze changes in the Enhanced Vegetation Index (EVI) from 1984 to 2016 and describe the spatial pattern and magnitude of vegetation change in the western Canadian Arctic. Our objective was to quantify changes in vegetation productivity and identify the biophysical variables that explain the spatial heterogeneity in observed trends. To accomplish this, we used Random Forests (RF) machine learning to model and evaluate the relationships between EVI trends and a suite of biophysical variables hypothesized to be influencing Arctic greening.

3.2 Methods

3.2.1 Study Area

The study area for this project encompassed approximately 800 000 km^2 of Arctic tundra in the Yukon, Northwest Territories and Nunavut (Fig. 3.1). Located between 63.5° N and 79.4° N and 141.0° W and 101.6° W, our study area consisted of the portion of western Canada defined as tundra by the circumpolar Arctic bioclimatic subzones map (Walker et al., 2005). This area spans the Taiga Cordillera, Taiga Plains, Taiga Shield, Northern

Arctic, and Southern Arctic ecozones and 22 ecoregions that contain mosaics of graminoid tundra, prostrate-shrub tundra, erect shrub tundra, wetland vegetation, and sparsely vegetated barrens (Olthof et al., 2009; Walker et al., 2005). Mean July temperature across the study area ranges from 10° C in the Taiga Cordillera to 4° C in the Northern Arctic ecozone (Ecosystem Classification Group, 2013).

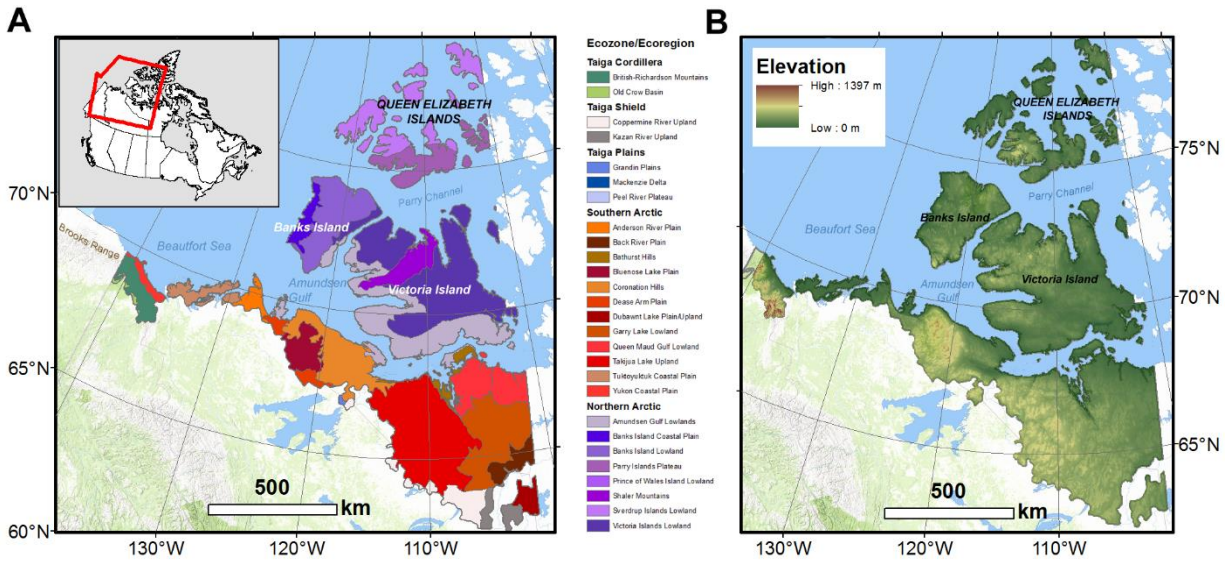

Figure 3.1 (A) Map of the study region in the western Canadian Arctic overlain with colours distinguishing ecoregions and ecozones located in the study area. (B) Map of the study area region overlaid with a digital elevation model. Inset map in the upper left shows the extent of the 80-million hectare study area in north-western Canada.

The terrain across our study area is highly variable. The western extent of our study area is located at the border of the Yukon and Alaska and is characterized by the low-lying Yukon Coastal Plain and glacial moraines that have been reworked by a range of periglacial processes, including hummock and thermokarst lake formation (Wolter et al., 2017). On the fringes of the Alaskan Brooks Range and south of the Beaufort Sea, this region extends inland westward through the Richardson Mountains, the Peel Plateau, and the Mackenzie

Delta, towards the Arctic Archipelago. Moist and more nutrient-rich low-lying areas in this region are occupied by wet sedge, low shrub, and tall shrub communities, whereas hilltops, and alpine and exposed environments are characterized by dwarf and herbaceous tundra (Smith et al., 2004; Ecosystem Classification Group, 2013). The islands of the Arctic Archipelago in the eastern extent of our study area are characterized by distinctive Northern and Southern Arctic ecoclimates. Northern Arctic regions like the Shaler Mountains, Banks Island Lowland and Parry Islands Plateau, are characterized by exposed bedrock, outwash deposits, glacial tills and plateaus. Upland vegetation in this region is mainly sparse and discontinuous, but in wet areas, a continuous cover of mosses, lichens, and low-growing forbs, sedges (including cottongrasses) can be found (Ecosystem Classification Group, 2013). Comparatively, vegetation in SouthernArctic regions like the Banks Island Coastal Plain and Amundsen Gulf Lowlands consists of near continuous dwarf shrub tundra which is often dominated by willows and sedges in wetter, warmer sites (Ecosystem Classification Group, 2013). The entire study area is located within the continuous permafrost zone, where a seasonally thawing active layer is found overlaying permafrost that ranges in depth from less than 100 m in areas with abundant water bodies to over 500 m in unglaciated regions (Burn and Kokelj, 2009). Cryosolic soils, characterized by the prevalence of permafrost, are the dominant soil order in this region (Tarnocai, 2004).

3.2.2 Enhanced Vegetation Index

To estimate shifts in vegetation status and productivity across our study area, we analyzed changes in the Enhanced Vegetation Index (EVI) calculated using Landsat imagery. EVI uses near infrared (NIR) and red wavelengths to relate biomass and photosynthetic activity,

and employs blue wavelengths for aerosol correction (Huete et al., 2002) to reduce the impact of spatially variable perturbations in the atmosphere.

$$EVI = 2.5 \times \frac{NIR - Red}{NIR + 6 \times Red - 7.5 \times Blue + 1}$$

Like the Normalized Difference Vegetation Index (NDVI), EVI has been used as a proxy for photosynthetic activity and productivity (Huete et al., 2002). In this analysis we used EVI because it has greater sensitivity to subtle vegetation changes, canopy structure, and leaf area index and can diminish possible distortions present in NDVI values, which results from ground cover below vegetation canopy (Xiao et al., 2005).

3.2.3 Landsat Trend Analysis

Changes in vegetation productivity were explored by calculating pixel-based trends in EVI using a time series of annual, gap-free, Landsat surface reflectance image composites with 30-m spatial resolution from 1984 to 2016 produced using the Composite2Change (C2C) algorithm (Hermosilla et al., 2016). First, Best Available Pixel (BAP) Landsat composites were annually generated through pixel selection using user-determined scores for four criteria: (1) sensor type, (2) acquisition day of year (August 1st ± 30 days), (3) distance to clouds and cloud shadow, and (4) atmospheric opacity. Scores are summed and pixels with the highest score are assigned as the best pixel in the final raster composite. Pixels where no observations were available (e.g., persistently cloudy locations) are labelled as data gaps (White et al., 2014). These BAP composites are further processed to remove unscreened noise (such as from haze or smoke) as well as non-permanent snow occurrences and fill any remaining data gaps with proxy surface reflectance values using spectral trend information derived the temporal analysis of the time series (Hermosilla et al., 2015).

To calculate per-pixel trends in the EVI time series, we used the Theil Sen slope estimator (Sen, 1968). This is a non-parametric regression method for trend evaluation where the median slope of all pairwise combinations is calculated. Repeated median estimates are more robust than ordinary least squares because they are less sensitive to outliers. All statistical analyses were performed in R (R Core Team, 2013) on Compute Canada's West Grid cloud-based high-performance computing infrastructure. We calculated the Theil estimator with the 'EcoGenetics' package (Roser et al., 2020) and evaluated trends with the 'Kendall' package (McLeod, 2011) by using the Mann-Kendall test for significance of monotonic trends in time series (Mann, 1945). Water masks derived from the Function of mask (Fmask) algorithm (Zhu and Woodcock, 2012) were used to remove water pixels and constrain the analysis to terrestrial pixels. Unlike areas of Scandinavia (Phoenix and Bjerke, 2016) and boreal Alaska (Verbyla, 2011) where significant decreases in productivity (browning) are spatially clustered and explicitly connected to specific regions and biophysical conditions, browning within our study area made up less than 1% of the total area and was not clustered. Since this small number of browning pixels was not clustered, we masked out browning trends and focused on EVI trends classified as either: (1) significantly greening or (2) non-significant change

3.2.4 Modelling Determinants of EVI Greening

We used Random Forests (RF) (Breiman, 2001) regression and classification modelling to examine the relationships between tundra greening (slope of significant EVI trends) and 12 biophysical variables hypothesized to influence landscape scale vegetation dynamics (Table 3.1). RF models are a machine learning ensemble method based on classification and regression trees (CART). This approach uses sample-with-replacement to derive many

sample subsets, or bootstrap samples. Different bootstrap samples are used to train each individual CART. Combining, or bootstrap aggregating (bagging) these CARTs creates the ensembled RF model. To calculate variance explained in our regression model we used out-of-bag (OOB) predictions to compute the percent of greening explained by data not used to train our model.

We conducted both a RF classification and regression model to separately evaluate the ability of biophysical factors to: (1) distinguish between areas with increasing and non-significant change in EVI trends (classification), and (2) predict the marginal differences in the magnitude of greening in areas with positively trended pixels (regression).

The ‘caret’ package (Kuhn, 2020) was used to downsample the majority class to address data imbalance in RF classification (Boulesteix et al., 2012). Models were constructed using a random subset of 1% of the significantly greening pixels ($p<0.05$) in the study area and performed using the ‘randomForest’ package (Liaw and Wiener, 2018). We used the ‘tidyverse’ and ‘dplyr’ packages (Wickham et al., 2020, 2019) to preprocess, organize, and compile the random sample subset.

To evaluate the proportion of greening observed within land cover types and ecozones we tested for equivalence (Foody, 2009). Two one-sided tests for equivalence were conducted using the ‘TOSTER’ package (Lakens, 2017) to test for equivalence in proportions (Tunes da Silva et al., 2009) between the proportion of greening of subgroups and the proportion of greening in our study area overall based on an equivalence margin of 5% (de Beurs et al., 2015).

Table 3.1 Description of environmental variables assessed as drivers of EVI trends

Variable	Data Set and Source	Description	Resolution/Scale
Land Cover	Northern Land Cover of Canada (Olthof et al., 2009)	Vegetation cover classification for Northern Canada	$30m^2$
Surficial Geology	Quaternary Geology of Canada and Greenland (Fulton, 1989)	Surficial geology classification	1: 5 000 000
Ecoregion	Terrestrial Ecoregions of Canada (Agriculture and Agri-Food Canada, 2016)	Subdivisions based on distinctive ecological features	1: 5 000 000
Elevation	Canada DEM (Natural Resources Canada, 2015)	Elevation above sea level	1: 250 000
Aspect		Polar transformed aspect in eight cardinal directions	
Slope		Slope in degrees	
Topographic Solar Radiation Index		Continuous scale from 0 (coolest/wettest orientation) to 1 (hottest, driest orientation)	
Historical Summer Temperature	Climatic Research Unit Time Series (I. Harris et al., 2014)	Mean near surface temperature for July 1984	0.5°
Historical Winter Temperature		Mean near surface temperature for January 1984	
Precipitation	University of East Anglia Climatic Research Unit (Harris et al., 2014)	Mean precipitation for 1984	0.5°
Substrate Chemistry	Circumpolar Arctic Vegetation Map (Walker et al., 2005)	Classification of soil and bedrock chemistry	$1\ km^2$
Lake Cover		Percent cover of lakes based on AVHRR data	

To improve modelling efficiency, ‘doParallel’ and ‘foreach’ packages (Weston, 2020, 2019) were used to implement multiple cores for parallel processing. To evaluate and visually assess models, we used three analysis tools: (1) partial dependence plots, (2) mean decrease in model accuracy (%IncMSE), and (3) mean decrease in node impurity (IncNodePurity). Partial dependence plots were used to visualize the marginal effects and patterns of the relationships between individual variables and modelled EVI trends when all other predictors are held constant. The y-axis of partial dependence plot shows the mean of all model predictions for a given the value of the predictor variable (x) (Jeong et al., 2016). We also used the variable importance function to rank the variables based on the percent increase in mean square (%IncMSE) when values for a variable of interest are randomly permuted, effectively mimicking the absence of that variable from the model. The most important biophysical variables for explaining EVI trend will have the greatest %IncMSE.

3.2.5 Biophysical Variables Datasets

Data for biophysical variables expected to influence trends in vegetation productivity were obtained from a range of sources (Table 3.1). Mean temperature and precipitation, which have been widely cited as the main driving forces of greening (Blok et al., 2011; Jia et al., 2009) were obtained from the University of East Anglia’s Climatic Research Unit (CRU) Time Series 4.02 dataset (Harris et al., 2014; Harris et al., 2020). This gridded dataset covers all global land regions at a resolution of 0.5° from1901 to 2017 and was derived using angular-distance weighted interpolation. We used data from July 1st and January 1st to assess both summer and winter historical temperatures from the beginning of the time series. Ecoregion data were acquired from the Terrestrial Ecoregions of Canada dataset

published by Agriculture and Agri-Food Canada (2013). This dataset delineates ecoregions based on distinctive regional differences in environmental factors such as climate, physiography, vegetation, soil, water, and fauna. Data on lake cover and substrate chemistry, were acquired from the Circumpolar Arctic Vegetation Mapping Project (Walker et al., 2005). Proximity to large water bodies and the effects on albedo have been suggested to contribute to vegetation greening along a forest-tundra gradient (Bonney et al., 2018) and hydrological changes associated with ice wedge degradation have altered surface water properties and vegetation across the western Arctic (Campbell et al., 2020; Liljedahl et al., 2016). Elevation data were obtained from the Canadian Digital Elevation Model (CDEM) (Natural Resources Canada, 2015). We used the 'spatialEco' package (Evans, 2020) to derive additional variables from the CDEM. These additional topographic variables included: slope, aspect, and the Roberts and Cooper (1989) topographic solar-radiation aspect index (TRASP), which transforms aspect to estimate relative solar radiation as continuous values from 0 to 1. Aerial photography and field research linking topographic position to increasing radial growth of *Betula glandulosa* demonstrates that variations in temperature and precipitation associated with terraces and hilltops can contribute to local heterogeneity of greening (Ropars et al., 2015). Data on surficial geology was taken from Fulton (1989) and aggregated into broad generic surficial units (ex. Lacustrine, Colluvial, Morainal, Fluvial). Spatial patterns of Arctic NDVI trends have been associated with landscape age and the effect of glacial history on vegetation type (Raynolds and Walker, 2009). Data on land cover were obtained from the Northern Land Cover of Canada dataset (Olthof et al., 2009). This land cover classification includes 15 classes north of the treeline (Timoney et al., 1992) and was derived from Landsat imagery

at 30-m spatial resolution. Experimental warming studies have shown that warming can elicit difference growth rates depending on cover type, where deciduous shrubs and graminoids have been observed to respond positively to warming while non-vascular plants such as mosses and lichens have responded negatively (Walker et al., 2006). All environmental datasets were reprojected to WGS84 reference ellipsoid and UTM coordinate system using nearest neighbour interpolation for categorical datasets and cubic convolution for continuous datasets and resampled to 30-m spatial resolution to match the resolution of the EVI data.

3.3 Results

3.3.1 EVI Trends

Trends in the Enhanced Vegetation Index indicated widespread increases in vegetation productivity across the western Canadian Arctic (Fig. 3.2). Over 68% (540 000 km^2) of the study area experienced significant ($p<0.05$) greening (EVI slope > 0) between 1984 and 2016 and only 31% of the study area (260 000 km^2) showed no significant trend in EVI over time. Land cover types where vegetation is less dense, such as sparsely vegetated till and barren had comparatively lower EVI slopes than denser vegetation types (Table 3.2). The highest levels of greening were observed within the Southern Arctic zone in dense vegetation cover types, including tall shrub, low shrub, tussock graminoid tundra, and graminoid and dwarf shrub tundra cover (Table 3.3).

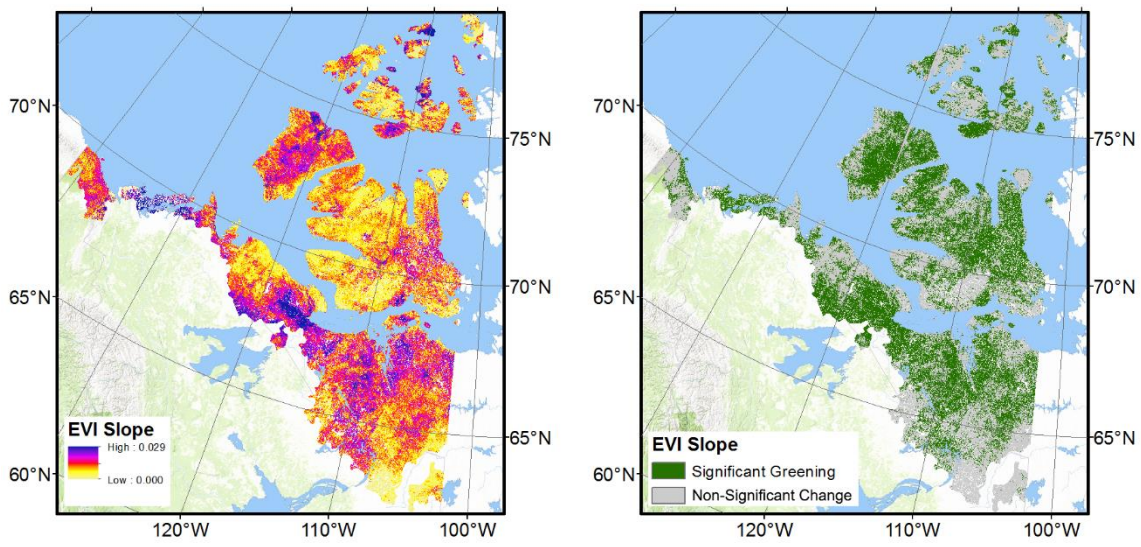

Figure 3.2 Enhanced Vegetation Index trends for the study area from 1984 to 2016. (A) Theil Sen slope of EVI trends (slope > 0) (B) Classification of Mann Kendall significance of EVI trends as either significantly greening ($p < 0.05$) or non-significant ($p > 0.05$).

3.3.2 EVI Classification Model

The RF classification of significantly greening versus non-significant pixels had an overall OOB user's accuracy rate of 73.5% and a per-class accuracy of 76.4% for greening pixels and 70.4% for stable pixels. The mean trend in non-significant pixels was 0.000005304 year $^{-1}$ and the mean trend in greening pixels was 0.001578 year $^{-1}$ (Table 2).The six most important variables for determining if a pixel had a significant trend were: land cover, slope, elevation, lake cover, historical winter temperature, and geology (Fig. 3). These variables all increased model accuracy by more than 50%. Land cover was the most important biophysical predictor in the classification tree model and improved model accuracy by nearly twice as much as the next most important variable (Fig. 3).

Table 3.2 Mean and median EVI trend by land cover type and the proportion of each cover type that experienced significant greening.

Land Cover Type	**Median EVI Trend (year^{-1})**	**Mean EVI Trend (year^{-1})**	**Proportion Greening (%)**
Tall Shrub	0.002155	0.002286	72.65
Low Shrub	0.001889	0.001990	**73.73**
Tussock Graminoid Tundra	0.001704	0.001774	**81.97*** **
Graminoid/Dwarf Shrub Tundra	0.001533	0.001625	**73.68**
Wet Sedge	0.001339	0.001414	**78.49*** **
Wetlands	0.001280	0.001452	**67.78*** **
Bare Soil/Frost Boils	0.001091	0.001179	**79.11*** **
Sparsely Vegetated Bedrock	0.001075	0.001434	**70.68**
Prostrate Dwarf-Shrub Tundra	0.001053	0.001219	**69.20**
Sparsely Vegetated Till	0.0007220	0.0008286	**67.24**
Barren	0.0005670	0.0007026	**58.68 +**
Total study area	0.001105	0.001289	72.39
Non-significant area	0.0004340	0.0005304	27.61
Total greening study area	0.001401	0.001578	100

*** indicates where the proportion of greening for the land cover is statistically greater than the proportion of greening for the study area based on an equivalence margin of Δ0.05.
+ indicates where the proportion of greening for the land cover is statistically less than the proportion of greening for the study area based on an equivalence margin of Δ0.05.
Bold text indicates where the difference between the proportion of greening for the land cover type is statistically different from zero based on alpha = 0.05.

Table 3.3 Proportion of land cover type within each ecozone that experienced significant greening.

Cover Type	Northern Arctic Proportion Greening (%)	Southern Arctic Proportion Greening (%)	Taiga (Proportion Greening%)
Tall Shrub	**73.08**	**76.85**	**57.21**
Low Shrub	**76.46**	**75.83**	**62.23*****
Tussock Graminoid Tundra	**64.37+**	**80.05*****
Graminoid Dwarf Shrub Tundra	77.59	**74.76**	**50.00+**
Wet Sedge	**80.83+**	**78.38**	55.89
Wetlands	**68.34+**	**65.33+**	**48.25+**
Bare Soil/Frost Boils	**74.74+**	**69.62+**	56.25
Sparsely Vegetated Bedrock	**72.79+**	**67.97+**	**35.70+**
Prostrate Dwarf-Shrub Tundra	**79.75*****
Sparsely Vegetated Till	**62.36+**	**60.32+**	**34.25+**
Barren	**63.09+**	**60.55+**	**44.22+**

*** indicates where the proportion of greening for the land cover is statistically greater than the proportion of greening for the study area based on an equivalence margin of 5%.
+ indicates where the proportion of greening for the land cover is statistically less than the proportion of greening for the study area based on an equivalence margin of 5%.
Bold text indicates where the difference between the proportion of greening for the land cover type is statistically different from zero based on alpha = 0.05.

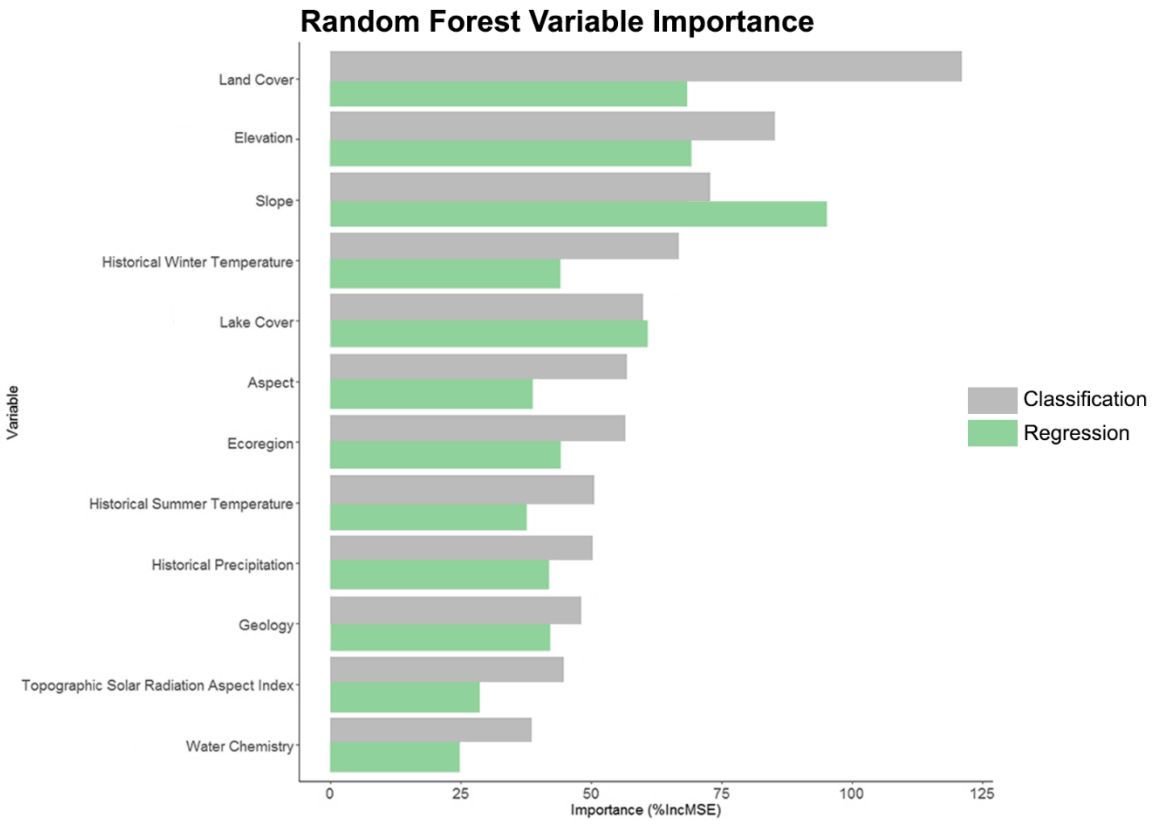

Figure 3.3 Importance of biophysical variables from classification (green) and regression (gray) tree Random Forests models. Variables are arranged by classification variable importance, which is measured as the increase in mean square error (%Inc MSE) when values of the predictor variable are randomly permuted and scaled by the normalized standard deviation of the differences.

The partial dependence plot for land cover shows that bare soil, tussock graminoid tundra, and wet sedge were the cover classes with the highest probability of being classified as greening (Fig. 3.4A). Comparatively, barrens, sparsely vegetated till, and tall shrubs had a lower probability of containing greening pixels.

A suite of variables related to topography including elevation, slope, and aspect also had a large impact on the accuracy of the classification tree model (Fig. 3.3). Pixels at elevations between 100 and 350 m above sea level were also more strongly associated with greening than mid-elevation or montane areas (Fig. 3.4C). The partial dependence plot for slope

indicated that flatter areas were more likely to be classified as greening (Fig. 4B) compared to sites with slopes greater than 5° (Fig. 3.4B). Glaciofluvial and glaciolacustrine geology types were more likely to be classified as greening. The overlap between the distribution of mountainous regions (Richardson Mountains, British Mountains, Shaler Mountains) in our study area and non-significant pixels is evident when comparing Figures 3.1 and 3.2. Our study area is predominantly flat, but southern and western slopes were more likely to be classified as greening, while northern and eastern slopes were more likely to be classified as non-significant (Fig. 3.4D). A higher probability of greening was also associated with cooler historic winter temperature between -36° and -28° C and warming historical summer temperatures between 6 and 10 °C, which occur primarily in the lower Northern Arctic and upper Southern Arctic regions, such as Banks Island and Victoria Island, the Yukon Coastal Plain, Tuktoyaktuk Coastlands, and British-Richardson Mountains (Fig. 3.4E). The Southern Arctic experienced more rapid greening than the High Arctic and High Subarctic (Table 3.3). The partial dependence plot for lake cover indicates that the highest probability of greening occurred in areas with low (<10%) or moderate (25-50%) lake coverage (Fig. 3.4F).

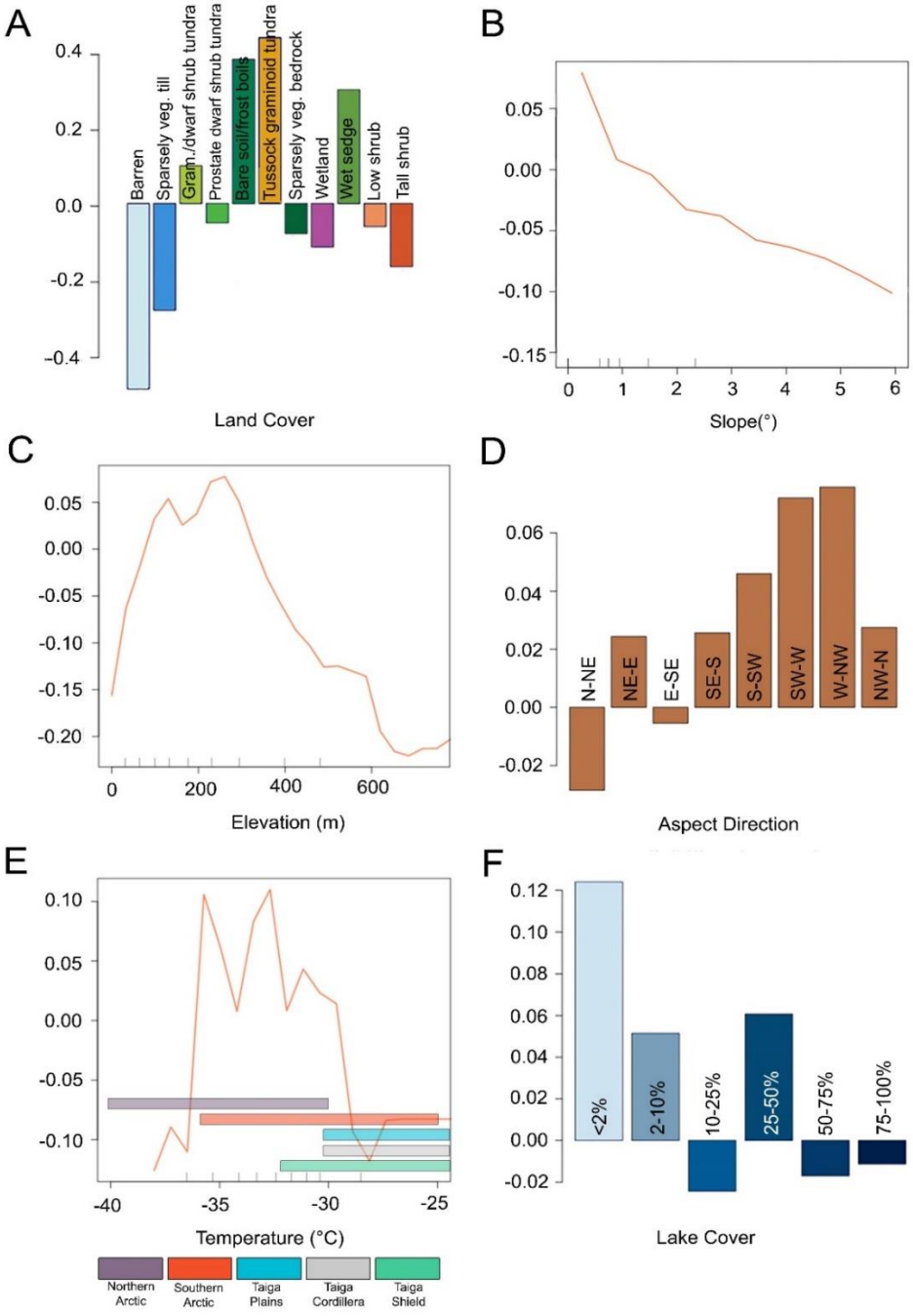

Figure 3.4 Partial dependence plots for the six most important variables in the by Random Forests classification model: (A) land cover (B) slope angle, (C) elevation, (D) aspect direction, (E) historical (1984) winter temperature with colored bars indicating temperature range at each ecozone, and (F) percent lake cover. Positive values on the y-axis indicates greater agreement between trees that a pixel is classified as greening at different values (x-axis) of a given explanatory variable, with the effect of other variables held constant (Friedman, 2001). Negative values indicate less agreement between trees that a level of the variable plotted was associated with greening.

3.3.3 EVI Regression Model

The biophysical variables used in RF regression model explained 48.4% of variance in EVI slope, based on the out-of-bag (OOB) predictions. The six most important variables in the regression Random Forests model were slope, elevation, land cover, lake cover, ecoregion classification and historical winter temperature (Fig. 3.3). Topographic variables (slope, elevation) had the greatest impact on the accuracy of the regression model (Fig. 3.3). The partial dependence plot for slope shows that tundra greening was most rapid in areas with slopes between 3 and 6° (Fig. 3.5A). The partial dependence plot for elevation shows that the rate of greening was highest at low elevations and declined with increasing elevation (Fig. 3.5B). Elevation greater than ~ 500 m above sea level were uncommon across the study area and had a below average trend in EVI of 0.00100 $year^{-1}$.

The partial dependence plot for land cover indicates that the magnitude of greening was greatest in areas of denser and shrub-dominated vegetation, such as low shrub, tall shrub, graminoid dwarf shrub, and tussock graminoid tundra (Fig. 3.5C). Comparatively, the slowest greening trends were associated with largely non-vegetated land covers, including barren and sparsely vegetated till (Fig. 3.5C). Glaciofluvial and morainal sediments experienced the fastest rates of greening while colluvium and marine sediments experienced the slowest rates. Rates of greening were similar across substrate chemistry classes.

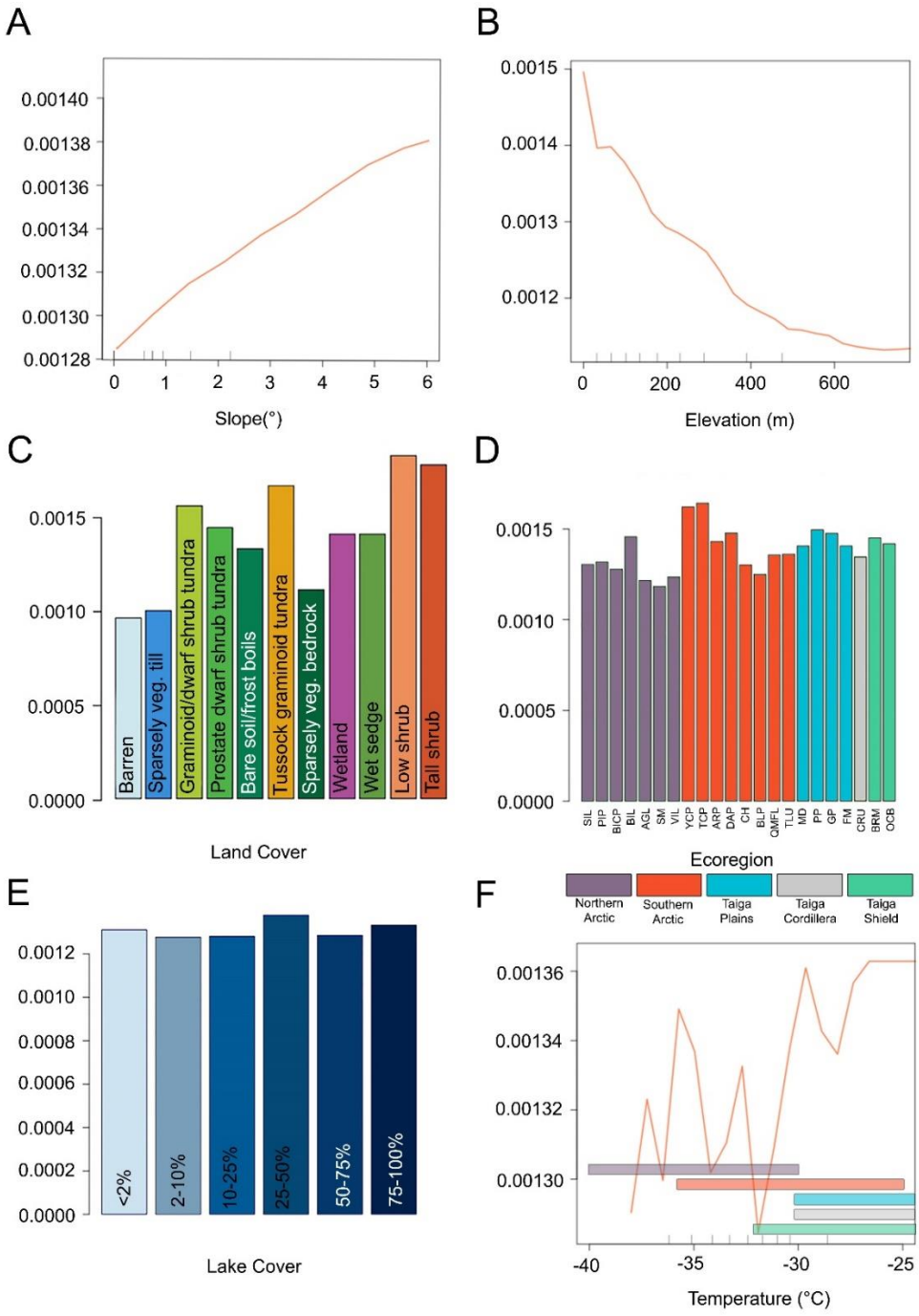

Figure 3.5 Partial dependence plots for six most important variables determined by Random Forests regression model: (A) slope angle, (B) elevation, (C) land cover, (D) ecoregion, (E) percent lake cover, and (F) historical (1984) winter temperature with colored bars indicating temperature range at each ecozone. The y-axis shows the average EVI trend slope predicted at different levels of a given explanatory variable, with the effect of other variables held constant (Friedman, 2001).

The rate of greening also varied among ecoregions, with the greatest increases occurring in southwestern ecoregions including the Peel Plateau, Tuktoyaktuk Coastal Plain, Mackenzie Delta, and Yukon Coastal Plain. In these areas median EVI trends were three to four times higher than the average across the entire study area (Fig. 3.5D, Table 3.2). The partial dependence plot for lake cover shows that the most rapid greening occurred in areas with moderate lake density, which are concentrated in the Mackenzie Delta, Tuktoyaktuk Coastal Plain, and Anderson River Plain. However, marginal differences among lake density classes were quite small (Fig. 3.5E). The relationship between winter temperature and EVI change showed considerable variation, but in general, winter temperatures below -30°C were associated with smaller changes in vegetation productivity (Fig. 3.5F) and historical summer temperatures between 6 and 10 ° C were associated with larger changes.

3.4 Discussion

Our observation that vegetation greening occurred across 68% of the study area and was common in all ecoregions suggests that this change was driven primarily by the rapid increases in temperature that have taken place across northwestern Canada (Vincent et al. 2015). Increases in average annual air temperature of 3° (Overland and Wang, 2016; Vincent et al., 2015) and an extension of the growing season by nearly two weeks (Pedlar et al., 2015) parallel the conditions imposed by plot-scale tundra warming experiments, which have driven increases in stem biomass (Bret-Harte et al., 2001) net primary productivity (Wahren et al., 2005), and canopy height (Elmendorf et al., 2012). The importance of climatic variables including historical winter temperature and elevation in our models of spatial variation in EVI trends also point to the importance of recent climate

warming as a driver of change (Bunn et al., 2006; Jia et al., 2009). Partial dependence plots of historic winter temperatures show that greening was most likely to occur, and was most rapid, at temperatures typical of the Southern Arctic portion of our study area. This observation is similar to other recent studies showing that vegetation productivity has increased more rapidly in the Southern Arctic, and Taiga compared to the Northern Arctic (Berner et al., 2011; Bolton et al., 2018; Bonney et al., 2018; Reichle et al., 2018; Ropars and Boudreau, 2012; Sulla-Menashe et al., 2018). This is likely because vegetation productivity in the Northern Arctic is more severely limited by cold temperatures and a short growing season than the Southern Arctic (Svoboda and Henry, 1987; Raynolds et al., 2008; Epstein et al., 2008), where temperature limitation of growth and reproduction have been surpassed by recent warming (Elmendorf et al., 2012; Lantz et al., 2013; Myers-Smith and Hik, 2018). This explanation is also consistent with our observation that sparsely vegetated cover types in the Northern Arctic (barren and till) had the lowest rates of EVI change and impacted the smallest area.

Recent studies in the Peel Plateau (Cameron and Lantz, 2016), the Tuktoyaktuk Coastlands (Fraser et al., 2014; Lantz et al., 2013; Travers-Smith and Lantz, 2020), and the Yukon Coastal Plain (Myers-Smith, et al., 2011) also show evidence of widespread vegetation change that is consistent with our observations of accelerated Southern Arctic greening. In the southern extent of our study area greening was likely lower because the productivity of the Taiga forest that dominates these areas has been negatively impacted by increased drought and fire severity (Myers-Smith et al., 2015; Schut et al., 2015; Sulla-Menashe et al., 2018). It is also possible that the more complex vegetation structure found in proximity to the forest-tundra transition zone (treeline) complicates the use of Landsat imagery to

detect tundra vegetation change (Boudreau and Villeneuve-Simard, 2012; McManus et al., 2012; Olthof and Fraser, 2007).

Although regional warming is likely the overarching driver of changes in productivity, our observation that slope, elevation, and aspect were among the most important variables in our classification and regression models, suggests that soil moisture and microclimate can also mediate the impacts of warming on tundra vegetation productivity. The increased likelihood of greening on flat or gentle slopes (Fig. 3.4B), and the higher magnitude of greening on moderate slopes (Fig. 3.6A) indicates that moist to mesic conditions are most conducive to change. This is consistent with a recent study showing that increases in the productivity of upland tundra on Banks Island, NWT here highest in flat areas accumulating moisture and nutrients from upslope (Campbell et al., 2020).

The higher probability of greening on southeasterly-south to west-northwesterly slopes also suggests that intermediate moisture conditions on moderately warm slopes have facilitated change (Dearborn and Danby, 2017). Partial dependence plots showing the effects of land cover and lake cover on EVI trends (Fig. 3.4A; Fig. 3.5C; Fig. 3.5E) also indicate that greening was more widespread in mesic-moist land cover types (tussock tundra, shrub tundra, wet sedge) corroborating findings from other studies showing that increased productivity has been particularly rapid in riparian corridors, floodplains, and along river valleys (Bonney et al., 2018; Loranty et al., 2016; Tape et al., 2012) and wetland-to-upland ecotones (Bunn et al., 2006; Ropars et al., 2015). It is likely that areas with mesic conditions are experiencing higher than expected greening because carbon uptake and photosynthesis are higher at mesic sites compared to dry and wet sites (Kwon et al., 2006; Oberbauer et al., 2007). The effects of experimental warming on functional

group abundance, community height, plant size, and leaf nitrogen content have also been shown to vary with temperature and soil moisture (Elmendorf et al., 2012; Bjorkman et al., 2018).

Our analysis also suggests that spatial variation in tundra greening is driven by differences in the temperature sensitivity of some plant functional groups. Greening rates in productive cover types typically dominated by upright shrubs were more than 1.5 times higher than the average greening rate (Fig 6; Table 2). Greening rates in sparsely vegetated cover types, characterized by low-growing herbs and prostrate shrubs, sedges, and mosses, were approximately half the average rate. These findings are also consistent with the results of experimental warming studies showing that shrub abundance has increased in response to warming at warm, mesic sites (Elmendorf et al., 2012). Plot-scale studies in the Southern Arctic also show that recent warming has increased the cover of upright shrubs including willow (Myers-Smith et al., 2011), dwarf birch (Moffat et al., 2016; Tremblay et al., 2012), and alder (Frost et al., 2018; Lantz et al., 2013; Travers-Smith and Lantz, 2020). Areas dominated by upright shrubs are likely more responsive to warming-induced increases in resource availability because these woody plants can more efficiently allocate increased availability of nitrogen and phosphorous to secondary growth and lateral expansion compared to other tundra species (Bret-Harte et al., 2001; Shaver et al., 2001). There are fewer plot-scale studies exploring the drivers of increased productivity in the Northern Arctic, but existing literature suggests that greening is linked with the accelerated growth of low-growing shrubs and herbs (Boulanger-Lapointe et al., 2014; Campbell et al., 2020; Edwards and Treitz, 2017; Weijers et al., 2017). Below average EVI trends in barren and

sparsely vegetated areas in the Northern Arctic (Table 3) suggests that greening is not being driven by recruitment into these areas.

Unlike our regression model, which showed that shrub dominated cover types were greening the most rapidly, our classification model predicted that shrub dominated areas were more likely to not show trends in increased productivity over time. This is likely because shrub density can be patchy in these terrain types (Lantz et al. 2010, Moffat et al., 2016; Frost et al., 2017) and may exhibit more variable responses than other terrain types. Areas completely dominated by upright shrubs likely have less potential for increased productivity than patches occupied by a mix of shrubs and other tundra species. This is consistent with research in the Tuktoyaktuk Coastlands showing that shifts in the cover of plant functional groups were more variable in terrain dominated by upright shrubs compared to area dominated by dwarf shrubs or graminoids (Moffat et al., 2016). At fine spatial scales, increases in shrub abundance have been greatest in areas that formerly had sparse cover of shrubs (Moffat et al. 2016; Cameron et al 2016).

Changes in tundra vegetation structure and composition are altering surface energy exchange (Chapin et al., 2005; Marsh et al., 2010), northern wildlife activity (Boelman et al., 2011; Van Hemert et al., 2015; Rickbeil et al., 2017), above and belowground carbon stocks (Schaefer et al., 2011; Schuur et al., 2015), and permafrost dynamics (Blok et al., 2010; Frost et al., 2018; Wilcox et al., 2019). Our study shows that greening is widespread across the western Canadian Arctic, but is more dominant and rapid in some areas. This indicates that the impacts of vegetation change on ecological processes will be heterogeneous and underscores the importance of fine-scale predictive models. Our analysis shows that changes have been most rapid in the Southern Arctic. Our work also

highlights the potential of Random Forests modeling and other machine learning methods to contribute to the development of predictive models of tundra vegetation change (Bonney et al., 2018; Greaves et al., 2016). Inconsistency among greening trends derived from coarse-scale remote sensing platforms (Fisher and Mustard, 2007; Rocha et al., 2018) also points to the need for more regional- and landscape-scale analyses (Myers-Smith et al., 2020). Based on differences between plot-scale studies and remote sensing change detection (Jorgenson et al., 2018; Goetz et al., 2019; Myers-Smith et al., 2020), we suggest that future studies continue to evaluate change across multiple spatial scales and make use of the increasing availability and quality of high spatial and temporal resolution data sources, such as micro-satellites and remotely piloted aerial systems (Fraser et al., 2016; Liu and Treitz, 2018; Myers-Smith et al., 2019). Research examining physiological responses to changes in soil micronutrients and shifts in the below-ground community are also needed to understand the proximal controls to greening (Martin et al., 2017). With anticipated feedbacks between shifting tundra vegetation structure and the frequency of fire and thermokarst (Loranty et al., 2016; Swanson, 2017; Tsuyuzaki et al., 2017), additional research will also be required to understand how shifting disturbance regimes will shape vegetation trajectories. More frequent and extreme weather events (Bret-Harte et al., 2013; Hansen et al., 2014; Vermaire et al., 2013) that alter growing conditions are also likely to influence how tundra landscapes respond to ongoing climate change (Lantz et al., 2015).

Bibliography

Agriculture and Agri-Food Canada. 2013. Terrestrial Ecoregions of Canada. https://sis.agr.gc.ca/cansis

Berner, L.T., Beck, P.S.A., Bunn, A.G., Lloyd, A.H., Goetz, S.J., 2011. High-latitude tree growth and satellite vegetation indices: Correlations and trends in Russia and Canada (1982–2008). J. Geophys. Res. 116, G01015. https://doi.org/10.1029/2010JG001475

Berner, L.T., Massey, R., Jantz, P., Forbes, B.C., Macias-Fauria, M., Myers-Smith, I., Kumpula, T., Gauthier, G., Andreu-Hayles, L., Gaglioti, B. V., Burns, P., Zetterberg, P., D'Arrigo, R., Goetz, S.J., 2020. Summer warming explains widespread but not uniform greening in the Arctic tundra biome. Nat. Commun. 11, 4621. https://doi.org/10.1038/s41467-020-18479-5

Bhatt, U., Walker, D., Raynolds, M., Bieniek, P., Epstein, H., Comiso, J., Pinzon, J., Tucker, C., Polyakov, I., 2013. Recent Declines in Warming and Vegetation Greening Trends over Pan-Arctic Tundra. Remote Sens. 5, 4229–4254. https://doi.org/10.3390/rs5094229

Bhatt, U.S., Walker, D.A., Raynolds, M.K., Bieniek, P.A., Epstein, H.E., Comiso, J.C., Pinzon, J.E., Tucker, C.J., Steele, M., Ermold, W., Zhang, J., 2017. Changing seasonality of panarctic tundra vegetation in relationship to climatic variables. Environ. Res. Lett. 12. https://doi.org/10.1088/1748-9326/aa6b0b

Blok, D., Heijmans, M.M.P.D., Schaepman-Strub, G., Kononov, A. V., Maximov, T.C., Berendse, F., 2010. Shrub expansion may reduce summer permafrost thaw in Siberian tundra. Glob. Chang. Biol. 16. https://doi.org/10.1111/j.1365-2486.2009.02110.x

Blok, D., Schaepman-Strub, G., Bartholomeus, H., Heijmans, M.P.D., Maximov, T.C., Berendse, F., 2011. The response of Arctic vegetation to the summer climate: Relation between shrub cover, NDVI, surface albedo and temperature. Environ. Res. Lett. 6. https://doi.org/10.1088/1748-9326/6/3/035502

Boelman, N.T., Gough, L., McLaren, J.R., Greaves, H., 2011. Does NDVI reflect variation in the structural attributes associated with increasing shrub dominance in arctic tundra? Environ. Res. Lett. 6, 035501. https://doi.org/10.1088/1748-9326/6/3/035501

Bolton, D.K., Coops, N.C., Hermosilla, T., Wulder, M.A., White, J.C., 2018. Evidence of vegetation greening at alpine treeline ecotones: Three decades of landsat spectral trends informed by lidar-derived vertical structure. Environ. Res. Lett. 13. https://doi.org/10.1088/1748-9326/aad5d2

Bonney, M.T., Danby, R.K., Treitz, P.M., 2018. Landscape variability of vegetation change across the forest to tundra transition of central Canada. Remote Sens.

Environ. 217. https://doi.org/10.1016/j.rse.2018.08.002

Boudreau, S., Villeneuve-Simard, M.P., 2012. Dendrochronological evidence of shrub growth suppression by trees in a subarctic lichen woodland. Botany. https://doi.org/10.1139/B11-089

Boulanger-Lapointe, N., Lévesque, E., Boudreau, S., Henry, G.H.R., Schmidt, N.M., 2014. Population structure and dynamics of Arctic willow (*Salix arctica*) in the High Arctic. J. Biogeogr. 41, 1967–1978. https://doi.org/10.1111/jbi.12350

Boulesteix, A.L., Janitza, S., Kruppa, J., König, I.R., 2012. Overview of random forest methodology and practical guidance with emphasis on computational biology and bioinformatics. Wiley Interdiscip. Rev. Data Min. Knowl. Discov. 2, 493–507. https://doi.org/10.1002/widm.1072

Breiman, L., 2001. Random Forests. Mach. Learn. 45, 5–32. https://doi.org/10.1023/A:1010933404324

Bret-Harte, M.S., Mack, M.C., Shaver, G.R., Huebner, D.C., Johnston, M., Mojica, C.A., Pizano, C., Reiskind, J.A., 2013. The response of Arctic vegetation and soils following an unusually severe tundra fire. Philos. Trans. R. Soc. B Biol. Sci. 368. https://doi.org/10.1098/rstb.2012.0490

Bret-Harte, S. M., Shaver, G. R., Zoerner, J. P., Johnstone, J. F., Wagner, J. L., Chavez, A. S., Gunkelman IV, R. F., Lippert, S. C., and Laundre, J. A. (2001). Developmental plasticity allows betula nana to dominate tundra subjected to an altered environment. *Ecology*, *82*(1), 18–32. https://doi.org/10.1890/0012-9658(2001)082[0018:dpabnt]2.0.co;2

Bunn, A.G., Goetz, S.J., Bunn, A.G., Goetz, S.J., 2006. Trends in Satellite-Observed Circumpolar Photosynthetic Activity from 1982 to 2003: The Influence of Seasonality, Cover Type, and Vegetation Density. Earth Interact. 10, 1–19. https://doi.org/10.1175/EI190.1

Burn, C.R., Kokelj, S. V., 2009. The environment and permafrost of the Mackenzie Delta area. Permafr. Periglac. Process. 20, 83–105. https://doi.org/10.1002/ppp.655

Cameron, E.A., Lantz, T.C., 2016. Drivers of tall shrub proliferation adjacent to the Dempster Highway, Northwest Territories, Canada. Environ. Res. Lett. 11. https://doi.org/10.1088/1748-9326/11/4/045006

Campbell, T.K.F., Lantz, T.C., Fraser, R.H., Hogan, D., 2020. High Arctic Vegetation Change Mediated by Hydrological Conditions. Ecosystems. https://doi.org/10.1007/s10021-020-00506-7

Chapin, F.S., Sturm, M., Serreze, M.C., McFadden, J.P., Key, J.R., Lloyd, A.H., McGuire, A.D., Rupp, T.S., Lynch, A.H., Schimel, J.P., Beringer, J., Chapman, W.L., Epstein, H.E., Euskirchen, E.S., Hinzman, L.D., Jia, G., Ping, C.L., Tape,

K.D., Thompson, C.D.C., Walker, D.A., Welker, J.M., 2005. Role of land-surface changes in arctic summer warming. Science (80-.). 310, 657–660. https://doi.org/10.1126/science.1117368

Christiansen, C.T., Lafreniére, M.J., Henry, G.H.R., Grogan, P., 2018. Long-term deepened snow promotes tundra evergreen shrub growth and summertime ecosystem net CO2 gain but reduces soil carbon and nutrient pools. Glob. Chang. Biol. 24, 3508–3525. https://doi.org/10.1111/gcb.14084

Cowtan, K., Way, R.G., 2014. Coverage bias in the HadCRUT4 temperature series and its impact on recent temperature trends. Q. J. R. Meteorol. Soc. 140, 1935–1944. https://doi.org/10.1002/qj.2297

de Beurs, K.M., Henebry, G.M., Owsley, B.C., Sokolik, I., 2015. Using multiple remote sensing perspectives to identify and attribute land surface dynamics in Central Asia 2001-2013. Remote Sens. Environ. 170, 48–61. https://doi.org/10.1016/j.rse.2015.08.018

de Jong, R., Verbesselt, J., Zeileis, A., Schaepman, M., 2013. Shifts in Global Vegetation Activity Trends. Remote Sens. 5, 1117–1133. https://doi.org/10.3390/rs5031117

Dearborn, K.D., Danby, R.K., 2017. Aspect and slope influence plant community composition more than elevation across forest-tundra ecotones in subarctic Canada. J. Veg. Sci. 28, 595–604. https://doi.org/10.1111/jvs.12521

Drake, T.W., Holmes, R.M., Zhulidov, A. V., Gurtovaya, T., Raymond, P.A., McClelland, J.W., Spencer, R.G.M., 2019. Multidecadal climate-induced changes in Arctic tundra lake geochemistry and geomorphology. Limnol. Oceanogr. 64, S179–S191. https://doi.org/10.1002/lno.11015

Ecological Regions of the Northwest Territories - Northern Arctic, 2013. . Yellowknife.

Edwards, R., Treitz, P., 2017. Vegetation Greening Trends at Two Sites in the Canadian Arctic. Arctic, Antarct. Alp. Res. 49, 601–619. https://doi.org/10.1657/AAAR0016-075

Elmendorf, Sarah C, Henry, G.H.R., Hollister, R.D., 2012. Plot-scale evidence of tundra vegetation change and links to recent summer warming. Nat. Clim. Chang. 2. https://doi.org/10.1038/NCLIMATE1465

Elmendorf, Sarah C., Henry, G.H.R., Hollister, R.D., Björk, R.G., Bjorkman, A.D., Callaghan, T. V., Collier, L.S., Cooper, E.J., Cornelissen, J.H.C., Day, T.A., Fosaa, A.M., Gould, W.A., Grétarsdóttir, J., Harte, J., Hermanutz, L., Hik, D.S., Hofgaard, A., Jarrad, F., Jónsdóttir, I.S., Keuper, F., Klanderud, K., Klein, J.A., Koh, S., Kudo, G., Lang, S.I., Loewen, V., May, J.L., Mercado, J., Michelsen, A., Molau, U., Myers-Smith, I.H., Oberbauer, S.F., Pieper, S., Post, E., Rixen, C., Robinson, C.H., Schmidt, N.M., Shaver, G.R., Stenström, A., Tolvanen, A., Totland, Ø., Troxler, T., Wahren, C.H., Webber, P.J., Welker, J.M., Wookey, P.A., 2012. Global assessment

of experimental climate warming on tundra vegetation: Heterogeneity over space and time. Ecol. Lett. https://doi.org/10.1111/j.1461-0248.2011.01716.x

Elmendorf, S.C., Henry, G.H.R., Hollister, R.D., Fosaa, A.M., Gould, W.A., Hermanutz, L., Hofgaard, A., Jónsdóttir, I.S., Jónsdóttir, I.I., Jorgenson, J.C., Lévesque, E., Magnusson, B., Molau, U., Myers-Smith, I.H., Oberbauer, S.F., Rixen, C., Tweedie, C.E., Walker, M.D., Walker, M., 2015. Experiment, monitoring, and gradient methods used to infer climate change effects on plant communities yield consistent patterns. Proc. Natl. Acad. Sci. U. S. A. 112, 448–52. https://doi.org/10.1073/pnas.1410088112

Epstein, H.E., Walker, D.A., Raynolds, M.K., Jia, G.J., Kelley, A.M., 2008. Phytomass patterns across a temperature gradient of the North American arctic tundra. J. Geophys. Res. 113, G03S02. https://doi.org/10.1029/2007JG000555

Evans, J.S., 2020. spatialEco: Spatial Analysis and Modelling Utilities.

Fisher, J.I., Mustard, J.F., 2007. Cross-scalar satellite phenology from ground, Landsat, and MODIS data. Remote Sens. Environ. 109, 261–273. https://doi.org/10.1016/j.rse.2007.01.004

Foody, G.M., 2009. Classification accuracy comparison: Hypothesis tests and the use of confidence intervals in evaluations of difference, equivalence and non-inferiority. Remote Sens. Environ. 113, 1658–1663. https://doi.org/10.1016/j.rse.2009.03.014

Fraser, R.H., Lantz, T.C., Olthof, I., Kokelj, S. V., Sims, R.A., 2014. Warming-Induced Shrub Expansion and Lichen Decline in the Western Canadian Arctic. Ecosystems 17, 1151–1168. https://doi.org/10.1007/s10021-014-9783-3

Fraser, R.H., Olthof, I., Lantz, T.C., Schmitt, C., 2016. UAV photogrammetry for mapping vegetation in the low-Arctic. Arct. Sci. 2, 79–102. https://doi.org/10.1139/as-2016-0008

Frost, G. V., Epstein, H.E., Walker, D.A., Matyshak, G., Ermokhina, K., 2018. Seasonal and Long-Term Changes to Active-Layer Temperatures after Tall Shrubland Expansion and Succession in Arctic Tundra. Ecosystems 21, 507–520. https://doi.org/10.1007/s10021-017-0165-5

Fulton, R.J., 1989. Quaternary geology of Canada and Greenland. Quat. Geol. Canada Greenl. https://doi.org/10.1130/dnag-gna-k1

Greaves, H.E., Vierling, L.A., Eitel, J.U.H., Boelman, N.T., Magney, T.S., Prager, C.M., Griffin, K.L., 2016. High-resolution mapping of aboveground shrub biomass in Arctic tundra using airborne lidar and imagery. Remote Sens. Environ. 184. https://doi.org/10.1016/j.rse.2016.07.026

Hansen, B.B., Isaksen, K., Benestad, R.E., Kohler, J., Pedersen, Å., Loe, L.E., Coulson, S.J., Larsen, J.O., Varpe, Ø., 2014. Warmer and wetter winters: Characteristics and

implications of an extreme weather event in the High Arctic. Environ. Res. Lett. 9. https://doi.org/10.1088/1748-9326/9/11/114021

Harris, I., Jones, P.D., Osborn, T.J., Lister, D.H., 2014. Updated high-resolution grids of monthly climatic observations - the CRU TS3.10 Dataset. Int. J. Climatol. 34, 623–642. https://doi.org/10.1002/joc.3711

Harris, I., Osborn, T.J., Jones, P., Lister, D., 2020. Version 4 of the CRU TS monthly high-resolution gridded multivariate climate dataset. Sci. Data 7, 1–18. https://doi.org/10.1038/s41597-020-0453-3

Hermosilla, T., Wulder, M.A., White, J.C., Coops, N.C., Hobart, G.W., 2015. An integrated Landsat time series protocol for change detection and generation of annual gap-free surface reflectance composites. Remote Sens. Environ. 158, 220–234. https://doi.org/10.1016/j.rse.2014.11.005

Hermosilla, T., Wulder, M.A., White, J.C., Coops, N.C., Hobart, G.W., Campbell, L.C., 2016. Mass data processing of time series Landsat imagery: pixels to data products for forest monitoring. Int. J. Digit. Earth. https://doi.org/10.1080/17538947.2016.1187673

Huete, A., Didan, K., Miura, T., Rodriguez, E.P., Gao, X., Ferreira, L.G., 2002. Overview of the radiometric and biophysical performance of the MODIS vegetation indices. Remote Sens. Environ. 83, 195–213. https://doi.org/10.1016/S0034-4257(02)00096-2

Jeong, J.H., Resop, J.P., Mueller, N.D., Fleisher, D.H., Yun, K., Butler, E.E., Timlin, D.J., Shim, K.-M., Gerber, J.S., Reddy, V.R., Kim, S.-H., 2016. Random Forests for Global and Regional Crop Yield Predictions. PLoS One 11, e0156571. https://doi.org/10.1371/journal.pone.0156571

Jia, G.J., Epstein, H.E., Walker, D.A., 2009. Vegetation greening in the canadian arctic related to decadal warming. J. Environ. Monit. 11, 2231–2238. https://doi.org/10.1039/b911677j

Jorgenson, J.C., Jorgenson, M.T., Boldenow, M.L., Orndahl, K.M., 2018. Landscape change detected over a half century in the Arctic National Wildlife Refuge using high-resolution aerial imagery. Remote Sens. 10, 1305. https://doi.org/10.3390/RS10081305

Jorgenson, M., Frost, G., Dissing, D., 2018. Drivers of Landscape Changes in Coastal Ecosystems on the Yukon-Kuskokwim Delta, Alaska. Remote Sens. 10, 1280. https://doi.org/10.3390/rs10081280

Ju, J., Masek, J.G., 2016. The vegetation greenness trend in Canada and US Alaska from 1984–2012 Landsat data. Remote Sens. Environ. 176, 1–16. https://doi.org/10.1016/J.RSE.2016.01.001

Kuhn, M., 2020. caret: Classification and Regression Training.

Kwon, H.J., Oechel, W.C., Zulueta, R.C., Hastings, S.J., 2006. Effects of climate variability on carbon sequestration among adjacent wet sedge tundra and moist tussock tundra ecosystems. J. Geophys. Res. Biogeosciences 111. https://doi.org/10.1029/2005JG000036

Lakens, D., 2017. Equivalence Tests: A Practical Primer for t Tests, Correlations, and Meta-Analyses. http://dx.doi.org/10.1177/1948550617697177. https://doi.org/10.1177/1948550617697177

Lantz, T.C., Kokelj, S. V., Fraser, R.H., 2015. Ecological recovery in an Arctic delta following widespread saline incursion. Ecol. Appl. 25, 172–185. https://doi.org/10.1890/14-0239.1

Lantz, T.C., Marsh, P., Kokelj, S. V., 2013. Recent Shrub Proliferation in the Mackenzie Delta Uplands and Microclimatic Implications. Ecosystems 16, 47–59. https://doi.org/10.1007/s10021-012-9595-2

Liaw, A., Wiener, M., 2018. randomForest: Breiman and Cutler's Random Forests for Classification and Regression.

Liljedahl, A.K., Boike, J., Daanen, R.P., Fedorov, A.N., Frost, G. V., Grosse, G., Hinzman, L.D., Iijma, Y., Jorgenson, J.C., Matveyeva, N., Necsoiu, M., Raynolds, M.K., Romanovsky, V.E., Schulla, J., Tape, K.D., Walker, D.A., Wilson, C.J., Yabuki, H., Zona, D., 2016. Pan-Arctic ice-wedge degradation in warming permafrost and its influence on tundra hydrology. Nat. Geosci. 9, 312–318. https://doi.org/10.1038/ngeo2674

Liu, N., Treitz, P., 2018. Remote sensing of Arctic percent vegetation cover and fAPAR on Baffin Island, Nunavut, Canada. Int. J. Appl. Earth Obs. Geoinf. 71, 159–169. https://doi.org/10.1016/j.jag.2018.05.011

Loranty, M.M., Lieberman-Cribbin, W., Berner, L.T., Natali, S.M., Goetz, S.J., Alexander, H.D., Kholodov, A.L., 2016. Spatial variation in vegetation productivity trends, fire disturbance, and soil carbon across arctic-boreal permafrost ecosystems. Environ. Res. Lett. https://doi.org/10.1088/1748-9326/11/9/095008

Mann, H.B., 1945. Nonparametric Tests Against Trend. Econometrica 13, 245. https://doi.org/10.2307/1907187

Martin, A., Jeffers, E., Petrokofsky, G., Myers-Smith, I., Macias-Fauria, M., 2017. Shrub growth and expansion in the Arctic tundra: an assessment of controlling factors using an evidence-based approach. Environ. Res. Lett. 12.

Mcguire, A.D., Anderson, L.G., Christensen, T.R., Scott, D., Laodong, G., Hayes, D.J., Martin, H., Lorenson, T.D., Macdonald, R.W., Nigel, R., 2009. Sensitivity of the carbon cycle in the Arctic to climate change. Ecol. Monogr.

https://doi.org/10.1890/08-2025.1

McLeod, A.I., 2011. Kendall: Kendall rank correlation and Mann-Kendall trend test.

McManus, K.M., Morton, D.C., Masek, J.G., Wang, D., Sexton, J.O., Nagol, J.R., Ropars, P., Boudreau, S., 2012. Satellite-based evidence for shrub and graminoid tundra expansion in northern Quebec from 1986 to 2010. Glob. Chang. Biol. 18, 2313–2323. https://doi.org/10.1111/j.1365-2486.2012.02708.x

Moffat, N.D., Lantz, T.C., Fraser, R.H., Olthof, I., 2016. Recent Vegetation Change (1980–2013) in the Tundra Ecosystems of the Tuktoyaktuk Coastlands, NWT, Canada. Arctic, Antarct. Alp. Res. https://doi.org/10.1657/AAAR0015-063

Myers-Smith, I.H., Elmendorf, S.C., Beck, P.S.A., Wilmking, M., Hallinger, M., Blok, D., Tape, K.D., Rayback, S.A., Macias-Fauria, M., Forbes, B.C., Speed, J.D.M., Boulanger-Lapointe, N., Rixen, C., Lévesque, E., Schmidt, N.M., Baittinger, C., Trant, A.J., Hermanutz, L., Collier, L.S., Dawes, M.A., Lantz, T.C., Weijers, S., JØrgensen, R.H., Buchwal, A., Buras, A., Naito, A.T., Ravolainen, V., Schaepman-Strub, G., Wheeler, J.A., Wipf, S., Guay, K.C., Hik, D.S., Vellend, M., 2015. Climate sensitivity of shrub growth across the tundra biome. Nat. Clim. Chang. 5, 887–891. https://doi.org/10.1038/nclimate2697

Myers-Smith, Isla H, Forbes, B.C., Wilmking, M., Hallinger, M., Lantz, T., Blok, D., Tape, K.D., Macias-Fauria, M., Sass-Klaassen, U., Lévesque, E., Boudreau, S., Ropars, P., Hermanutz, L., Trant, A., Collier, L.S., Weijers, S., Rozema, J., Rayback, S.A., Schmidt, N.M., Schaepman-Strub, G., Wipf, S., Rixen, C., Ménard, C.B., Venn, S., Goetz, S., Andreu-Hayles, L., Elmendorf, S., Ravolainen, V., Welker, J., Grogan, P., Epstein, H.E., Hik, D.S., 2011. Shrub expansion in tundra ecosystems: dynamics, impacts and research priorities. Environ. Res. Lett. 6, 045509. https://doi.org/10.1088/1748-9326/6/4/045509

Myers-Smith, I.H., Hik, D.S., 2018. Climate warming as a driver of tundra shrubline advance. J. Ecol. 106, 547–560. https://doi.org/10.1111/1365-2745.12817

Myers-Smith, Isla H., Hik, D.S., Kennedy, C., Cooley, D., Johnstone, J.F., Kenney, A.J., Krebs, C.J., 2011. Expansion of canopy-forming willows over the twentieth century on Herschel Island, Yukon Territory, Canada. Ambio 40, 610–623. https://doi.org/10.1007/s13280-011-0168-y

Myers-Smith, I.H., Grabowski, M.M., Thomas, H.J.D., Angers-Blondin, S., Daskalova, G.N., Bjorkman, A.D., Cunliffe, A.M., Assmann, J.J., Boyle, J.S., McLeod, E., McLeod, S., Joe, R., Lennie, P., Arey, D., Gordon, R.R., Eckert, C.D., 2019. Eighteen years of ecological monitoring reveals multiple lines of evidence for tundra vegetation change. Ecol. Monogr. 89, e01351. https://doi.org/10.1002/ecm.1351

Oberbauer, S.F., Tweedie, C.E., Welker, J.M., Fahnestock, J.T., Henry, G.H.R., Webber, P.J., Hollister, R.D., Walker, M.D., Kuchy, A., Elmore, E., Starr, G., 2007. Tundra CO2 fluxes in response to experimental warming across latitudinal and moisture

gradients. Ecol. Monogr. 77, 221–238. https://doi.org/10.1890/06-0649

Ohse, B., Ohse, B., Jansen, F., Wilmking, M., 2012. Do limiting factors at Alaskan treelines shift with climatic regimes? Environ. Res. Lett. 7. https://doi.org/10.1088/1748-9326/7/1/015505

Olthof, I., Fraser, R.H., 2007. Mapping northern land cover fractions using Landsat ETM+. Remote Sens. Environ. 107, 496–509. https://doi.org/10.1016/j.rse.2006.10.009

Olthof, I., Latifovic, R., Pouliot, D., 2009. Development of a circa 2000 land cover map of northern canada at 30 m resolution from landsat. Can. J. Remote Sens. 35, 152–165. https://doi.org/10.5589/m09-007

Overland, J.E., Wang, M., 2016. Recent extreme arctic temperatures are due to a split polar vortex. J. Clim. 29, 5609–5616. https://doi.org/10.1175/JCLI-D-16-0320.1

Pedlar, J.H., McKenney, D.W., Lawrence, K., Papadopol, P., Hutchinson, M.F., Price, D., 2015. A comparison of two approaches for generating spatial models of growing-season variables for Canada. J. Appl. Meteorol. Climatol. 54, 506–518. https://doi.org/10.1175/JAMC-D-14-0045.1

Phoenix, G.K., Bjerke, J.W., 2016. Arctic browning: extreme events and trends reversing arctic greening. Glob. Chang. Biol. 22, 2960–2962. https://doi.org/10.1111/gcb.13261

Pithan, F., Mauritsen, T., 2014. Arctic amplification dominated by temperature feedbacks in contemporary climate models. Nat. Geosci. 7, 181–184. https://doi.org/10.1038/ngeo2071

Raynolds, M.K., Comiso, J.C., Walker, D.A., Verbyla, D., 2008. Relationship between satellite-derived land surface temperatures, arctic vegetation types, and NDVI. Remote Sens. Environ. 112, 1884–1894. https://doi.org/10.1016/j.rse.2007.09.008

Raynolds, M.K., Walker, D.A., 2009. Effects of deglaciation on circumpolar distribution of arctic vegetation. Can. J. Remote Sens. 35, 118–129. https://doi.org/10.5589/m09-006

Raynolds, M.K., Walker, D.A., Maier, H.A., 2006. NDVI patterns and phytomass distribution in the circumpolar Arctic. Remote Sens. Environ. 102, 271–281. https://doi.org/10.1016/j.rse.2006.02.016

Reichle, L.M., Epstein, H.E., Bhatt, U.S., Raynolds, M.K., Walker, D.A., 2018. Spatial Heterogeneity of the Temporal Dynamics of Arctic Tundra Vegetation. Geophys. Res. Lett. 45, 9206–9215. https://doi.org/10.1029/2018GL078820

Rickbeil, G.J.M., Hermosilla, T., Coops, N.C., White, J.C., Wulder, M.A., Lantz, T.C., 2018. Changing northern vegetation conditions are influencing barren ground

caribou (Rangifer tarandus groenlandicus) post-calving movement rates. J. Biogeogr. 45, 702–712. https://doi.org/10.1111/jbi.13161

Rocha, A. V., Blakely, B., Jiang, Y., Wright, K.S., Curasi, S.R., 2018. Is arctic greening consistent with the ecology of tundra? Lessons from an ecologically informed mass balance model. Environ. Res. Lett. 13, 125007. https://doi.org/10.1088/1748-9326/aaeb50

Ropars, P., Boudreau, S., 2012. Shrub expansion at the foresttundra ecotone: Spatial heterogeneity linked to local topography. Environ. Res. Lett. 7. https://doi.org/10.1088/1748-9326/7/1/015501

Ropars, P., Lévesque, E., Boudreau, S., 2015. How do climate and topography influence the greening of the forest-tundra ecotone in northern Québec? A dendrochronological analysis of *Betula glandulosa*. J. Ecol. 103, 679–690. https://doi.org/10.1111/1365-2745.12394

Roser, L., Vilardi, J., Saidman, B., Ferreyra, L., 2020. EcoGenetics: Management and Exploratory Analysis of Spatial Data in Landscape Genetics.

Rozema, J., Weijers, S., Broekman, R., Blokker, P., Buizer, B., Werleman, C., Yaqine, H. El, Hoogedoorn, H., Fuertes, M.M., Cooper, E., 2009. Annual growth of Cassiope tetragona as a proxy for Arctic climate: developing correlative and experimental transfer functions to reconstruct past summer temperature on a millennial time scale. Glob. Chang. Biol. 15, 1703–1715. https://doi.org/10.1111/j.1365-2486.2009.01858.x

Schaefer, K., Zhang, T., Bruhwiler, L., Barrett, A.P., 2011. Amount and timing of permafrost carbon release in response to climate warming. Chem. Phys. Meteorol. 63, 165–180. https://doi.org/10.1111/j.1600-0889.2010.00527.x

Schut, A.G.T., Ivits, E., Conijn, J.G., ten Brink, B., Fensholt, R., 2015. Trends in Global Vegetation Activity and Climatic Drivers Indicate a Decoupled Response to Climate Change. PLoS One 10, e0138013. https://doi.org/10.1371/journal.pone.0138013

Schuur, E.A.G., McGuire, A.D., Schädel, C., Grosse, G., Harden, J.W., Hayes, D.J., Hugelius, G., Koven, C.D., Kuhry, P., Lawrence, D.M., Natali, S.M., Olefeldt, D., Romanovsky, V.E., Schaefer, K., Turetsky, M.R., Treat, C.C., Vonk, J.E., 2015. Climate change and the permafrost carbon feedback. Nature. https://doi.org/10.1038/nature14338

Sen, P.K., 1968. Estimates of the Regression Coefficient Based on Kendall's Tau. J. Am. Stat. Assoc. 63, 1379–1389. https://doi.org/10.1080/01621459.1968.10480934

Serreze, M.C., Walsh, J.E., Chapin, F.S., Osterkamp, T., Dyurgerov, M., Romanovsky, V., Oechel, W.C., Morison, J., Zhang, T., Barry, R.G., 2000. Observational evidence of recent change in the northern high-latitude environment. Clim. Change 46, 159–207. https://doi.org/10.1023/A:1005504031923

Silapaswan, C.S., Verbyla, D.L., Mc Guire, A.D., 2001. Land cover change on the seward peninsula: The use of remote sensing to evaluate the potential influences of climate warming on historical vegetation dynamics. Can. J. Remote Sens. 27, 542–554. https://doi.org/10.1080/07038992.2001.10854894

Smith, C.A.S., Meikle, J.C., Roots, C.F., 2004. Ecoregions of the Yukon Territory: Biophysical properties of Yukon landscapes. Summerland, BC.

Stocker, T.F., Qin, D., Plattner, G.-K., Tignor, M.M.B., Allen, S.K., Boschung, J., Nauels, A., Xia, Y., Bex, V., Midgley, P.M., 2013. The Physical Science Basis: Working Group I Contribution to the Fifth Assessment Report of the Intergovernmental Panel on Climate Change.

Sulla-Menashe, D., Woodcock, C.E., Friedl, M.A., 2018. Canadian boreal forest greening and browning trends: An analysis of biogeographic patterns and the relative roles of disturbance versus climate drivers. Environ. Res. Lett. 13. https://doi.org/10.1088/1748-9326/aa9b88

Svoboda, J., R Henry, G.H., 1987. Succession in Marginal Arctic Environments. Arct. Alp. Res. 19, 373–384. https://doi.org/10.1080/00040851.1987.12002618

Swanson, D., 2017. Trends in Greenness and Snow Cover in Alaska's Arctic National Parks, 2000–2016. Remote Sens. 9, 514. https://doi.org/10.3390/rs9060514

Syndonia Bret-Harte, M., Mack, M.C., Shaver, G.R., Huebner, D.C., Johnston, M., Mojica, C.A., Pizano, C., Reiskind, J.A., n.d. The response of Arctic vegetation and soils following an unusually severe tundra fire. https://doi.org/10.1098/rstb.2012.0490

Tape, K.D., Hallinger, M., Welker, J.M., Ruess, R.W., 2012. Landscape Heterogeneity of Shrub Expansion in Arctic Alaska. Ecosystems 15, 711–724. https://doi.org/10.1007/s10021-012-9540-4

Tarnocai, C., 2004. Classification of Cryosols in Canada, in: Cryosols. Springer Berlin Heidelberg, pp. 599–610. https://doi.org/10.1007/978-3-662-06429-0_30

Timoney, K.P., La Roi, G.H., Zoltai, S.C., Robinson, A.L., 1992. The high subarctic forest-tundra of northwestern Canada: position, width, and vegetation gradients in relation to climate. Arctic 45, 1–9. https://doi.org/10.14430/arctic1367

Travers-Smith, H., Lantz, T.C., 2020. Leading edge disequilibrium in sub-Arctic alder and spruce populations. Ecosphere.

Tremblay, B., Lévesque, E., Boudreau, S., 2012. Recent expansion of erect shrubs in the Low Arctic: evidence from Eastern Nunavik. Environ. Res. Lett. 7, 035501. https://doi.org/10.1088/1748-9326/7/3/035501

Tsuyuzaki, S., Iwahana, G., Saito, K., 2017. Tundra fire alters vegetation patterns more

than the resultant thermokarst. Polar Biol. 1–9. https://doi.org/10.1007/s00300-017-2236-7

Tunes da Silva, G., Logan, B.R., Klein, J.P., 2009. Methods for Equivalence and Noninferiority Testing. Biol. Blood Marrow Transplant. 15, 120–127. https://doi.org/10.1016/j.bbmt.2008.10.004

Van Hemert, C., Flint, P.L., Udevitz, M.S., Koch, J.C., Atwood, T.C., Oakley, K.L., Pearce, J.M., 2015. Forecasting Wildlife Response to Rapid Warming in the Alaskan Arctic. Bioscience. https://doi.org/10.1093/biosci/biv069

Verbyla, D., 2011. Browning boreal forests of western North America. Environ. Res. Lett. 6, 041003. https://doi.org/10.1088/1748-9326/6/4/041003

Vermaire, J.C., Pisaric, M.F.J., Thienpont, J.R., Courtney Mustaphi, C.J., Kokelj, S. V., Smol, J.P., 2013. Arctic climate warming and sea ice declines lead to increased storm surge activity. Geophys. Res. Lett. 40, 1386–1390. https://doi.org/10.1002/grl.50191

Vincent, L.A., Zhang, X., Brown, R.D., Feng, Y., Mekis, E., Milewska, E.J., Wan, H., Wang, X.L., 2015. Observed trends in Canada's climate and influence of low-frequency variability modes. J. Clim. 28, 4545–4560. https://doi.org/10.1175/JCLI-D-14-00697.1

Wahren, C.H.A., Walker, M.D., Bret-Harte, M.S., 2005. Vegetation responses in Alaskan arctic tundra after 8 years of a summer warming and winter snow manipulation experiment. Glob. Chang. Biol. 11, 537–552. https://doi.org/10.1111/j.1365-2486.2005.00927.x

Walker, D.A., Raynolds, M.K., Daniëls, F.J.A., Einarsson, E., Elvebakk, A., Gould, W.A., Katenin, A.E., Kholod, S.S., Markon, C.J., Melnikov, E.S., Moskalenko, N.G., Talbot, S.S., Yurtsev, B.A.., The other members of the CAVM Team, 2005. The Circumpolar Arctic vegetation map. J. Veg. Sci. 16, 267–282. https://doi.org/10.1111/j.1654-1103.2005.tb02365.x

Walker, M.D., Wahren, C.H., Hollister, R.D., Henry, G.H.R., Ahlquist, L.E., Alatalo, J.M., Bret-Harte, M.S., Calef, M.P., Callaghan, T. V, Carroll, A.B., Epstein, H.E., Jónsdóttir, I.S., Klein, J.A., Magnússon, B., Molau, U., Oberbauer, S.F., Rewa, S.P., Robinson, C.H., Shaver, G.R., Suding, K.N., Thompson, C.C., Tolvanen, A., Totland, Ø., Turner, P.L., Tweedie, C.E., Webber, P.J., Wookey, P.A., 2006. Plant community responses to experimental warming across the tundra biome. Proc. Natl. Acad. Sci. U. S. A. 103, 1342–6. https://doi.org/10.1073/pnas.0503198103

Weijers, S., Buchwal, A., Blok, D., Löffler, J., Elberling, B., 2017. High Arctic summer warming tracked by increased *Cassiope tetragona* growth in the world's northernmost polar desert. Glob. Chang. Biol. 23, 5006–5020. https://doi.org/10.1111/gcb.13747

Weston, S., 2020. foreach: Provides Foreach Looping Construct.

Weston, S., 2019. doParallel: Foreach Parallel Adaptor for the “parallel” Package.

White, J.C., Wulder, M.A., Hobart, G.W., Luther, J.E., Hermosilla, T., Griffiths, P., Coops, N.C., Hall, R.J., Hostert, P., Dyk, A., Guindon, L., White, ©j C, 2014. Pixel-Based Image Compositing for Large-Area Dense Time Series Applications and Science. Can. J. Remote Sens. 40, 192–212. https://doi.org/10.1080/07038992.2014.945827

Wickham, H., Averick, M., Bryan, J., Chang, W., McGowan, L.D., François, R., Grolemund, G., Hayes, A., Henry, L., Hester, J., Kuhn, M., Pedersen, T.L., Miller, E., Bache, S.M., Müller, K., Ooms, J., Robinson, D., Seidel, D.P., Spinu, V., Takahashi, K., Vaughan, D., Wilke, C., Woo, K., Yutani, H., 2019. Welcome to the {tidyverse}. J. Open Source Softw. 4, 1686. https://doi.org/10.21105/joss.01686

Wickham, H., François, R., Henry, L., Müller, K., 2020. dplyr: A Grammar of Data Manipulation.

Wilcox, E.J., Keim, D., de Jong, T., Walker, B., Sonnentag, O., Sniderhan, A.E., Mann, P., Marsh, P., 2019. Tundra shrub expansion may amplify permafrost thaw by advancing snowmelt timing. Arct. Sci. 5, 202–217. https://doi.org/10.1139/as-2018-0028

Wolter, J., Lantuit, H., Herzschuh, U., Stettner, S., Fritz, M., 2017. Tundra vegetation stability versus lake-basin variability on the Yukon Coastal Plain (NW Canada) during the past three centuries. The Holocene 27, 1846–1858. https://doi.org/10.1177/0959683617708441

Wulder, M.A., Loveland, T.R., Roy, D.P., Crawford, C.J., Masek, J.G., Woodcock, C.E., Allen, R.G., Anderson, M.C., Belward, A.S., Cohen, W.B., Dwyer, J., Erb, A., Gao, F., Griffiths, P., Helder, D., Hermosilla, T., Hipple, J.D., Hostert, P., Hughes, M.J., Huntington, J., Johnson, D.M., Kennedy, R., Kilic, A., Li, Z., Lymburner, L., McCorkel, J., Pahlevan, N., Scambos, T.A., Schaaf, C., Schott, J.R., Sheng, Y., Storey, J., Vermote, E., Vogelmann, J., White, J.C., Wynne, R.H., Zhu, Z., 2019. Current status of Landsat program, science, and applications. Remote Sens. Environ. 225, 127–147. https://doi.org/10.1016/j.rse.2019.02.015

Xiao, X., Zhang, Q., Hollinger, D., Aber, J., Berrien, M., 2005. Modeling gross primary production of an evergreen needleleaf forest using modis and climate data. Ecol. Appl. 15, 954–969. https://doi.org/10.1890/04-0470

Zhu, Z., and Woodcock, C. E. (2012). Object-based cloud and cloud shadow detection in Landsat imagery. Remote Sensing of Environment, 118, 83–94. https://doi.org/10.1016/j.rse.2011.10.028

4 Conclusion

4.1 Study Synthesis

The objective of my MSc research was to understand the response of Arctic tundra vegetation to ongoing climate change and more severe tundra fire. In Chapters 2 and 3 of this thesis I conducted two independent studies to meet this objective and enhance our understanding of tundra vegetation dynamics.

In Chapter 2, I used remote sensing and field observations of biotic and abiotic recovery to evaluate how tundra landscapes are responding to increasing burn severity. Specifically, I calculated the differenced Normalized Burn Ratio and used it to classify moderate and severely burned areas and adjacent unburned controls at six recent tundra fires in the Northwest Territories. Field sampling was used to investigate variation in plant community composition and edaphic conditions across severity classes. My results demonstrate that tundra plant communities are resilient to lower severity fire and experienced rapid recovery of aboveground biomass, but indicate that severe fire still alters vegetation structure, community composition, and soils after six years and may have ongoing effects on long-term vegetation recovery. My work also suggests that severe tundra may promote the success of deciduous shrub tundra on decadal scales, but additional monitoring is required to evaluate the stability of deciduous shrub tundra communities under ongoing fire regime change.

In Chapter 3, I utilized the Landsat satellite archive to calculate trends in the Enhanced Vegetation Index (EVI) from 1984-2016 across a study area spanning the western Canadian Arctic from the Yukon Coast to the western Arctic Archipelago. I found that two-thirds of the western Canadian Arctic experienced significant increases in vegetation

productivity from 1984-2016. The most rapid change occurred in the Low Arctic region and was associated with lower elevation, moderately sloping terrain, and areas dominated by upright shrubs. Climate warming is widespread across the Arctic, but the biophysical controls that mediate how tundra vegetation responds to warming are heterogeneous. Using Random Forests modelling, I also showed that changes in tundra vegetation productivity are mediated by differences among plant functional types and localized variations in biophysical properties. The role that topography (slope, elevation, and aspect), microclimate, and moisture can have on finer-scale tundra vegetation change demonstrates the complex interactions that can occur between climate warming and regional and landscape biophysical variation.

Overall, my thesis research indicates that ongoing warming (Vincent et al., 2015) and more frequent and intense tundra fires (Wang et al. 2020) will contribute to the increased dominance of deciduous shrubs across the tundra biome (Elmendorf, Henry, Hollister, et al., 2012; Lantz et al., 2013; Myers-Smith, et al., 2011). My findings in Chapter 2 show shrub tundra communities are resilient to fire and that under current tundra fire regimes in the Northwest Territories they are anticipated to prevail following fire disturbance. My findings in Chapter 3 show that some of the most drastic rates of greening being experienced in the past three decades in the western Canadian Arctic (Yukon, Northwest Territories, western Nunavut) are being driven by increased productivity at shrub-dominated sites.

4.2 Limitations and Future Research Opportunities

My thesis research makes an important contribution our understanding of the dynamics of tundra ecosystems, but it has several limitations, which provide opportunities for future research.

In Chapter 2, I generated burn severity maps for all six of the fire sites visited, but limitations in time and financial resources restricted the number of sites within each burn and total area that could be visited in the field. Tundra ecosystems are heterogeneous at fine scales (He et al., 2019) and it is likely that additional sampling could bridge the gap in spatial discrepancies between satellite and field data. Collection of unmanned aerial vehicle (UAV) imagery was conducted at all six of my fire sites and these 1.5-3 cm resolution surveys provide a very high-resolution dataset for future spatial analysis and to evaluate finer scale patterns in burn severity and recovery. My research is one of the only studies on the effects of tundra fire in the western Canadian Arctic, but the fact that all of the fires we sampled burned in 2012 leaves considerable uncertainty regarding longer term successional trajectories (Lantz et al., 2010). The rapid resprouting success of deciduous shrubs, combined with conditions known to promote their growth (Bret-Harte et al., 2001; Racine et al., 2004; Schuur et al., 2007), suggest that deciduous shrub communities will dominate tundra landscapes. However, ongoing monitoring is required to track successional change on decadal scales (Moritz et al., 2012). While deciduous shrub tundra may thrive under current climate and fire regimes, the stability of shrub communities remains uncertain in the face of a warming Arctic. The nature of my field season limited my ability to evaluate the rates of above and belowground recovery and monitor progress over time. Longer-term monitoring to quantify continued recovery at these sites is

necessary to better understand the long-term response of tundra communities to severe burning and the impacts of changing fire regimes in the western Canadian Arctic. The installation of two thermistors in each of the six different tundra fires (n=12) provides a potential opportunity for future monitoring to assess the rate of abiotic recovery. Repeat UAV surveys can allow for ongoing fine-scale monitoring and also account for heterogeneity that is unresolved by coarser satellite surveying (Siewert and Olofsson, 2020).

In Chapter 3, I demonstrated the application of RF modelling for understanding the relationships between multi-decadal greening trends and different biophysical properties at the landscape-scale. Greening was widespread across the western Canadian Arctic, but a national scale investigation that captures trends in the eastern Canadian Arctic may allow for a more comprehensive evaluation of relationships between productivity trends, warming, and biophysical properties. Furthermore, my analysis focused on greening trends, but there is an opportunity to build on this study by evaluating browning trends as well as interannual variability and finer-scale moisture variation. The underlying causes of greening and browning trends across the Circumpolar Arctic remain highly uncertain (Myers-Smith et al., 2020) and future research that investigates interannual variability may reveal patterns that are not captured by long-term trend analysis.

The spatial scale of the satellite imagery I utilized in both Chapter 2 and 3 of my thesis also limited fine-scale analysis. In both studies, remote sensing analyses utilized Landsat data, which has a resolution of 30 m. In Chapter 2, my field observations suggest the Normalized Burn Ratio calculated using Landsat oversimplified fine-scale differences in burn severity. Previous comparisons of plot-scale field observations and landscape-scale satellite

observations have found that measurements of increased productivity from the field may not always be detectable using remote sensing (Goetz et al., 2019). Additionally, the spatial resolution of Landsat has limited ability to capture shifts in dominant plant species and functional groups (Wang et al., 2019), making Landsat insufficient for conducting ongoing monitoring of vegetation responses to disturbance or for evaluating shifts in vegetation structure. In Chapter 3, I found that variation in moisture, terrain, and microclimate influenced changes in vegetation productivity. However, tundra ecosystems are known to exhibit variation at spatial scales less than 1 m (Assmann et al., 2020) and it is likely that Landsat-scale imagery may be insufficient for quantifying variation in biophysical factors at the appropriate scale. The recent developments of satellite platforms (Sentinel-2, CubeSat) with higher spatial (<30 m) and temporal (<5 days) resolution enables the generation of more detailed vegetation indices (Normalized Burn Ratio, Normalized Differenced Vegetation Index, Enhanced Vegetation Index) imagery. I recommend that future research utilize these data sources to better evaluate finer scale variations in vegetation change. As higher resolution platforms are developed and becoming more readily available for ecological research (Riihimäki et al., 2019), there will also be greater opportunities for future monitoring to incorporate both high spatial and temporal resolution data. My research contributes to the ongoing effort to understand the relationships between climate change, disturbance, vegetation change, and biophysical properties of tundra landscapes. Continued monitoring of fine-scale changes and multi-scale research is necessary to improve our understanding on the long-term dynamics of tundra communities under future climate change.

Bibliography

Assmann, J. J., Myers-Smith, I. H., Kerby, J., Cunliffe, A., and Daskalova, G. (2020). *Drone data reveal heterogeneity in tundra greenness and phenology not captured by satellites*. https://doi.org/10.32942/osf.io/tqekn

Barrett, K., Rocha, A. V, Van De Weg, J., and Shaver, G. (2012). Vegetation shifts observed in arctic tundra 17 years after fire. *Remote Sensing Letters*, *3*(8), 729–736. https://doi.org/10.1080/2150704X.2012.676741

Bhatt, U., Walker, D., Raynolds, M., Bieniek, P., Epstein, H., Comiso, J., Pinzon, J., Tucker, C., and Polyakov, I. (2013). Recent Declines in Warming and Vegetation Greening Trends over Pan-Arctic Tundra. *Remote Sensing*, *5*(9), 4229–4254. https://doi.org/10.3390/rs5094229

Blok, D., Heijmans, M. M. P. D., Schaepman-Strub, G., Kononov, A. V., Maximov, T. C., and Berendse, F. (2010). Shrub expansion may reduce summer permafrost thaw in Siberian tundra. *Global Change Biology*, *16*(4). https://doi.org/10.1111/j.1365-2486.2009.02110.x

Blok, D., Schaepman-Strub, G., Bartholomeus, H., Heijmans, M. P. D., Maximov, T. C., and Berendse, F. (2011). The response of Arctic vegetation to the summer climate: Relation between shrub cover, NDVI, surface albedo and temperature. *Environmental Research Letters*, *6*(3). https://doi.org/10.1088/1748-9326/6/3/035502

Bret-Harte, S. M., Shaver, G. R., Zoerner, J. P., Johnstone, J. F., Wagner, J. L., Chavez, A. S., Gunkelman Iv, R. F., Lippert, S. C., and Laundre, J. A. (2001). DEVELOPMENTAL PLASTICITY ALLOWS BETULA NANA TO DOMINATE TUNDRA SUBJECTED TO AN ALTERED ENVIRONMENT. In *Ecology* (Vol. 82, Issue 1). https://doi.org/10.1890/0012-9658(2001)082[0018:DPABNT]2.0.CO;2

Bush, E., and Lemmen, D. S. (2019). *Canada's Changing Climate Report*. http://www.changingclimate.ca/CCCR2019

Drake, T. W., Holmes, R. M., Zhulidov, A. V., Gurtovaya, T., Raymond, P. A., McClelland, J. W., and Spencer, R. G. M. (2019). Multidecadal climate-induced changes in Arctic tundra lake geochemistry and geomorphology. *Limnology and Oceanography*, *64*(S1), S179–S191. https://doi.org/10.1002/lno.11015

Elmendorf, S. C., Henry, G. H. R., and Hollister, R. D. (2012). Plot-scale evidence of tundra vegetation change and links to recent summer warming. *Nature Climate Change*, *2*. https://doi.org/10.1038/NCLIMATE1465

Elmendorf, S. C., Henry, G. H. R., Hollister, R. D., Björk, R. G., Bjorkman, A. D., Callaghan, T. V., Collier, L. S., Cooper, E. J., Cornelissen, J. H. C., Day, T. A., Fosaa, A. M., Gould, W. A., Grétarsdóttir, J., Harte, J., Hermanutz, L., Hik, D. S., Hofgaard, A., Jarrad, F., Jónsdóttir, I. S., … Wookey, P. A. (2012). Global

assessment of experimental climate warming on tundra vegetation: Heterogeneity over space and time. In *Ecology Letters*. https://doi.org/10.1111/j.1461-0248.2011.01716.x

Hanes, C. C., Wang, X., Jain, P., Parisien, M.-A., Little, J. M., and Flannigan, M. D. (2019). Fire-regime changes in Canada over the last half century. *Canadian Journal of Forest Research*, *49*(3), 256–269. https://doi.org/10.1139/cjfr-2018-0293

He, J., Loboda, T. V., Jenkins, L., and Chen, D. (2019). Mapping fractional cover of major fuel type components across Alaskan tundra. *Remote Sensing of Environment*, *232*, 111324. https://doi.org/10.1016/j.rse.2019.111324

Hu, F. S., Brubaker, L. B., Gavin, D. G., Higuera, P. E., Lynch, J. A., Rupp, T. S., and Tinner, W. (2006). How climate and vegetation influence the fire regime of the Alaskan boreal biome: The Holocene perspective. *Mitigation and Adaptation Strategies for Global Change*, *11*(4), 829–846. https://doi.org/10.1007/s11027-005-9015-4

Jia, G. J., Epstein, H. E., and Walker, D. A. (2009). Vegetation greening in the canadian arctic related to decadal warming. *Journal of Environmental Monitoring*, *11*(12), 2231–2238. https://doi.org/10.1039/b911677j

Jiang, Y., Rocha, A. V., O'Donnell, J. A., Drysdale, J. A., Rastetter, E. B., Shaver, G. R., and Zhuang, Q. (2015). Contrasting soil thermal responses to fire in Alaskan tundra and boreal forest. *Journal of Geophysical Research: Earth Surface*, *120*(2), 363–378. https://doi.org/10.1002/2014JF003180

Jones, B. M., Grosse, G., Arp, C. D., Miller, E., Liu, L., Hayes, D. J., and Larsen, C. F. (2015). Recent Arctic tundra fire initiates widespread thermokarst development. *Scientific Reports*, *5*, 15865. https://doi.org/10.1038/srep15865

Ju, J., and Masek, J. G. (2016). The vegetation greenness trend in Canada and US Alaska from 1984-2012 Landsat data. *Remote Sensing of Environment*, *176*. https://doi.org/10.1016/j.rse.2016.01.001

Lantz, T. C., Gergel, S. E., and Henry, G. H. R. (2010). Response of green alder (Alnus viridis subsp. fruticosa) patch dynamics and plant community composition to fire and regional temperature in north-western Canada. *Journal of Biogeography*, *37*(8), no-no. https://doi.org/10.1111/j.1365-2699.2010.02317.x

Lantz, T. C., Marsh, P., and Kokelj, S. V. (2013). Recent Shrub Proliferation in the Mackenzie Delta Uplands and Microclimatic Implications. *Ecosystems*, *16*(1), 47–59. https://doi.org/10.1007/s10021-012-9595-2

Loranty, M. M., Goetz, S. J., and Beck, P. S. A. (2011). Tundra vegetation effects on pan-Arctic albedo. *Environmental Research Letters*, *6*(2), 029601. https://doi.org/10.1088/1748-9326/6/2/029601

Mack, M. C., Bret-Harte, S. M., Hollingsworth, T. N., Jandt, R. R., Schuur, E. A. G., Shaver, G. R., and Verbyla, D. L. (2011). Carbon loss from an unprecedented Arctic tundra wildfire. *Nature*, *475*. https://doi.org/10.1038/nature10283

Moritz, M. A., Parisien, M.-A., Batllori, E., Krawchuk, M. A., Van Dorn, J., Ganz, D. J., and Hayhoe, K. (2012). Climate change and disruptions to global fire activity. *Ecosphere*, *3*(6), art49. https://doi.org/10.1890/es11-00345.1

Myers-Smith, I. H., Forbes, B. C., Wilmking, M., Hallinger, M., Lantz, T., Blok, D., Tape, K. D., Macias-Fauria, M., Sass-Klaassen, U., Lévesque, E., Boudreau, S., Ropars, P., Hermanutz, L., Trant, A., Collier, L. S., Weijers, S., Rozema, J., Rayback, S. A., Schmidt, N. M., … Hik, D. S. (2011). Shrub expansion in tundra ecosystems: dynamics, impacts and research priorities. *Environmental Research Letters*, *6*(4), 045509. https://doi.org/10.1088/1748-9326/6/4/045509

Myers-Smith, I. H., Hik, D. S., Kennedy, C., Cooley, D., Johnstone, J. F., Kenney, A. J., and Krebs, C. J. (2011). Expansion of canopy-forming willows over the twentieth century on Herschel Island, Yukon Territory, Canada. *Ambio*, *40*(6), 610–623. https://doi.org/10.1007/s13280-011-0168-y

Myers-Smith, I. H., Kerby, J. T., Phoenix, G. K., Bjerke, J. W., Epstein, H. E., Assmann, J. J., John, C., Andreu-Hayles, L., Angers-Blondin, S., Beck, P. S. A., Berner, L. T., Bhatt, U. S., Bjorkman, A. D., Blok, D., Bryn, A., Christiansen, C. T., Hans, J., Cornelissen, C., Cunliffe, A. M., … Wipf, S. (2020). Complexity revealed in the greening of the Arctic. *Nature Climate Change*, *10*, 106–117. https://doi.org/10.1038/s41558-019-0688-1

Natali, S. M., Schuur, E. A. G., Trucco, C., Hicks Pries, C. E., Crummer, K. G., and Baron Lopez, A. F. (2011). Effects of experimental warming of air, soil and permafrost on carbon balance in Alaskan tundra. *Global Change Biology*, *17*(3), 1394–1407. https://doi.org/10.1111/j.1365-2486.2010.02303.x

Nauta, A. L., Heijmans, M. M. P. D., Blok, D., Limpens, J., Elberling, B., Gallagher, A., Li, B., Petrov, R. E., Maximov, T. C., Van Huissteden, J., and Berendse, F. (2015). Permafrost collapse after shrub removal shifts tundra ecosystem to a methane source. *Nature Climate Change*. https://doi.org/10.1038/nclimate2446

Racine, C., Jandt, R., Meyers, C., and Dennis, J. (2004). Tundra Fire and Vegetation Change along a Hillslope on the Seward Peninsula, Alaska, U.S.A. *Source: Arctic, Antarctic, and Alpine Research Arctic, Antarctic, and Alpine Research*, *36*(1), 1–10. http://www.jstor.org/stable/1552423

Schuur, E. A. G., Crummer, K. G., Vogel, J. G., and MacK, M. C. (2007). Plant species composition and productivity following permafrost thaw and thermokarst in Alaskan tundra. *Ecosystems*, *10*(2), 280–292. https://doi.org/10.1007/s10021-007-9024-0

Siewert, M. B., and Olofsson, J. (2020). Scale-dependency of Arctic ecosystem properties revealed by UAV. *Environmental Research Letters*, *15*(9), 94030.

https://doi.org/10.1088/1748-9326/aba20b

Smith, L. C., Sheng, Y., MacDonald, G. M., and Hinzman, L. D. (2005). Atmospheric Science: Disappearing Arctic lakes. *Science*, *308*(5727), 1429. https://doi.org/10.1126/science.1108142

Tarnocai, C., Canadell, J. G., Schuur, E. A. G., Kuhry, P., Mazhitova, G., and Zimov, S. (2009). Soil organic carbon pools in the northern circumpolar permafrost region. *Global Biogeochemical Cycles*, *23*(2). https://doi.org/10.1029/2008GB003327

Veraverbeke, S., Rogers, B. M., Goulden, M. L., Jandt, R. R., Miller, C. E., Wiggins, E. B., and Randerson, J. T. (2017). Lightning as a major driver of recent large fire years in North American boreal forests. *Nature Climate Change*, *7*(7), 529–534. https://doi.org/10.1038/nclimate3329

Vincent, L. A., Zhang, X., Brown, R. D., Feng, Y., Mekis, E., Milewska, E. J., Wan, H., and Wang, X. L. (2015). Observed trends in Canada's climate and influence of low-frequency variability modes. *Journal of Climate*, *28*(11), 4545–4560. https://doi.org/10.1175/JCLI-D-14-00697.1

Wang, J. A., Sulla-Menashe, D., Woodcock, C. E., Sonnentag, O., Keeling, R. F., and Friedl, M. A. (2020). Extensive land cover change across Arctic–Boreal Northwestern North America from disturbance and climate forcing. *Global Change Biology*, *26*(2), 807–822. https://doi.org/10.1111/gcb.14804